The Role of Coenzyme Q10 in Statin Treated Zebrafish (*Danio rerio*)

by

Rand Pasha

Thesis submitted to the
Faculty of Graduate and Postdoctoral Studies
University of Ottawa
In partial fulfillment of the requirements for the
M.Sc. degree in the
Chemical and Environmental Toxicology Program
Ottawa-Carleton Institute of Biology

Thèse soumise à
L'École des Études Supérieures et Postdoctorales
Université d'Ottawa
En vue de l'obtention d'une Maîtrise dans le
Programme de
Toxicologie Chimiques et Environnemental
L'Institut de Biologie Ottawa-Carleton

Abstract

Atorvastatin (ATV) is a member of the statin family of pharmaceuticals sold as Lipitor™ by Pfizer Pharmaceuticals. Statins inhibit HMG-Coenzyme A reductase (HMG-CoAR), thus inhibiting the biosynthesis of cholesterol and other isoprenoid compounds including Coenzyme Q10 (CoQ10). This study evaluated the role of CoQ10 in preventing ATV-induced myotoxicity using the zebrafish *Danio rerio* as a model organism. ATV reduced spontaneous swimming, response to tactile stimuli, whole body enzyme activities (citrate synthase, cytochrome oxidase and lactate dehydrogenase) as well as increased pericardial sac edema in larvae. Transcript abundance of muscle atrophy markers (*atrogen-1, murf*) and the mitochondrial biogenesis marker (*pgc-1α*) were also altered. Additionally, acute toxicity of adult zebrafish resulted in no change in locomotor behaviour; however tissue enzyme activities and transcript abundance were altered. These findings demonstrate the protective effect of CoQ10 against larval ATV-meditated reduction in responses to tactile stimuli and enzyme activities suggesting CoQ10 does play a role in ATV-mediated toxicity.

Résumé

L'atorvastatine (ATV) est un membre de la famille de produits pharmaceutiques des statines vendus sous le nom de Lipitor ™ par Pfizer Pharmaceuticals. Les statines inhibent la HMG coenzyme A-réductase (HMG-CoA), inhibant ainsi la biosynthèse du cholestérol et d'autres composés isoprénoïdes dont la coenzyme Q10 (CoQ10). Cette étude a évalué le rôle de la CoQ10 dans la prévention de la myotoxicité induite par l'ATV en utilisant le poisson zèbre (*Danio rerio*) comme organisme modèle. L'ATV a réduit la nage spontanée, la réponse à des stimuli tactiles, des activités enzymatiques du corps entier (la citrate synthase, la cytochrome oxydase et la lactate déshydrogénase), et a causé l'inflammation de l'œdème du sac péricardique chez les larves. Les marqueurs de l'atrophie musculaires (*atrogin-1, murf*) et le marqueur de la biogenèse mitochondriale (*pgc- 1α*) ont également été modifiés. De plus, la toxicité aiguë du poisson zèbre adulte n'a pas entraîné de changement dans le comportement locomoteur, mais les activités enzymatiques et l'abondance des transcrits ont été modifiés. Ces résultats démontrent l'effet protecteur de la CoQ10 chez les larves contre la réduction des réponses à des stimuli tactiles et les activités enzymatiques induit par l'ATV suggérant que la CoQ10 joue un rôle dans la toxicité induite par l'ATV.

Table of Contents

List of Figures

List of Tables

List of Abbreviations

ATV – Atorvastatin

CS – Citrate synthase

COX – cytochrome synthase

DMSO – Dimethyl sulfoxide

LDH – Lactate dehydrogenase

PTS – Polyoxyethanyl-α-tocopheryl sebacate

PTU – 1-Phenyl 2-thiourea inhibitor

EM – Embryo medium

CoQ10 – Coenzyme Q10

HMG-CoAR – 3-hydroxy-3-methyl-glutaryl-coenzyme A reductase

FDA – U.S.A food and drug administration

MCT – H^+-monocarboxylic carrier transporter

P-glycoprotien – permeability glycoprotein

ETC – electron transport chain

OATP – organic anion transporting polypeptide

CYP – cytochrome P450

UGT – uridinediphosphoglucuronyl transferase

STP – sewage treatment plant

PGS – primordial germ cells

GGPP – geranylgeranyl pyrophosphate

PP – pyrophosphate

CPK – creatine phosphokinase

ROS – reactive oxygen species

ATP – adenosine triphosphate

PFA – 4% Paraformaldehyde

PBST – phosphate buffered saline with tween 20

DMSO – Dimethyl sulfoxide

OCT – optimal cutting temperature

SOD2 – superoxide dismutase 2

GPX1 – glutathione peroxidase 1

Atrogen-1 – protein

atrogen-1– mRNA

Pgc-1α – protein

pgc-1α – mRNA

murf – mRNA

Acknowledgements

To begin, I wish to express my deepest gratitude and appreciation to my supervisor, Dr. Thomas W. Moon, for providing me with the opportunity to join his lab. His continuous guidance and support as well as his efforts have made this journey a pleasant learning experience in which I will be forever grateful. I would also like to express my sincerest appreciations to my committee members, Drs. Bill Willmore, Charles Darveau, and Marc Ekker, for their valuable effort and contribution to this project.

Moreover, I would like to thank my colleagues in the Moon lab, Kim Mitchell, Paul Craig, Shahram Eisa-Beygi, Andrey Massarsky, and Marilyn Chang who have always lend a hand when needed as well as Kelly Levesque, Félix Morin, Ali Taha, Justine Labarre, Carol Truong, Kevin Yoon, Maurice Lam who have provided me with support along with valued friendship. Furthermore, I would like to extend a special thanks to Phillip Pelletier at the Common Molecular Facility for providing his expertise in the use of the equipment as well as to William "Bill" Fletcher and Vishal Saxena at the aquatics care facility for providing care to my zebrafish and for the maintenance of aquariums.

Lastly, I would like to express special appreciations to my husband, Justin Lajoie, to my parents, Challang Pasha and Niran Al-Obaydi, and to my siblings, Banar and Tanya. I also would like to thank my in-laws for their continuous support throughout the project. They are Fernand Campeau and Lyse Marleau, Sylvie Beaupré, Jacques Lajoie and Laurie Filion, Jean-Francois Beaupré, Simon-Pierre Lajoie and Kimberly McClean, and Marie-Ève Lajoie and Joel Stang.

Funding for this research was provided by the Natural Science and Engineering Council (NSERC) to Dr. Thomas W. Moon.

"When the last tree is cut down, the last fish eaten, and the last stream poisoned, you will realize that you cannot eat money"

~Native American Proverb

Chapter 1 – General Introduction

1.1. Rationale for the Study

Statin drugs (or statins) are the most highly prescribed medication for the treatment of hypercholesterolemia (Gotto, 2002; Charlton-Menys and Durrington, 2008; IMS, 2011; Jackevicius *et al.*, 2012). In comparison to other cholesterol-lowering drugs, statins have little known side effects, and this contributes to their common use (Palinski, 2001). Globally, heart disease rates are predicted to increase exponentially as more and more countries adopt western-style diets and coronary disease-prone lifestyles (Heart and Stroke Foundation, 2012), which will increase the need for statins. However, in recent years concerns pertaining to the potential impacts of statins on non-target aquatic species have been raised. Inevitably, the increasing prescription rates of these drugs will lead to increased release into aquatic environments. In fact, statins are now present at detectable levels in sewage treatment plant (STP) effluents and surface and ground waters in Canada and elsewhere (Miao and Metcalfe, 2003; Lee *et al.*, 2009; Metcalfe *et al.*, 2003). Generally, the concentrations detected in the environment are in the ng L^{-1} range (see Table 1.1) (Metcalfe and Miao, 2003; Lee *et al.*, 2009). Nonetheless, even at these low environmental concentrations, statins could negatively impact non-target aquatic organisms, especially considering the continuous addition of statins into the aquatic system (Gagné *et al.*, 2006).

Although pharmaceuticals are designed to alter physiological functions and induce specific effects in humans, they can have similar effects in non-target species, particularly among vertebrates, which share many evolutionarily conserved physiological processes

(Doughton and Ternes, 1999; Fent *et al.*, 2006; Corcoran *et al.*, 2010). The most vulnerable species to these aquatic contaminants are fish since they are often exposed over their entire life cycle (Doughton and Ternes, 1999; Spitsbergen and Kent, 2003). Therefore, it is important to monitor the impacts of pharmaceuticals, including statins, on non-target aquatic species (Metcafe and Miao, 2003).

Table 1.1: Detected ATV concentrations in bodies of water.

Country	ATV Detected Concentration (ng L^{-1})
Canada	44[1]
U.S.	25[2]
Spain	2[3]
Italy	23[4]

Sources: [1]Metcalfe *et al*., (2003), [2] Benotti *et al*., (2009), [3] Jelic *et al*., (2011) and [4] Pojana *et al*., (2011).

The following sections provide an overview of the role of statins in blocking cholesterol biosynthesis, as well as their general characteristics, pharmacokinetics, and pharmacodynamics. Since my thesis investigates the impact of statins on Coenzyme Q10 (CoQ10), which is synthesized within the cholesterol biosynthesis pathway, the importance of this biomolecule in the mitochondrial electron transport chain (ETC), its chemical properties, as well as its role in energy production will also be discussed.

1.2. Statins

1.2.1. Overview

Statins are a class of fungal metabolites that inhibit 3-hydroxy-3-methyl-glutaryl-coenzyme A reductase (HMG-CoAR, EC1.1.1.88), the rate-limiting enzyme in cholesterol biosynthesis (Endo, 2010; Lyons *et al.*, 2011). Historically, the first compound with statin-like properties was isolated in 1976 from a rice mold (*Penicillium citrinum*) and named Compactin (later renamed mevastatin). However, it was not until 1987, when lovastatin

isolated from soil mold, *Aspergillus terrestrius* was given FDA approval in the US to become the first commercial statin compound on the market (Vagelos, 1991). Since the introduction of lovastatin to the market, seven additional structural analogs have been developed, including two semi-synthetic (simvastatin and pravastatin) and four synthetic (fluvastatin, atorvastatin, rosuvastatin, cerivastatin, and pitavastatin) versions (Endo, 2010). However, in 2001 cerivastatin was withdrawn from the market due to reports of fetal rhabdomyolysis (Maggini *et al.*, 2004; see section 1.4 for more details), leaving only 6 analogs on the market today (Fig. 1.1).

1.2.2. General characteristics and mode of action of statin drugs

Statins share many beneficial features; nonetheless, their structural differences play an important role in dictating their clinical utility and effectiveness in modifying risk for cardiovascular disease. Pleiotropic effects of statins, including antioxidant, anti-inflammatory, and anti-proliferative effects (Anand *et al.*, 2008; Hajipour *et al.*, 2010), have recently emerged leading to the expansion of their use to treat cancer, stroke, inflammatory conditions, and polycystic ovarian syndrome (Kishi *et al.*, 2009; Sathyapalan and Atkin, 2010; Vasyuk *et al.*, 2010).

Although the clinical benefits of statins are generally significant, some statin analogs are more potent than others. Statins act by inhibiting the conversion of HMG-CoA to mevalonate by competitive inhibition of HMG-CoAR (Lyons *et al.*, 2011). Statins bind to HMG-CoAR through van der Waals forces, competing with HMG-CoA for the substrate binding site on the enzyme (McKenney, 2003). Upon binding, statins alter the conformation and prevent HMG-CoAR from attaining its functional configuration (Corsini *et al.*, 1999; Schachter, 2005; Gazzero *et al.*, 2012).

The degree of statin binding to the enzyme and how well statins fit into the binding pocket of the enzyme are determined by the statin base structure. X-ray crystallographic studies of the statin-HMG-CoAR complexes have allowed the characterization of the base structures of each statin analog (McKenney, 2003). The synthetic statins including fluvastatin, atorvastatin, and rosuvastatin, contain a fluorinated phenol group and other moieties that enhance their binding to the substrate pocket of the enzyme (McKenney, 2003; Gazzerro *et al.*, 2012). Rosuvastatin has the strongest binding affinity to HMG-CoAR compared with the other statins due to its polar bond with the enzyme. Both atorvastatin and rosuvastatin form additional hydrogen bonds, making them more potent than the other statin analogs (McKenney, 2003; Schachter, 2005).

1.2.3. Atorvastatin

This thesis focuses on atorvastatin (ATV), which is better known by its trade name Lipitor™. Although its market share is decreasing after losing patent protection in 2011, it is still the most prescribed statin drug on the market today (IMS, 2011; Jackevicius *et al.*, 2012). ATV is a synthetic statin, and is administered in its acid form (Charlton-Menys and Durrington, 2008). ATV was first synthesized in 1985 by Bruce Roth while working for the Parke-Davis pharmaceutical company (bought by Pfizer pharmaceutical company in 2000). After co-marketing with Pfizer in 1997, Lipitor™ was the fourth HMG-CoAR inhibitor to be approved by the FDA and introduced to the market (Rea, 2008).

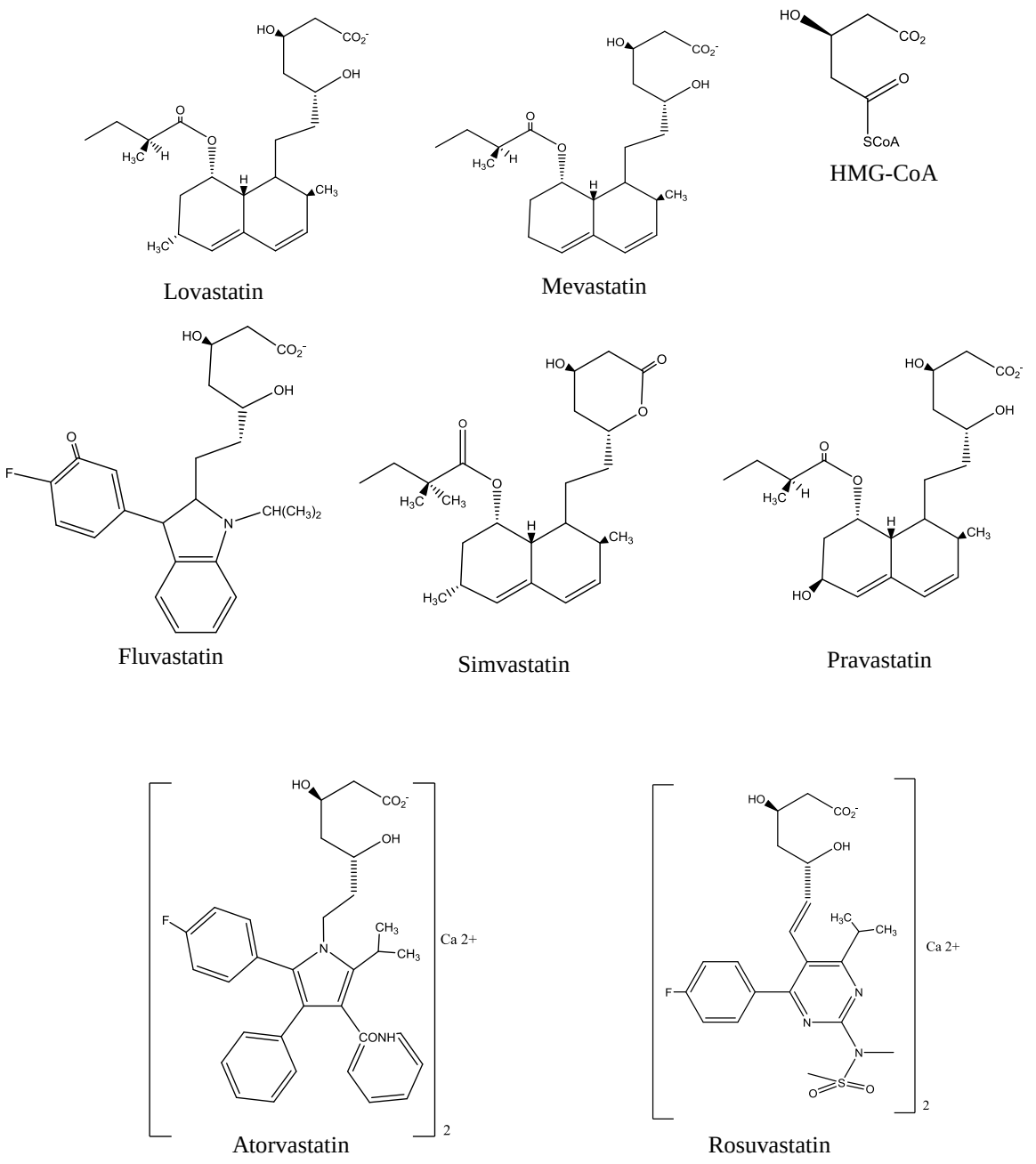

Figure 1.1: Structures of HMG-CoAR inhibitors (statins). Lovastatin, mevastatin and simvastatin are administered in the lactone form and converted to their hydroxy acids in the liver. Pravastatin, fluvastatin, atorvastatin and rosuvastatin are salts of their hydroxy acids. The common structural characteristics of these drugs are the HMG-CoA group which competes with HMG-CoA binding to the HMG-CoAR (modified from Charlton-Menys and Durrington, 2008).

As mentioned above, the different functional groups of statins make some analogs more potent than others. For example, ATV and rosuvastatin form a hydrogen bond with the Ser565 residue in HMG-CoAR through the carbonyl oxygen in ATV or through the sulfone oxygen in rosuvastatin. These differences in the number and types of interactions between the statin and enzyme may explain the relatively greater efficacy of ATV and rosuvastatin in lowering cholesterol (McKenny, 2003).

ATV is administered orally as a calcium salt of the active hydroxy acid (Cilla *et al.*, 1996). The dosage used clinically is 10-80 mg day^{-1} (Lennernas, 2003). ATV has a log K_{ow} of 4.5 and is therefore relatively lipophilic (Hernando *et al.*, 2007). Generally, it takes 4 weeks after the initiation of ATV therapy for the patient's cholesterol to reach 90% reduction (Stern *et al.*, 1998). Although ATV-acid has complete intestinal absorption due to high solubility and permeability, the drug is subjected to first pass metabolism by oxidation and glucuronidation in the gut wall and the liver (Lennernas, 2003). As a result, the absolute bioavailability (i.e. the fraction of the administered dose of unchanged drug that reaches the systemic circulation) of the ATV-acid after a 10 mg oral dose is 14%. The time to reach peak plasma concentration is 1-2 h and the elimination half-life is 14 h after administration (Gibson *et al.*, 1997; Lennernas, 2003). Intake of food does not impact intestinal absorption of ATV; therefore ATV can be administrated with or without food (Lennernas, 2003).

1.2.4. Statin absorption, distribution, metabolism, and excretion

Once ATV is ingested, primary uptake occurs by transporters and/or passive diffusion (Randall *et al.*, 1998; Lennernas, 2003). Wu *et al.* (2000) suggested the absorption of ATV was a result of the H^+-monocarboxylic carrier transporter (MCT) and

that passive diffusion was of lesser importance. Moreover, P-glycoprotein transport was also found to contribute to intestinal absorption of ATV (Lennernas, 2003).

Once in the circulatory system, ATV is taken up by the liver (Lennernas, 2003). In humans the transporters involved in the hepatic uptake of statins are localized at the basolateral or apical membranes of polarized cells in the liver. These transporters are classified as either influx (uptake into cells) or efflux (excretion out of cells) (Gazzerro *et al.*, 2012). The influx transporters associated with ATV are the organic anion transporting polypeptide (OATP) 1B1 and OATP C, members of OATP family of transporters located at the canalicular membrane of the liver (Fojo *et al.*, 1987; Hsiang *et al.*, 1999).

The metabolism of statins in mammals occurs within the liver and involves the well-known xenobiotic metabolism system, which includes the Phase I and II reactions. Phase I reactions involve changes that are made to the drug, such as oxidation, reduction, and hydrolysis, that are primarily mediated by the cytochrome P450 (CYP) family of enzymes (Ho and Kim, 2005). Whereas Phase II reactions use an endogenous compound, such as glucuronic acid, glutathione, or sulfate, to produce a more polar end-product of the drug that can be ultimately excreted from the body through urine and/or feces (Ho and Kim, 2005). In humans, the enzyme responsible for ATV metabolism in the gut wall and the liver is the CYP3A4 isozyme (see Table 1.2) (Lennernas, 2003). The ATV Phase I reaction undergoes metabolism by oxidation into active metabolites, while ATV Phase II reaction involves uridinediphosphoglucuronyl transferase (UGT)-mediated glucuronidation, more specifically UGT1A1 and 1A3 in human is involved in the elimination of the active metabolites in the liver (Prueksaritanont *et al.*, 2002a; 2002b; 2002c; Lennernas, 2003).

The bile to urine excretion ratios of different analogs of statins varies with respect to statin lipophilicity (see Table 1.2). Due to its lipophilicity, ATV requires efflux transporters to be excreted into the bile and ultimately the feces (Konig *et al.*, 2000; Ho and Kim, 2005; Gazerro *et al.*, 2012). Hsiang *et al.* (1999) has shown in an *in vitro* study using a colon cell line, that ATV-acid is a substrate for both the efflux protein P-glycoprotein and OATP C, thus suggesting P-glucoprotein and OATP C are responsible for biliary secretion of ATV and its metabolites.

1.2.5. Statin environmental fate and uptake by fish

Drugs and active metabolites enter the aquatic ecosystem generally through sewage treatment plants (STP) effluents (Daughton and Ternes, 1999; Halling-Sorensen *et al.*, 1998). The major source of statins in the aquatic environment is patient excretion following therapy (Kolpin *et al.*, 2002). Nonetheless, improper disposal of unused or expired statins from manufacturing facilities and homes, hospital wastewater, and landfill leachate also contribute to the environmental load (Daughton and Ternes, 1999; Christensen *et al.*, 2009).

Two processes are important for the elimination of pharmaceuticals in the STP: 1) adsorption to suspended solids (sewage sludge), and 2) biodegradation. Adsorption to suspended solids depends on hydrophobic and electrostatic interactions of the pharmaceutical with particulates in the environment (Fent *et al.*, 2006). Ottmar *et al.* (2010) suggested that statin sorption occurs via solubilisation of the hydrophobic part of the molecule onto the sorbent organic matter. In general, acidic pharmaceuticals occur as ions at neutral pH, thus have little tendency to adsorb to the sludge. Due to its lipophilic nature, ATV adsorption to sludge does not play a major role in the elimination process. In

contrast, ATV biodegradation is considered to be the more important elimination process from wastewater and surface water (Fent *et al.*, 2006). Elimination rate studies of pharmaceuticals are mainly based on measurements of influent and effluent concentrations in STPs.

Previous studies indicated that STP elimination efficiencies can cover a wide range (0-99%) (Ternes, 1998; Stumpf *et al.*, 1999; Carballa *et al.*, 2004). This variation is due to a number of factors including the construction and treatment technology, hydraulic retention time, season, and the performance of the STP (Fent *et al.*, 2006). Once in surface waters, biotransformation of pharmaceuticals occurs through biodegradation. In addition, photodegradation is important; however, the efficiency of photodegradation depends on the strength of the solar irradiation, and therefore season (Fent *et al.*, 2006). Due to its lipophilicity (log K_{ow} 4.5), the ATV taken up by fish is thought to occur by diffusion across the gills, while uptake through ingestion plays a minor role (Randall *et al.*, 1998). Statins are bioavailable to aquatic species (Lahti *et al.*, 2011) since many drugs are small molecules (<600 da) and are relatively lipophilic including ATV, the transfer across the gills would be favored (Huckins *et al.*, 1990; Randall *et al.*, 1998; Ellesat *et al.*, 2012). Fish embryos can similarly take-up xenobiotics largely through the chorion pore canals. For example, zebrafish (*Danio rerio*) chorion pore canals are approximately 0.5-0.7 µm in diameter, with distances between pores of 1.5-2.5 µm, which allows for the passive diffusion of small xenobiotic molecules into the embryo (Rawson *et al.*, 2000; Lee *et al.*, 2007). Once embryos hatch, oxygen uptake occurs through diffusion of gasses across the larval skin and gills, as a result, small xenobiotic agents are similarly taken up across the larval skin (McGrath and Li, 2008).

Table 1.2: Pharmacological characteristics of different statin analogs (Han *et al.*, 2012; Hernando *et al.*, 2007; Pan *et al.*, 1991).

Parameter	Lovastatin	Pravastatin	Simvastatin	Fluvastatin	Atorvastatin	Rosuvastatin
Oral absorption	30%	34%	61-85%	98%	30%	NDA
Absolute bioavailability	5%	17%	<5%	24%	12%	NDA
Protein binding	>95%	55-60%	94-98%	98%	>98%	88%
Volume of distribution (L Kg^{-1})	NDA	0.5	NDA	34%	565	NDA
Elimination half-life (hours)	1.1-1.7	1.5-3.2	1.9	0.5-3.1	14	19
Log K_{ow}	4.3	NDA	4.7	4.9	4.5	NDA
Clearance						
• **Urine**	NDA	47%	13%	<6%	<2%	NDA
• **Bile**	NDA	53%	53%	90%	>98%	NDA
Metabolism CYP	CYP 3A4	No significant metabolism	CYP 3A4	CYP 2C9	CYP 3A4	CYP 2C9, CYP 2C19
Significant Drug interaction	Food Warfarin, Propranolol	Warfarin, Propranolol	Warfarin, Digoxin	Warfarin, Digoxin	Digoxin	NDA
Dissolubility	Lipophilic	Hydrophilic	Lipophilic	Lipophilic	Lipophilic	Hydrophobic
Origin	Natural	Natural	Semi-Synthetic	Synthetic	Synthetic	Synthetic

NDA= No Data Available

Given that vertebrates share evolutionary conserved physiological processes, fish share similar receptors and/or signal transduction pathways that can influence ATV bioavailability. Thus, ATV is expected to be bioavailable to fish, however, Zhang *et al.* (2010) demonstrated that ATV does not bioaccumulate in fish muscle tissues. This was attributed to the low ATV log K_{ow} resulting in sufficient excretion from fish and therefore insufficient bioaccumulation in tissues (Zhang *et al.*, 2010).

1.2.6. Past studies on statins and fish

Two forms of HMG-CoAR have been identified in zebrafish, *hmgcr1* and *hmgcr2* (Thorpe *et al.*, 2004), and Estey *et al.* (2008) reported a 79 to 87% sequence similarity of the rainbow trout HMG-CoAR to that of humans. Previous studies demonstrated that statins inhibit HMG-CoAR in fish species including the zebrafish (Hanai *et al.*, 2007), rainbow trout (*Oncorhynchus mykiss*) (Estey *et al.*, 2008), and Japanese medaka (*Oryzias latipes*) (Kurokawa *et al.*, 2006).

A previous study by Thorpe *et al.* (2004) reported that treatment of zebrafish embryos with 10 µM (5.58 mg L^{-1}) ATV resulted in germ cell migration defects and morphologic abnormalities as a result of disruption in primordial germ cells (PGC) migration. The authors observed that ATV-induced PGC migration defects were rescued by both geranylgeraniol, an alcohol involved in post-translational modification (geranylgeranylation) and farnesol, suggesting the potential role for geranylgeranyl transferase or farnesyl transferase activities in this process (Thorpe *et al.*, 2004). The germ cell migration defects were also observed in medaka embryos treated with ATV, but only during the later somitogenesis stage of development (Kurokawa *et al.*, 2006). Kurokawa *et al.* (2006) demonstrated that ATV did not result in germ cell migration defects in medaka

embryos up to early somitogenesis, however at subsequent stages, most PGC did not move to posterior regions of the embryo.

Another study by Eisa-Beygi *et al.* (2013) demonstrated that a concentration of 0.5 mg L^{-1} ATV resulted in cerebral hemorrhage early in zebrafish development resulting from the loss of vascular integrity. The hemorrhage was rescued by exogenous supplementation of geranylgeranyl pyrophosphate (GGPP), a metabolite of the mevalonate pathway (see Fig. 1.2), required for the membrane localization and activation of Rho GTPases for vascular stability (Eisa-Beygi *et al.*, 2013).

Moreover, Hanai *et al.* (2007) reported that lovastatin induced concentration-dependent muscle damage in zebrafish larvae by formation of gaps in muscle fibers and fiber disruption. By knocking down the HMG-CoAR gene (*z–HMG-CoA reductase*) in zebrafish embryos using missense and antisense morpholino oligonucleotides targeting the ATG region of the HMG-CoAR gene (ATG morpholino), the authors confirmed that lovastatin's effect on zebrafish muscle was due to the inhibition of HMG-CoA reductase. Lovastatin also induced the expression of *atrogen-1*, a key marker of skeletal muscle atrophy (Hanai *et al.*, 2007).

A study using the rainbow trout PLHC-1 cell line (topminnow hepatocyte cell line) demonstrated that ATV exposure decreased in activities of P-glycoprotein, a member of the ABC family of transporters that are involved in efflux transportation of statins in trout hepatocytes (Caminada *et al.*, 2008). Furthermore, *in vivo* ATV exposure resulted in intracellular accumulation of statins in the gills, thereby resulting in up-regulation of mRNA transcript abundance of genes involved in membrane transport (*pgp, mrp1*), the oxidative stress response (*sod, mt*), apoptosis (*bax*) and drug biotransformation (*sult2b*) (Ellesat *et al.*, 2012).

Although the above studies used statin concentrations well above those found in the environment (Kurokawa *et al.*, 2006; Hanai *et al.*, 2007; Caminada *et al.*, 2008; Estey *et al.*, 2008; Eisa-Beygi *et al.*, 2013), these studies demonstrated the importance of the mevalonate pathway during normal fish development. However, little attention has been given to whether ATV induces muscle damage or the role that CoQ10 might play in mitigating ATV-induced damage. Regardless, these studies do support ATV-induced muscle damage and morphological abnormalities due to inhibition of HMG-CoAR.

1.3. The Biochemical Significance of CoQ10 and its Relation to Statins

1.3.1. Overview

The popularity of statins in medical research increased dramatically after it become a commonly prescribed medication for high blood cholesterol and other health issues that exploit the pleiotropic benefits associated with statin use (Stancu and Sima, 2001; McKenney, 2003). As noted above, statins work by inhibiting the conversion of HMG-CoA to mevalonate early within the mevalonate pathway that leads to the production of cholesterol and other isoprenoids (Fig. 1.2) (Endo, 2010; Lyons *et al.*, 2011). The blockade of mevalonate production reduces the availability of all subsequent products of the mevalonate pathway including the production of farnesyl pyrophosphate (PP), which is an intermediate in the synthesis of decaprenyl-PP that leads to CoQ10, geranylgeranyl-PP that leads to prenylated proteins, and cholesterol (Stancu and Sima, 2001; McKenney, 2003; Marcoff and Thompson, 2007; Endo, 2010).

1.3.2. Functional description of CoQ10

Coenzyme Q10 (CoQ10) or ubiquinone, is the predominant member of the coenzyme Q family. The Q refers to the quinone chemical group and the number refers to the total amount of isoprene chemical subunits in its tail (Ernster and Dallner, 1995).

CoQ10 was first isolated from beef heart by Fredrick L. Crane and colleagues at the University of Wisconsin in 1957 (Crane *et al.*, 1957). The essential amino acid tyrosine or phenylalanine is converted to 4-hydroxybenzoic acid, which when combined with decaprenyl-PP (derived from the mevalonate pathway) in the presence of a specific transferase ultimately generates CoQ10 (Ernster and Dallner, 1995; Tran and Clarke, 2007) (see Fig. 1.3). CoQ10 exists in three oxidation states (Fig. 1.4), enabling it to both accept and donate electrons. This property makes CoQ10 an essential molecule for the Electron Transport Chain (ETC) within the mitochondria, where CoQ10 acts as an important electron shuttle that is crucial for generating the proton gradient across the mitochondrial membrane that is used for the production of ATP (Fig. 1.5). Reduction in the amount of CoQ10 within the mitochondria could potentially cause oxidative stress and ultimately mitochondrial dysfunction (Gold and Cohen, 2001; Musumeci *et al.*, 2001). Since CoQ10 has the same important function in every cell of the body, impairing its synthesis could be detrimental to all tissues, but in particular those tissues with high energy requirements such as cardiac muscle, red oxidative muscle, brain, liver, and kidney (Abou-Sleiman *et al.*, 2006; Molyneux *et al.*, 2009).

CoQ10 is synthesized in all cells of the body and is found in the mitochondria, peroxisomes, lysosomes, plasma membrane, Golgi vesicles, and endoplasmic reticulum of cells (Kalen *et al.*, 1987; Shapiro and Saliou, 2001). Coenzymes Q1 through 7 have been reported to have enzymatic functions in quinone biosynthesis in the cell (Jonassen and Clarke, 2001; Gin *et al.*, 2003); however the mode of transport of CoQ10 to the mitochondrial membrane is still unexplained (Spisni *et al.*, 1978; Quinn and Esfahani, 1980; Ulrich *et al.*, 1985; Fato *et al.*, 1986; Di Bernardo *et al*., 1998; Jemiota-Rzeminska 2001; Geromel *et al.*, 2002).

Although many organisms contain more than one member of the CoQ family, CoQ10 is predominant in humans, birds, and fish, whereas CoQ9 is predominant in rats and mice (Battino *et al.*, 1990; Lenaz *et al.*, 1993; Albano *et al.*, 2002; Kyoto Encyclopedia of genes and genomes, 2012). The major function of some CoQ members is to act as an electron carrier in the mitochondrial respiratory chain (Schindler *et al.*, 1984). In the inner mitochondrial membrane, electrons from NADH and succinate pass through the ETC and ultimately reduce oxygen to water. The transfer of electrons through the ETC provides energy to complexes I, III, and IV to pump protons through the inner mitochondrial membrane, creating a proton gradient. ATP synthase uses this electrochemical potential to generate ATP from ADP. CoQ10 functions as an electron carrier from enzyme complex I and enzyme complex II to complex III (Fig. 1.5).

1.3.3. Therapeutic uses of CoQ10

The findings of Tran and Clarke (2007) demonstrated that under normal physiological conditions, all cells can synthesize CoQ10; therefore cells are not reliant upon an exogenous (dietary) supply of CoQ10 (Bhagavan and Chopra, 2006). However more recent studies indicate that dietary supplements of CoQ10 do alleviate symptoms of familial encephalomyopathy (Rotig *et al.*, 2000), mitochondrial cytopathy (Gold and Cohen, 2001), cardiomyopathy that develops in Friedreich ataxia (Campuzano *et al.*, 1996), Duchenne, Becker, and limb-girdle dystrophies, myotonic dystrophy, Charcot-Marie-Tooth disease, Welander disease (Folkers *et al.*, 1985), and cases of cerebellar ataxia and cerebellar atrophy (Musumeci *et al.*, 2001) are all ascribed to CoQ10 deficiency. These findings suggest that abnormalities in cell function resulting in reduced endogenous CoQ10 levels may benefit from exogenous supplementation of CoQ10.

CoQ10 is photosensitive, very stable at 37 ^{o}C, and highly lipophilic (Kommuru *et al.,* 1999). Exogenous (dietary or supplementary) CoQ10 is absorbed across intestinal enterocytes, similar to vitamin E and other lipophilic substances.

CoQ10 is first incorporated into chylomicrons following absorption, and transported by the circulation. In humans 95% of CoQ10 in the circulation exists in its fully reduced form or ubiquinol (Fig. 1.4) (Elmberger *et al.*, 1989). Following absorption, ubiquinol first appears as a part of mesenteric triacylglycerol-rich lipoproteins. These particles are converted to chylomicron remnants in the circulation by lipoprotein lipase and then taken up rapidly by the liver, where CoQ10 is repackaged mostly into very low-density lipoprotein or low-density lipoprotein particles and re-released back into the circulation to help cells manage oxidative stress (Elmberger *et al.*, 1989; Greenberg, 1990; Traber *et al.*, 1992; Bhagavan and Chopra, 2006). Although studies on CoQ10 metabolism in humans and animals are limited, the fecal excretion was found to be the main route of elimination of ^{14}C-labeled CoQ7 in rats (Fujita *et al.*, 1971). Moreover, the authors reported that CoQ7 was absorbed via the lymphatic system and concentrated mainly in the liver (Fujita *et al.*, 1971).

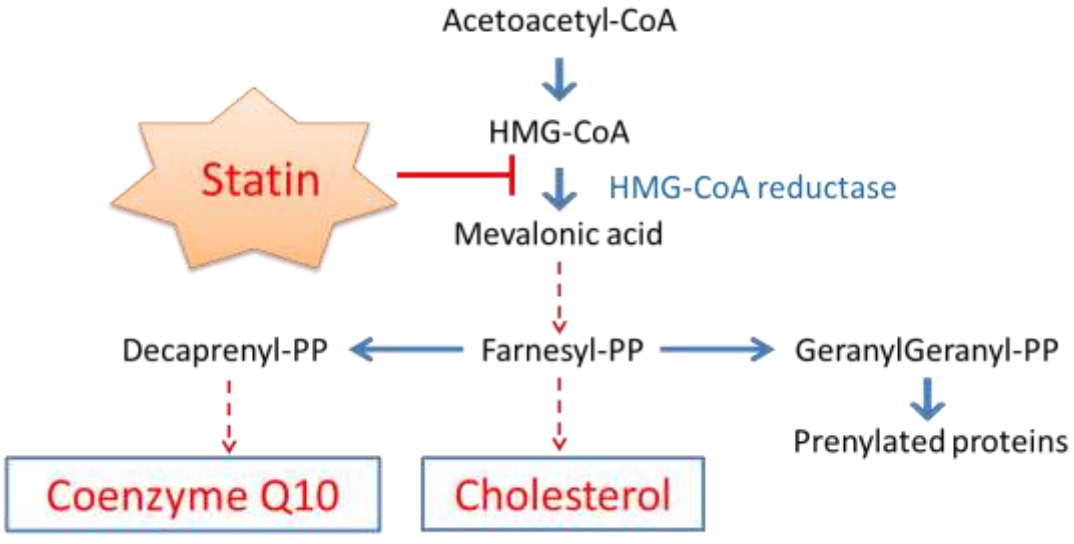

Figure 1.2: An abbreviated mevalonic acid pathway illustrating the major steps in the biosynthesis of cholesterol, Coenzyme Q10 and prenylated proteins. Statins inhibit the enzyme hydroxy-methylglutaryl-Coenzyme A (HMG-CoA) reductase (EC 1.1.1.88), thus interfering with the conversion of HMG-CoA to mevalonate and therefore blocking the production of farnesyl pyrophosphate (PP), an intermediate in the synthesis of Coenzyme Q10 and other key compounds (modified from Charlton-Menys and Durrington, 2008).

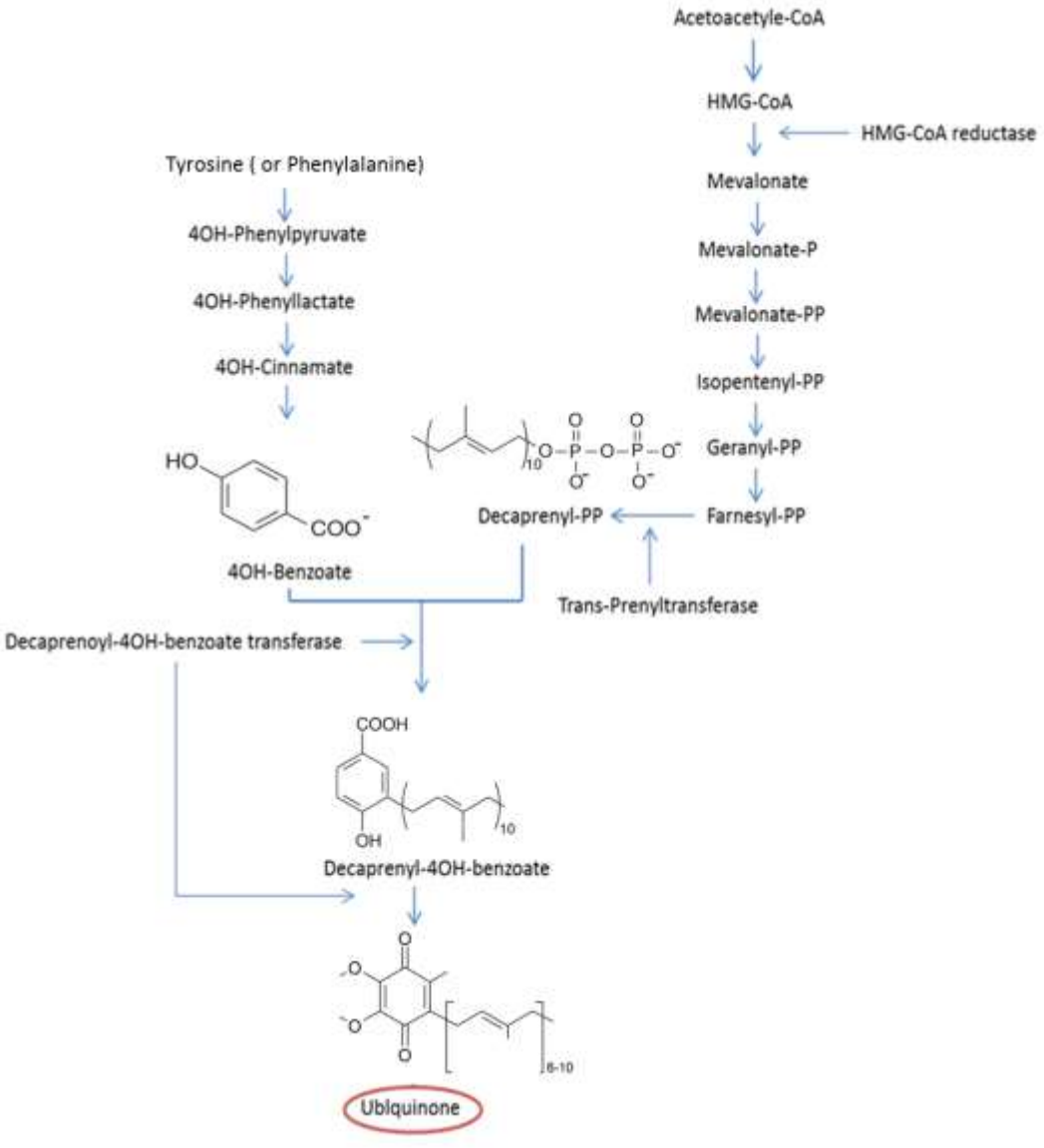

Figure 1.3: The synthesis of CoQ10 from tyrosine (or phenylalanine) and polyisopreny chains derived from the mevalonic acid pathway (Ernster and Dallner, 1995). Permission was obtained from the journal to reuse this figure in the thesis.

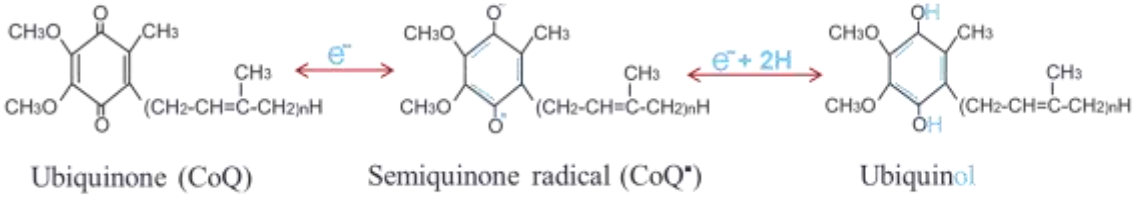

Figure 1.4: An illustration of 1,4-benzoquinone in its three oxidative states: the fully oxidized ubiquinone, the radical semiquinone intermediate, and the fully reduced ubiquinol (modified from Mancini *et al.*, 2011).

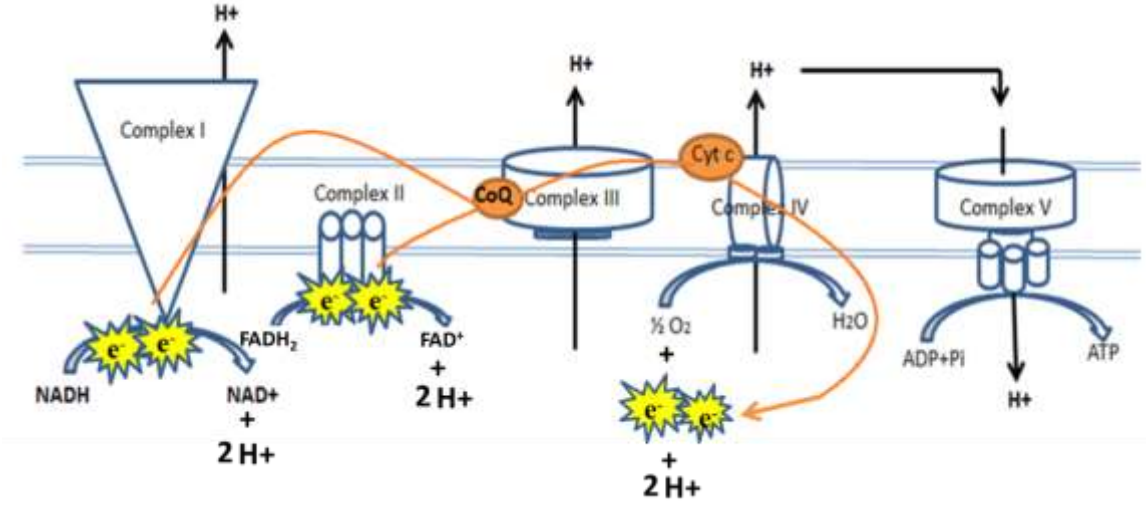

Figure 1.5: An illustration of the components of the Electron Transport Chain (ETC) in the inner mitochondrial membrane (modified from Abou-Sleiman *et al.*, 2006).

1.4. Literature Review on Statin Effects and Key genes Involved in Muscle Atrophy

Although statins have many benefits, one clinical downside is rhabdomyolysis (breakdown of muscle cells) (Itagaki *et al.*, 2009). In a large clinical study that examined rhabdomyolysis in a hospital population, the average incidence was found to be 0.44 % for ATV (Sathasivam and Lecky, 2008). Studies have shown that different statins can result in muscle damage in humans (Sathasivam and Lecky, 2008), mice (Elhaleem and Elsayed, 2011), and zebrafish larvae (Hanai *et al.*, 2007). A study involving mice exposed to statins found that muscle damage correlated with reduced levels of CoQ10 and that the damage was rescued with CoQ10 treatment (Elhaleem and Elsayed, 2011). Alternatively, Hanai *et al.* (2007) demonstrated that lovastatin exposure in zebrafish larvae resulted in thinning of muscle fibers as well as elevation in *atrogen-1* gene, an early marker of muscle degeneration.

Elhaleem and Elsayed (2011) evaluated the effects of CoQ10 supplementation to prevent statin-induced myotoxicity. The authors assessed adult male Sprague Dawley rats given an oral dose of 1.44 mg day^{-1} for 3 months, which was equivalent to adult human therapeutic dose of 100 mg day^{-1} of ATV and simvastatin. They assessed the activities of creatine phosphokinase (CPK) and lactate dehydrogenase (LDH), as well as myoglobin, potassium, creatinine, and CoQ10 levels in the plasma, and skeletal muscle histopathological changes. Significant elevation of CPK and LDH activities as well as potassium and myoglobin levels was observed. Moreover, a depletion of CoQ10 levels and histological muscle damage were noted. These effects were more evident in skeletal muscle tissues treated with ATV than with simvastatin. Upon co-treatment with CoQ10 at 1.8 mg day^{-1} equivalent to adult human therapeutic dose of 100 mg day^{-1}, Elhaleem and Elsayed (2011) noted significant recovery in CPK, LDH, potassium, and myoglobin concomitant

with restoration of depleted CoQ10 levels and decreased damage to muscle tissue. This study demonstrated the protective effect of CoQ10 against myotoxicity induced by simvastatin and ATV, proposing its use in the treatment of statin-induced damage in skeletal muscle tissue.

Atrogen-1 is an early marker of muscle degradation during muscle atrophy in mammals and fish (Gomes *et al.*, 2001; Sacheck *et al.*, 2004; Hanai *et al.*, 2007). It is a muscle-specific F-box protein (MAFbx) and is an E3, ATP-dependent ubiquitin ligase that mediates proteolytic events that occur during atrophy in skeletal muscle (Adams *et al.*, 2007). This gene is one of the few examples of an F-box protein or Ub-protein ligase (E3) expressed in a tissue-specific manner that is enhanced with proteolysis, leading to muscle atrophy (Gomes *et al.*, 2001).

In a study by Amaral and Johnston (2011), adult zebrafish were deprived of food for 7 days to investigate the transcriptional responses to this applied stress. They reported that the expression of the muscle-specific E3 ubiquitin ligases *fbxo32* (MARF/*atrogen-1*) and *murf* (annotated as *zgc: 86757*) was up-regulated in zebrafish by 13.3 and 2.7-fold, respectively, between 9 and 144 h after the initiation of fasting. *Atrogen-1* and *murf* transcriptions were down-regulated by 55% (*fbxo*) and 77% (*murf*) within 45 min after re-feeding. These results are in agreement with studies in mammals (Gomes *et al.*, 2001; Adams *et al.*, 2007; Bdolah *et al.*, 2007; Cao *et al.*, 2009; Galasso *et al.*, 2010; Elhaleem and Elsayed, 2011), rainbow trout (Sacheck *et al.*, 2004; Salem *et al.*, 2006; Seiliez *et al.*, 2008; Cleveland and Evenhuis, 2010; Wang *et al.*, 2011), and zebrafish (Hanai *et al.*, 2007; Cao *et al.*, 2009) in that *atrogen-1* and *murf* are up-regulated as an early marker of muscle degradation.

Another useful marker is the peroxisome proliferator-activated receptor (PPAR)-γ coactivator 1α (*pgc-1α*) that regulates mitochondrial biogenesis and metabolism (Puigserver and Spiegelman, 2003). This marker is involved in multiple biological responses related to energy homeostasis, thermal regulation, and glucose metabolism; it also promotes mitochondrial biogenesis and respiration in muscle (Puigserver and Spiegelman, 2003). Interference with mitochondrial respiration will result in reduced *pgc-1α* mRNA abundance; therefore it can be used as an indicator for mitochondrial dysfunction (Puigserver and Spiegelman, 2003).

1.5. Zebrafish as a Model Organism

The zebrafish continues to gain more and more recognition as a vertebrate model in many fields including medical and toxicological research (Helenius and Yeh, 2012; Lessman, 2011; Spitsbergen and Kent, 2003) since zebrafish embryos rapidly absorb hydrophilic and lipophilic agents (Spitsbergen and Kent, 2003). Moreover, due to their optical clarity in the early stages of development, short lifespan, small size and frequent breeding, zebrafish are cost effective in the laboratory and many protocols have already been established to enable their use (Lessman, 2011; Spitsbergen and Kent, 2003). The zebrafish genome has also been thoroughly characterized (Helenius and Yeh, 2012), which have led to the discovery of novel gene functions for a number of human disease processes and disorders (Barros *et al.*, 2008; Amsterdam and Hopkins, 2006). Moreover, the CoQ10 biosynthesis pathways (Kyoto Encyclopedia of genes and genomes, 2012) as well as HMG-CoAR were found to be similar to those in mammals (Thorpe *et al.*, 2004). Therefore, the zebrafish is a well suited system for the study of the effects of waterborne statins on fish and the role of CoQ10 in mitigating statin-induced effects.

1.6. Hypotheses and Objectives of this Study

The hypothesis that I tested in this work was that ATV-exposed zebrafish embryos and adults would demonstrate cardiac and skeletal muscle damage and that this damage could be rescued by the addition of CoQ10. Given that ATV blocks the activity of HMG-CoAR, thereby blocking the production of CoQ10, it is predicted that reduction in CoQ10 synthesis will reduce localization of CoQ10 in the ETC of the mitochondria. This can lead to reduced proton gradient within the mitochondrial membrane. Given that the proton gradient is essential for ATP production, low CoQ10 will ultimately result in reduced ATP production. Thus, it is predicted that ATV will alter energy production and locomotor behaviours in larval and adult zebrafish. Spontaneous displacement in zebrafish larvae was previously demonstrated to be reduced as a result of a number of contaminant treatments including propranolol, clozapine, fluoxetine, melatonin, diazepam, and pentobarbital (Airhart *et al.*, 2007; Boehmler *et al.*, 2007; Fraysse *et al.*, 2006; Zhdanova *et al.*, 2001) suggesting that zebrafish are an appropriate model to test locomotor activity upon drug treatment for the early identification of potential pharmaceutical effects. If ATV reduces CoQ10, the mitochondrial membrane potential would decrease and ATP synthesis would decrease. As a result, enzyme activities that are recognized markers of oxidative capacity such as cytochrome oxidase and mitochondrial abundance such as citrate synthase would be reduced in ATV-exposed fish, leading to decreased tissue aerobic metabolism and to cytotoxicity that result in muscle atrophy (Lemasters *et al.*, 1999). Thus, it is predicted that ATV exposure will result in increased anaerobic enzyme activities as indicated by lactate dehydrogenase. Furthermore, it is predicted that ATV exposure will increase muscle atrophy markers including *atrogen-1* and *murf* mRNA abundance as well as depletion of the marker of mitochondrial biogenesis, *pgc-1α*.

The objectives of this study were to assess the physiological and behavioral responses to ATV exposure in the larvae and adult zebrafish *Danio rerio*. Toxicological endpoints in larvae such as the LC_{50} and LE_{50}, behavioral responses, tissue enzyme activities as well as transcript abundance were estimated to address the hypothesis. The specific objectives of this study were:

1) To assess toxicological endpoints including LC_{50} and EC_{50} in ATV-exposed embryos;
2) To assess larvae morphology and cardiac and skeletal muscle histology in ATV-exposed zebrafish;
3) To assess heart rate in ATV-exposed embryos and whether treatments of CoQ10 (PTS) or PTS (vehicle) rescues such effects;
4) To assess spontaneous displacement, response to tactile stimuli, tissue enzyme activities and changes in mRNA transcript abundance in ATV-exposed embryos and whether treatments with CoQ10 or PTS rescues such effects; and,
5) To assess swimming behavior, tissue enzyme activities and changes in mRNA transcript abundance in ATV-exposed adult zebrafish.

The overall goal of this thesis was to assess whether ATV was capable of inducing muscle damage and potentially threatening fish development, fecundity, and ultimately performance. Furthermore, the research will establish the role of CoQ10 in mitigating statin-induced cardiac and skeletal muscle damage in fish.

Chapter 2 – Materials and Methods

2.1. Chemicals

Atorvastatin (ATV) was a generous gift from Pfizer Inc. (Groton, CT, USA). The stock solution of ATV was prepared in dimethyl sulfoxide (DMSO, 10 mg mL^{-1}) and diluted to working concentrations in embryo medium (EM; 5 mmol L^{-1} NaCl, 0.17 mmol L^{-1} KCl, 0.33 mmol L^{-1} $CaCl_2$, 0.33 mmol L^{-1} $MgSO_4$, including 0.00001% methylene blue) or in tank water. Polyoxyethanyl-α-tocopheryl sebacate (PTS stock solution 150 mg mL^{-1} water) and CoQ10+PTS solution (50 mg mL^{-1}) were generous gifts from Dr. Jagdeep Sandhu, National Research Council (Ottawa, ON, Canada). All other chemicals were purchased from Sigma-Aldrich Chemical Co. (Oakville, ON, Canada) unless stated otherwise.

2.2. Fish

Wild-type adult zebrafish (*Danio rerio*) were obtained from a local supplier (AQUAlity, Mississauga, ON, Canada) and were maintained in the University of Ottawa Aquatic Facility. The fish were acclimated in 2.75 L plastic tanks under 14 h light:10 h dark photoperiod in an Aquatic Habitat Multi-Rack system (Apopka, FL, USA). Tanks were supplied with flowing 28^0C dechloraminated aerated city of Ottawa tap water. The fish were fed 12 mg/tank of food pellets containing 50% zebrafish complete diet (Zeigler™, Gardners, PA, USA), 25% Golden pearls (Artemia International LLC, McKinney, TX, USA) and 25% spirulina flakes (Ocean Star International Inc., Coral Springs, FL, USA) for a total of 1 mg/day/zebrafish (represents 5% of body weight daily). All experiments were approved by the University of Ottawa Protocol Review Committee and adhere to the guidelines established by the Canadian Council on Animal Care for the use of animals in research and teaching.

2.3. Experiments Using Zebrafish Embryos/Larvae

2.3.1. Embryo Collection

Adult zebrafish were collected from several holding tanks and distributed evenly among 1-L zebrafish breeding tanks (Aquatic Habitat, Apopka, FL, USA) between 3-4 pm. Pair-wise trap methods were employed in which 2 females and 1 male were placed in a breeding trap and were separated by a transparent divider that was removed at 9 am the following morning. Embryos were collected within one hour of spawning between 10-10:30 am. Embryos from several breeding traps were pooled and randomly assigned to glass petri dishes containing EM and were incubated at 28 ± 1 °C until separated into treatment groups.

2.3.2. Drug Exposure

Two separate embryo/larvae experiments were carried out. Experiment 1 assessed mortality to permit the calculation of a LC_{50} (lethal concentration at which 50% of the embryos died) and LE_{50} (effective concentration at which 50% of the embryos had edema in pericardial sac). The concentrations to which embryos and larvae were exposed ranged from 0.045 mg L^{-1} (1000x environmental concentration; Metcalfe *et al.*, 2003) to 7 mg L^{-1}. Experiments were performed on embryos collected from four separate breeding events that involved randomly breed adults as noted above (n = 4). Thirty-five embryos were transferred to each 5 cm glass petri dish containing 35 mL EM. Not every ATV concentration was tested for each breeding session, due to insufficient embryo numbers. The embryos were exposed to ATV starting at 2 hpf (hours post fertilization) for 4 days in a 28 ± 1°C incubator, with the EM and ATV dose renewed daily. The incidences of embryo/larval mortality and edema of the pericardial sac were assessed daily by inspection using a Leica WILD M10 light dissecting microscope (Leica Microsystems Inc., Concord,

ON, Canada) and dead embryos were removed. The 96 h LC_{50} and EC_{50} were calculated from these results.

Experiment 2 assessed the effects of ATV on heart rate, total displacement, response to a tactile stimulus, and the effect of CoQ10 (rescue experiments). Embryos were collected, maintained, and exposed as in Experiment 1. Heart rate, total displacement and response to a tactile stimulus were assessed at 96 hpf in ATV alone or in combination with CoQ10 (rescue experiment) or PTS (vehicle control). Larvae from each treatment group were collected for subsequent enzymatic and molecular analyses. Twenty five 96 hpf larvae from each treatment group were collected into a 1.5 mL conical centrifuge tubes representing one sample. The EM was removed using a plastic pasteur pipette and the larvae were immediately frozen in liquid nitrogen and stored at -80°C until analyzed.

2.3.3. Heart rate

The zebrafish heart beat is first detectable at 24 hpf and is an important indicator of health (Asharani *et al.*, 2008). Each larva was placed in a 9 mm diameter dish containing EM and allowed to acclimate for 2 min prior to video capture. In total 3 larvae per treatment per breeding session were assessed for a total of 4 breeding sessions (n = 4). The larval heart beat was recorded with a high speed camera (Grasshopper, Point Grey Research Inc., Richmond, BC) linked to a microscope (Leica MZ12.5, Meyer Instruments, Houston, TX, USA). Ten second recordings were taken and single frames were captured using a computer and analysed with Windows Live Movie Maker, Version 2011(Microsoft, Redmond, WA, USA). Video recordings were used to calculate the heart rate by counting the number of beats in a 10 s interval. The number of beats was then extrapolated to beats per minute. The average total of two recordings per larvae was taken.

2.3.4. Response to a tactile stimulus

The response of 96 hpf zebrafish larvae to tactile stimulation was examined according to Xi *et al.* (2010) with slight modifications. In total, 30 larvae per treatment per breeding session were assessed for a total of 4 breeding sessions (n = 4). Each larva was placed in a 9 mm petri dish and allowed to acclimate for 2 min. Larvae response to a tactile stimulus was assessed by a gentle touch using a needle to the tail of the larva. In total, two stimuli were applied to each larva. Immediate response was defined as responding to both stimuli, while delayed response was defined as responding to only one stimulus. Absence of response to both stimuli was defined as no response. Values are expressed as a percentage of larval response.

2.3.5. Spontaneous displacement

Zebrafish larvae spontaneous displacement was assessed according to methods described in Xi *et al.* (2010). Each larva was placed in a 9 mm diameter petri dish containing EM and allowed to acclimate for 2 min. In total, four larvae per treatment per breeding session were assessed for a total of 4 breeding sessions (n = 4). The larvae displacement was recorded for 2 min using a high-speed camera (Grasshopper, Point Grey Research Inc., Richmond, BC, Canada) linked to a microscope (Leica MZ12.5, Meyer Instruments, Houston, TX, USA). Single frames were captured onto a computer. Tracking was performed manually using Transparentizer (Fridgesoft, Konstanz, Germany) with Microsoft Paint (Microsoft, Redmond, WA, USA), in an attempt to trace the motion over the video in an image file. The spontaneous displacement of each larva was calculated using Mousotron (Blacksun Software, Turnhout, Belgium). Values are expressed as total displacement in centimeters and calculated as the mean + SEM.

In a follow-up experiment embryos/larvae were exposed for 96 h to ATV (0.5 mg L^{-1}) alone or in the presence of CoQ10 (4.5 mg L^{-1}) or PTS (vehicle control). After exposure the larvae were transferred into fresh EM for 24 h. The following day, total displacement of 120 hpf larvae was measured and plotted as described above.

2.3.6. TUNEL and ROS Assay

A separate experiment was conducted to assess the effect of ATV on apoptotic cells and reactive oxygen species. Adult zebrafish were bread and embryos were collected as noted above (see section 2.2.1). In total, 5 larvae per treatment per breeding session were assessed for a total of 3 breeding sessions (n = 3). Thirty five embryos were placed in a petri dish containing EM with ATV concentrations of 0, 0.045, 0.5, or 1 mg L^{-1}. Embryos were pre-treated with the inhibitor 1-phenyl 2-thiourea (PTU, 0.2 mM) throughout the experiment starting at 2 hpf to inhibit the expression of melanocytes in the growing embryo. At 96 hpf, images of the larvae were captured using a stereomicroscope (SMZ1500. Nikon Instruments Inc., Montreal, QC, Canada) connected to a high definition color camera head (DS-Fi1, Nikon Instruments Inc., Montreal, QC, Canada). Images were taken using NIS-Elements Microscope Imaging Software (Nikon Instruments Inc., Melville, NY, USA). These embryos/larvae were then used for TUNEL and reactive oxygen species (ROS) assays.

2.3.6.1. Reactive oxygen species (ROS) detection

The relative levels of ROS in zebrafish larvae were estimated using methods previously described in Wu *et al.* (2011). In brief, 5 PTU pre-treated larvae from each treatment group at 96 hpf were placed in a 1.5 mL conical centrifuge tube containing 1 mL of fresh EM. In total, 5 larvae per treatment per breeding session were assessed for a total of 3 breeding session (n = 3). Cell-permeable CM-H_2DCFDA (50 µg, Invitrogen, Eugene,

OR, USA) was dissolved in 50 µL of DMSO. From this stock solution, 1µL was added to each conical centrifuge tubes and incubated at room temperature (RT) for 2 h in the dark. After a series of washes in EM, embryos were examined on a stereomicroscope at 40x magnification.

2.3.6.2. TUNEL assay

Whole-mount PTU pre-treated larvae were fixed with 4% Paraformaldehyde (PFA) overnight at 4°C as previously described in Eisa-Beygi *et al.* (2013). The following day, samples were washed with Phosphate Buffered Saline with Tween 20 (PBST contains 3.2 mM Na_2HPO_4, 0.5 mM KH_2PO_4, 1.3 mM KCl, 135 mM NaCl, with 0.05% Tween 20, pH 7.4) three times for 5 min. Apoptotic cells were detected in whole-mount larvae using ApopTag® Peroxidase In Situ Apoptosis Detection Kit, according to the manufacturer's instructions (EMD Millipore, MA**,** USA). Briefly, tissues were digested with proteinase K (10 µg mL^{-1}) for 40 min at RT. Following tissue digestion, larvae were fixed with 4% PFA for 30 min at RT, and then washed five times for 5 min each. Equilibration buffer was applied to samples for 30 s, followed by application of working strength TdT enzyme (77% Reaction buffer, 33% TdT enzyme) and incubated overnight at 37°C. The following day, Stop/Wash buffer (1 mL Stop/Wash buffer in 34 mL water) was added. Once stop/Wash buffer was added, samples were rocked for 15 s then incubated at RT for 15 min. The tissues were then incubated with Anti-DIG peroxidase for 1 h at RT. Five PBST washes; 2 min each, preceded the addition of 1X working solution DAB Substrate (10X DAB/metal concentrate diluted with peroxide buffer, Roche) and incubated for 5 min at RT. The samples were then washed 5 times with PBST. Images were captured using a stereomicroscope at 40x magnification as above (*2.3.6.1*).

2.4. Experiments Using Adult Zebrafish

Zebrafish were purchased and maintained as above (see section 2.1) and were held in quarantine for 2 weeks. Adult zebrafish experiments were done on fish received from the same stock. Following the quarantine period, zebrafish (weight 387.9 ± 7 mg, n = 192) from multiple holding tanks were randomly assigned to treatment groups. Each trial took place for a period of 30 days and involved two treatment groups, control (DMSO) and an Atorvastatin (ATV) treatment at 0.045 mg L^{-1}. In total, four separate trials were carried out, with 24 fish per treatment group in each trial. Twelve fish were held in an 8 L tank at 28 ± 1^0C for the duration of the experiment (30 days) and were fed daily at 10 am except for the last day of the experiment. The fish were fed 12 mg/tank of food pellets containing 50% zebrafish complete diet (Zeigler™, Gardners, PA, USA), 25% Golden pearls (Artemia International LLC, McKinney, TX, USA) and 25% spirulina flakes (Ocean Star International Inc., Coral Springs, FL, USA) for a total of 1 mg/day/zebrafish (represents 5% of body weight daily). Adequate oxygenation was ensured using air stones and an air pump. The water and the dosing were renewed daily 30 min after feeding. In addition, pH (Combo pH & EC; HI 98129, HANA Instruments, Rhode Island, USA), O_2 (Alpha Probe; OxyGard®, Birkerod, Denmark), ammonia (Ammonia NuTrafin Test® A7820; Hagen®, QC, Canada), and total nitrite levels (Nitrite Nutrafin Test® A7825; Hagen®, QC, Canada) were monitored daily. The ATV dose was administrated directly to the tanks in tank water. Behavioural assessment and the exercise test were conducted prior to tissue collection. The fish were terminated with an overdose of tricane mesylate (ethyl 3-aminobenzoate methanesulfonate; Syndel Laboratories Ltd., B.C., Canada). Cardiac and skeletal muscle tissues were immediately collected and frozen in liquid nitrogen then stored at -80°C until analyzed. Tissues to be used for staining were fixed in PFA. A total of 4 zebrafish hearts

were pooled into one 1.5 mL conical centrifuge tube representing one sample. Skeletal muscle tissue was collected from the trunk region between the tail and anal fin as it contains both white and red muscle.

2.4.1. Swimming behavior

Behavioral traits for adult ATV-treated zebrafish were assessed according to Cachet *et al.* (2010). Each trial involved an ATV (0.045 mg L^{-1}) and a control group. In total, 15 fish per treatment group were assessed (n = 15). Trapezoidal 1.5 L fish tanks were filled with 1.25 L of 28 °C system water and set on a table 0.5 m away from a video recorder (SiMPLEFLiX; Slick VC-120, Southern Telcom, Brooklyn, NY, USA). The tank was surrounded by styrofoam sheets on three sides, to remove environmental cues that may affect fish behaviour; however, the top of the tank remained uncovered to allow adequate light (Fig. 2.1). The tank water was changed between each fish tested. The video recorder was turned on and a single fish was carefully netted and placed into this observation tank. The fish were videotaped for a total of 15 min and were left undisturbed during this period. Analysis of the videos involved manually tracking fish every 500 ms over the 15 min period using the data collection software Logger Pro® 3.8.6.1 (Vernier Software & Technology, Beaverton, OR, USA). An origin point was placed at the centre of the tank and all x, y, z coordinates were generated relative to this origin point. These coordinates were then uploaded to Matlab version 8.1.0.604 (R2013a) (MathWorks Inc., Natick, MA, USA) and Python version 2.7.3 (Pérez and Granger, 2007) using modules Numpy and Matplotlib. The Matlab program commands were written by Dr. John Lewis (Biology, uOttawa) and the Python program commands were written by PhD candidate Antony Dean St-Jacques. The commands are provided in Appendix A and B. The variables calculated were average speed, total displacement and maximum novel test speed.

2.4.2. Swim tunnel test

Each exercise trial involved the two groups, ATV (0.045 mg L^{-1}) and control (n=8 for each group, average body length 3.02 ± 0.04 cm). In total, 8 fish per treatment group were assessed. Fish were transferred from the 10 L glass experimental tank in 1 L of tank water and placed into the swim tunnel by gently pouring the water and fish into the swim tunnel. The Blazka-style swimming tunnel was constructed at the University of Ottawa and had dimensions of 39.8 cm (L) and 5.1 cm (D) (Fig. 2.2). Using a submersible suction pump (1/40 HP, 2 series, Little Giant), the water current was generated and the pump speed was controlled by a variable transformer (Staco Energy Product, 120V input, Dayton, OH). Using a turbine-type flow meter (Onicon Inc., Fish pond F-1100, Clearwater, FL), a calibration curve relating voltage and water velocities was generated by plotting the absolute water velocities corresponding to each voltage increments (Fig. 2.2). This calibration curve was then used to calculate the swimming speed for each experiment. Once a fish was placed into the tunnel, it was acclimated for 5 min and then subjected to a velocity of 4 cm s^{-1} for 2 min, the velocity was then increased with increments of 2 cm s^{-1} at 1 min intervals, until the fish fatigued. Fatigue was defined as the point when the fish could no longer maintain its position against the current and was swept against a mesh screen downstream within the tunnel. Once the fish could no longer remove itself from the screen within 10 s, the swimming test was terminated.

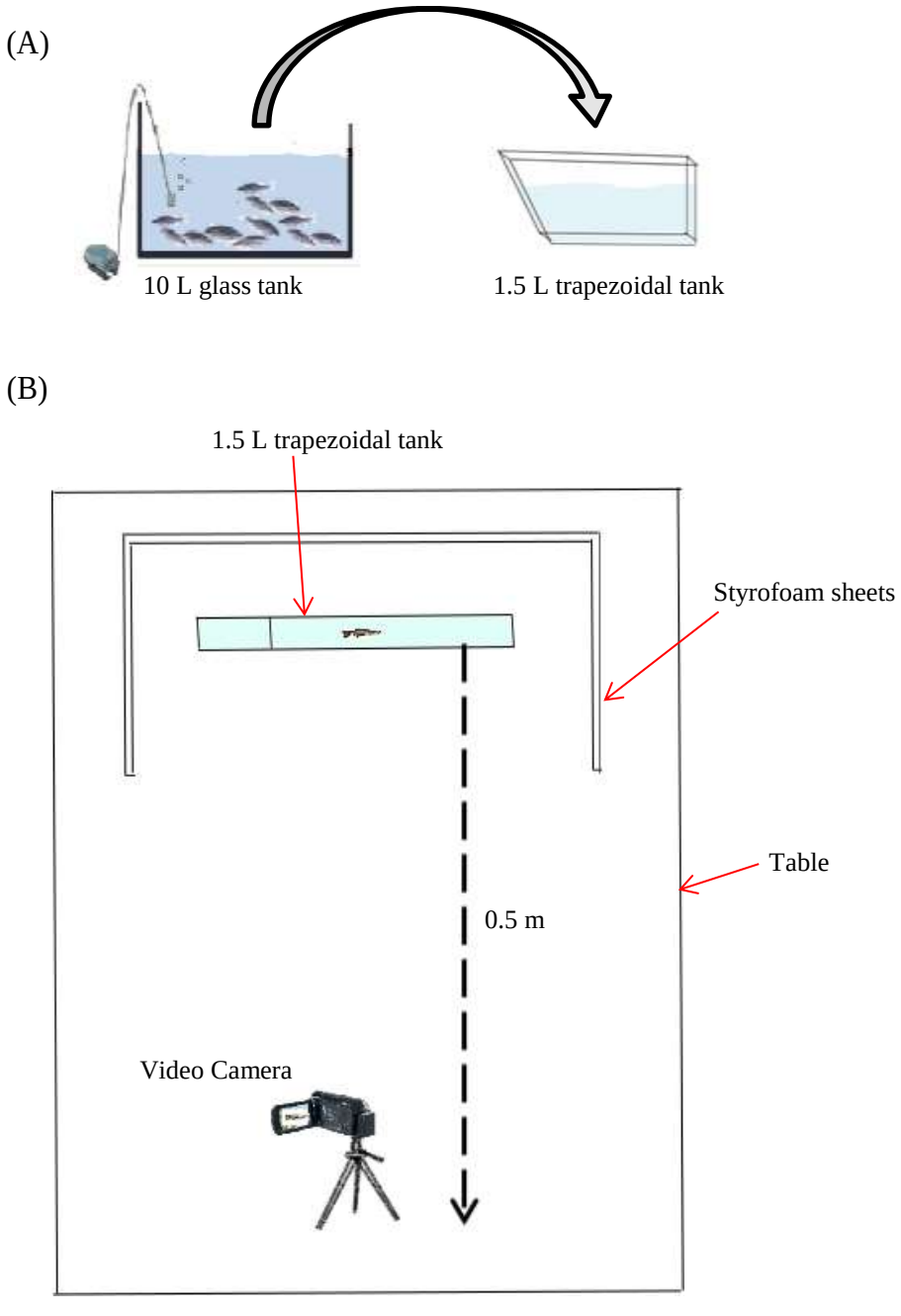

Figure 2.1: Novel tank test experimental setup. (A) A single adult zebrafish, control (DMSO) or ATV- treated for a period of 30 days, was net transferred into the 1.5 L trapezoidal tank where it was videotaped for 15 min. (B) The novel tank was located on a table facing a video camera 0.5 m away. A bird's-eye view.

(A)

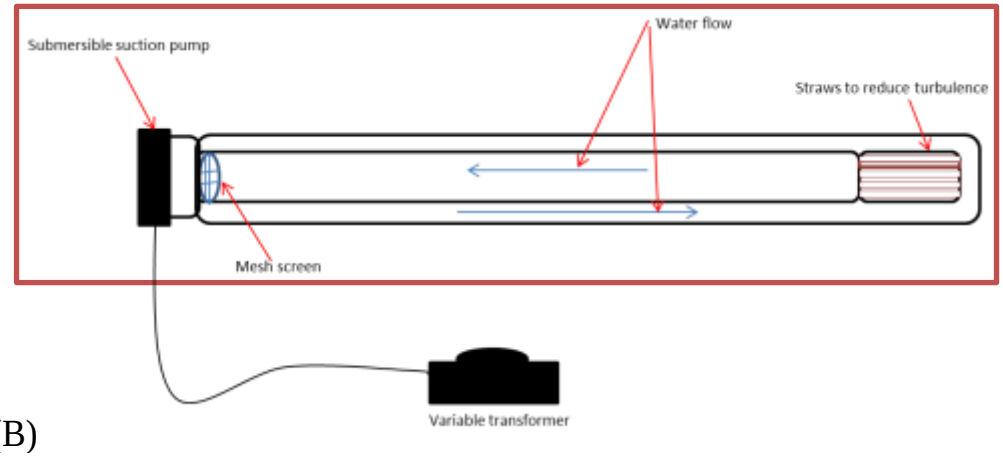

(B)

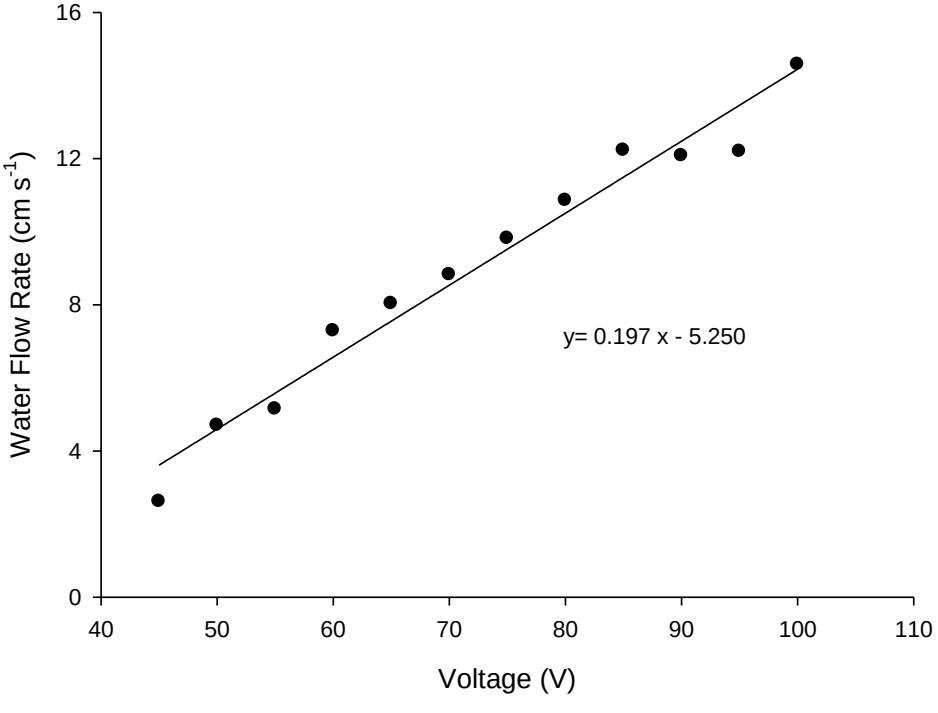

Figure 2.2: (A) Swimming test experimental set-up that was held in a large box filled with water to maintain constant temperatures at 28°C. A single adult zebrafish, control (DMSO) or ATV-treated for a period of 30 days, was transferred into the swim tunnel where water velocity was increased using variable transformer.(B) Calibration curve that was generated and used to calculate the swimming speed for swim tunnel test.

2.4.3. Staining and Tissue Histology

Cardiac and skeletal muscles were fixed with 4% PFA overnight at 4°C (Eisa-Beygi *et al.*, 2013). The following day, tissues were incubated for 1 h at RT in 15% sucrose. Tissues were then transferred to 30% sucrose and kept overnight at 4 °C. The next day, tissues were embedded in optimal cutting temperature compound (OCT) and frozen at -20 °C prior to sectioning. Tissues were sectioned (10 µm) using a microtome (CM 1850, Leica Microsystems; Concord, ON, Canada) and transferred to silane-coated slides to dry. These slides were then used for hematoxylin and eosin staining and TUNEL assay.

2.4.3.1. Hematoxylin and eosin staining

Hematoxylin and eosin staining was performed according to methods previously described in Kiernan (1999). Briefly, prepared slides were placed in Mayer's haemalum (193.6 mM aluminum potassium sulphate, 3.3 mM haematoxylin, 0.505 mM sodium iodate, 5.2 mM citric acid and 0.302 M chloral hydrate) for 3 min, the slides were then rinsed with distilled water for a few seconds followed by tap water for 5 min. Slides were placed in acid-alcohol (70% ethanol and 1% HCl) for 10 s and washed twice with tap water for 1 min, followed by a wash with distilled water for 2 min. Following the rinse, slides were placed in Eosin (12.05 mM eosin Y and 0.16% glacial acetic acid) for 30 s. Once the slides were differentiated they were rinsed again in running tap water, and then dehydrated in 70%, 95% and twice in 100% ethanol (EtOH) for 3 min each. Lastly, slides were placed in xylene for 2 min. Images were captured using a stereomicroscope at 40x magnification (SMZ1500, Nikon Instruments Inc.; Montreal, QC, Canada) connected to a high definition color camera head (DS-Fi1, Nikon Instruments Inc.). Images were captured using NIS-Elements Microscope Imaging Software (Nikon Instruments Inc., Melville, NY, USA).

From the images, cell size in red and white muscle was assessed in treated and control and plotted for statistical analysis (Fig. IV).

2.4.3.2. TUNEL Assay

Cardiac muscle from control and ATV-treated adult zebrafish was fixed with 4% PFA overnight at 4 °C. Staining followed methods described above (section *2.3.6.2.*). Cardiac muscle samples were sliced to 10 µm thick using a microtome (CM 1850, Leica Microsystems) and transferred to silane-coated slides. Photos were captured as mentioned above (see section *2.4.3.1*).

2.5. Enzyme Activities

Adult zebrafish skeletal and cardiac muscle samples were grounded individually with a mortar and pestle in liquid nitrogen to keep the sample frozen during grinding. They were then transferred to 1.5 mL conical centrifuge tubes, and placed on ice. Zebrafish larvae samples were homogenized in 10 vol of imidazole buffer (50 mM, pH 7.5), while cardiac and skeletal muscle samples were homogenized in 250 µL of the same buffer using a ground glass tissue homogenizer. All enzyme activities were carried out using 96-well plates and assessed using a SPECTRAmax Plus Spectrophotometer (Molecular Devices, Sunnyvale, CA, USA) at 25 °C. The enzyme activities (in µmol mg of protein^{-1} min^{-1}) were assessed using the SOFTmax Pro software of the plate reader. Cytochrome c oxidase (COX; EC 1.9.3.1), citrate synthase (CS; EC 2.3.3.1) and lactate dehydrogenase (LDH; EC. 1.1.1.27) were assayed as previously described (McClelland *et al.* 2005). The assay for COX was carried out immediately after homogenization, whereas the homogenates were frozen at – 80 °C prior to analyses of the other enzymes. All enzyme activities are reported based on protein concentrations assessed using the bicinchoninic acid (BCA; Sigma

Chemical Co.) assay method and bovine serum albumin (BSA) as a standard (Fig. I, II & III).

2.5.1. Cytochrome oxidase (COX) (E.C. 1.9.3.1)

The COX activity was assessed within 60 min following preparation of the reduced cytochrome c solution. Cytochrome c solution was prepared as previously described (Spinazzi *et al.*, 2012). In brief, 1 mM reduced cytochrome c was prepared by dissolving oxidized cytochrome c in 20 mM of potassium phosphate buffer (20 mM K_2HPO_4 and 20 mM KH_2PO_4, pH 7.0) followed by adding a few grains of sodium dithionite. A ratio of the absorbance values at 550 nm versus 565 nm greater than 6 indicated effective cytochrome c reduction.

Sample homogenates (10 µL) were added to a 100 µL mixture of Tris-HCl (20 mM, pH 8.0) and 0.5% Tween incubated at 28 °C for 10 min, followed by addition of 100 µL Tris-HCl (20 mM, pH 8.0), 0.5 % Tween and reduced cytochrome c (100 µM). The plate was shaken and the absorbance a 550 nm was followed for up to 5 min. Enzyme activity was adjusted to enzyme blanks and substrate was calculated based on extinction coefficient of reduced cytochrome C 28.5 mM^{-1} cm^{-1}.

2.5.2. Citrate synthase (CS) (E.C. 2.3.3.1)

Samples were thawed on ice and 10 µL were added to a mixture of Tris-HCl (50 mM, pH 8.0), Acetyl-CoA (0.3 mM), 5, 5′-dithiobis-(2-nitrobenzoic acid) (0.1 mM). Activities were followed after the addition of oxaloacetate (0.5 mM) and the increase in absorbance at 412 nm was followed for up to 30 min. Enzyme activity was calculated as above (section 2.5.1) using the extinction coefficient of DTNB 13.6 mM^{-1} cm^{-1}.

2.5.3. Lactate dehydrogenase (LDH) (E.C. 1.1.1.27)

LDH activity was assayed as previously described (McClelland *et al.,* 2005) with a simple modification. In brief, samples were thawed on ice and sample homogenates (2.5 µL) were added to a mixture of 100 µL imidazole buffer (50 mM, pH 7.0) that contained 10 µL NADH (0.35 mM). This was followed by the addition of 10 µL pyruvate (4.5 mM) and the decrease in absorbance at 340 nm were followed for up to 30 min. Enzyme activity was calculated as above (see 2.5.1) using the extinction coefficient of NADH 6.22 mM^{-1} cm^{-1}.

2.6. Molecular Procedures

2.6.1. RNA extraction

Adult zebrafish skeletal and cardiac muscle samples were grounded individually with a mortar and pestle in liquid nitrogen to keep the sample frozen during grinding. They were then transferred to 1.5 ml conical centrifuge tube, and placed on ice. Zebrafish embryo, adult skeletal and cardiac muscle sample total RNA was extracted using TRIzol reagent (Invitrogen, Carlsbad, CA, USA) according to manufacturer's protocol. One mL TRIzol reagent was added to each tube and sonicated on ice with a Kontes microultrasonic cell disruptor. The sonicator was rinsed with 70% ethanol and distilled water and was dried thoroughly with a Kimwipe between each sample. Following sonication, 0.5 mL chloroform was added to each tube and shaken vigorously for 15 s. The samples were left to sit at RT for 5 min before being centrifuged at 12,000 g, 4 °C for 15 min. The supernatant was transferred to a new RNAase-free tube and 1 mL isopropanol was added. The tubes were inverted 5 times and left to sit at RT for 10 min. The tubes were then centrifuged at 12,000 g, 4°C for 15 min. The isopropanol was removed from each tube

using a plastic transfer pipette, and the pellets were rinsed with 1 mL 75% ethanol followed by centrifugation at 7500 g, 4°C for 5 min. The ethanol was removed and the samples were washed again with 1 mL 75% ethanol and centrifuged at 7500 g, 4°C for 5 min. As much of the ethanol was removed as possible and then the samples were left to air dry for 4 min in a fume hood. Samples were suspended in 20-60 µL RNAase-free water depending on the size of the RNA pellet present then incubated at 60 °C for 10 min. Total RNA quantity and quality were assessed using the Nanodrop ND-1000 (Fisher Scientific, Wilmington, DE, USA). The RNA quality was verified using 1.5% agarose gel electrophoresis.

2.6.2. cDNA synthesis

cDNA was synthesized from equal concentrations of template RNA (1 µg) using QuantiTect® Reverse Transcription Kit (Qiagen, Valencia, CA, USA) according to manufacturer's protocol. gDNA Wipeout Buffer, Quantiscript RT buffer, RT Primer mix, and RNase-free water were thawed at RT, while Quantiscript® Reverse Transcriptase was thawed on ice. Prior to cDNA synthesis, a total reaction volume of 14 µL was obtained for the genomic DNA elimination reaction in which it contained 1 µg template RNA, 2 µL 7x gDNA Wipeout Buffer and the appropriate amount of RNase-free water. The samples were then incubated at 42 °C for 2 min. Following incubation, tubes were placed immediately on ice. A master mix of reverse-transcription master mix (1 µL), Quantiscript RT Buffer, 5x (4 µL), and RT primer mix (1 µL) was made and from this 6 µL were aliquoted into each sample tube previously containing the 14 µL template RNA from the genomic DNA elimination reaction. The samples were incubated for 15 min at 42 °C then inactivated at 95 °C for 5 min. Following the incubation and inactivation steps, the samples were placed on ice. Samples were diluted 1:5 by adding 80 µL UltraPure water to each tube containing 1st

strand cDNA. cDNA that was to be used as real-time PCR standard curves were diluted to 4x, 16x, 64x and 256x by adding 45 µL UltraPure water to 15 µL of 1st strand cDNA. Using the 4x standard curve cDNA, a serial dilutions was performed to make the 16x, 64x and the 256x respectively.

2.6.3. Quantitative real-time PCR (qPCR)

mRNA transcript abundance was assessed in duplicate on a Rotor-Gene Q (Qiagen, Valencia, CA, USA) real-time PCR machine by using a Rotor-Gene™ SYBR® Green PCR Master Mix(Qiagen, Valencia, CA, USA). Data analysis as well as melting curve analysis to verify the PCR products were conducted using Rotor-Gene Q software (Version 2.0.3, Model: 2-Plex HRM, Valencia, CA, USA). Each reaction contained 5 µL SYBR® Green mix, 1 µL of each forward and reverse primers (1 µM), 2 µL RNase/DNase-free H_2O, and 1 µL cDNA template. Cycling conditions were as follows: 5 min initial denaturation at 95 °C (DNA polymerase activation), 40 cycles of 95 °C for 5 s (denaturation), and 60 °C for 10 s (annealing). Standard curves were constructed for each gene using a serial dilution of 1x cDNA of the stock cDNA as described above to account for differences in amplification efficiencies in samples. All samples were normalized using NORMA-gene (Macro V1.1) to the expression level of the β-actin and Ef1α mRNAs. Both a water and no-template cDNA were assayed to ensure there was no contamination present. Primers were designed using Invitrogen primer design software (OligoPerfect™ Designer) and targets were verified by gel electrophoresis. Target genes of interest and primers used are found in Table 2.1.

Table 2.1: Primer sequences used for qPCR analysis of mRNA expression in zebrafish.

Gene	Accession number	Primer	Sequence (5' to 3')	Amplicon size (base pairs)
		FORWARD	GTCAGTCTGGGTCAAGTGTG	
atrogin-1[1]	(NM_200917)	REVERSE	AAGAGGATGTGGCAGTGTG	233
		FORWARD	TGAGGAAAATGAGGCCAACT	
pgc-1α	(FJ710604)	REVERSE	AGCTTCTTCAGCAGGGAAGG	198
		FORWARD	CCTGGCTTTGAGAGTATGGACC	
murf	(BC071428)	REVERSE	GCCCCTTGCCTCACAGTTAT	225
		FORWARD	TGAATCCCAAAGCCAACAGAG	
b-actin[2]	(AF057040)	REVERSE	CCAGAGTCCATCACAATACCAG	139
		FORWARD	GTGCTGTGCTGATTGTTGCT	
ef1α[2]	(AY422992)	REVERSE	TGTATGCGCTGACTTCCTTG	201

[1]*atrogin-1* was taken from Al-Hebsi (2012). [2]*b-actin* and *ef1α* will be used as a housekeeping gene (LeMoine and Walsh, 2013).

2.7. Statistical Analysis

Statistical analyses and graphs were generated using SigmaPlot, Version 11.0 (Systat Software Inc., San Jose, CA, USA). All experimental results are presented as means ± standard error of the mean (SEM). Statistical significance between treatments for the adult zebrafish behavioral analyses, enzyme activities, enzyme ratios and mRNA transcript abundance was assessed using a one-way ANOVA with Tukey's post hoc test. Spontaneous swimming displacement of 120 hpf larvae was analyzed using a one-way ANOVA with Tukey's post hoc test to compare results between treatment and control groups. Larval rescue experiments for enzyme activities, mRNA transcripts, response to tactile stimulus, total spontaneous displacement, heart rate, and percent edema in pericardial cavity were assessed using a two-way ANOVA with Holm-Sidak post-hoc test. The two factors were treatment and ATV concentrations. $P < 0.05$ was considered significant in all cases. Some two-way ANOVA with Holm-Sidak post-hoc test did not meet the assumption of normality and/or equal variance; however, this is unlikely to have an impact since generally p-values were smaller than 0.001.

Chapter 3 – Results

3.1. Zebrafish embryos/larvae

3.1.1. Effects of ATV on mortality, pericardial sac edema, and heart rate

Zebrafish embryo mortality was significantly increased by ATV exposure at concentrations ≥ 3 mg L^{-1} in a dose-dependent manner (Fig. 3.1A). Using Probit analysis, the calculated LC_{50} value at 96 hpf was 3.30 mg L^{-1} (Fig. 3.1B). Sub-lethal ATV concentrations ≥ 1 mg L^{-1} significantly increased the incidence of pericardial sac edema in a dose-dependent manner in 96 hpf larvae (Fig. 3.2A) with a calculated LE_{50} value of 1 mg L^{-1} (Fig. 3.2B). Based on this LE_{50} and the fact that mortality was not affected at this ATV concentration, 1 mg L^{-1} was chosen as the highest concentration for all subsequent embryo/larvae experiments, which examined ATV toxicity in more details. In these subsequent experiments there were no detectable changes observed in larval morphology; length were similar across the treatment groups (Fig. 3.3). Treatment with CoQ10 was unable to decrease the incidence of pericardial sac edema in larvae exposed to 1 mg L^{-1} ATV; in fact, there was a significant increase at that dose compared to larvae treated with ATV alone (Fig. 3.4). Treatment with the vehicle (PTS) showed a similar pattern to the larvae treated with ATV alone.

Given the higher incidence of pericardial sac edema in ATV-exposed larvae, the larval heart rate was also assessed as it is an important indicator of health (Asharani *et al.*, 2008). The larval heart rate at 96 hpf was not significantly affected by ATV exposure, although there was a trend towards a decrease in the heart rate with increased concentrations of ATV (Table 3.1). Furthermore, heart rate was altered by treating larvae with CoQ10 and the vehicle control (PTS). A two-way ANOVA indicated a difference

between treatments with CoQ10 and vehicle control (PTS) compared with the ATV treatment alone; however, a Holm-Sidak post-hoc test could not identify exactly where these differences occurred (Table 3.1).

3.1.2. Effects of ATV on locomotor behavior

Spontaneous movement and the response to tactile stimuli can be observed and easily assessed during early larval stages (Granato *et al.*, 1996). Thus the effects of ATV on larval locomotor behavior were assessed to further examine ATV-mediated toxicity and the potential role of CoQ10 on these effects. Spontaneous displacement of 96 hpf larvae was significantly decreased by ATV exposure at all ATV concentrations assessed and at ATV concentrations of 0.5 and 1 mg L^{-1}, spontaneous displacement was absent (Fig. 3.5). This was also true of larvae exposed to ATV in the presence of CoQ10 or only the vehicle control (PTS) (Fig. 3.5B).

To address whether the absence of spontaneous movement was a result of unidentified drug interactions, a follow-up experiment was conducted. Embryos/larvae were exposed from 2 hpf to ATV (0.5 mg L^{-1}) alone or in the presence of CoQ10 (4.5 mg L^{-1}) or PTS until 96 hpf, and then reared in fresh EM without additions for an additional 24 h. Similar to the above results, there was a significant decrease in spontaneous displacement of larvae that were treated with ATV in the presence or absence of CoQ10 or PTS (Fig. 3.6).

A second experiment to assess any ATV-mediated locomotor affects used responses to tactile stimuli. In total, two stimuli were applied using a needle to each larva and responses noted. Response to tactile stimuli in 96 hpf larvae was significantly decreased in ATV-treated larvae in a dose-dependent manner. There was a decrease in the

incidence of ‘complete response’ (i.e. response to both stimuli) and a corresponding dose-dependent increase in the incidence of ‘no response’ (i.e. no response to either stimuli) starting at 0.045 mg L^{-1} ATV (Fig. 3.7A). Interestingly, CoQ10 treatment abolished the ATV effects on the tactile response as indicated by the exposed larvae not differing from their respective control counterparts (Fig. 3.7B). Moreover, the impact of ATV on the larval response to tactile stimuli was also reduced in the presence of the vehicle PTS; however, there remained significant ATV-associated effects, but not to the same extent as in the ATV group (Fig. 3.7C).

3.1.3. Reactive oxygen species (ROS) generation and apoptosis

ROS generation and apoptosis were evaluated in larvae to assess whether any of the ATV-mediated effects were associated with ROS generation or programmed cell death. Evaluation of ROS generation between treatments was based on previous study by Massarsky et al. 2013. No discernible changes were observed in either ROS generation (CM-H_2DCFDA staining, Fig. 3.8) or apoptosis cell counts (TUNEL staining, Fig. 3.9) in ATV-treated and control embryos.

3.1.4. Effects of ATV on enzyme activities associated with oxidative capacity and mitochondrial function

De Pinieux *et al.* (1996) reported that patients treated with lovastatin, simvastatin, pravastatin, or fluvastatin had an increased lactate to pyruvate blood serum ratio. The authors suggested that the increase in this ratio is indicative of a shift toward anaerobic metabolism in the presence of statins. To test whether this occurred in ATV-treated zebrafish larva, enzyme activities of cytochrome oxidase (COX), citrate synthase (CS), and lactate dehydrogenase (LDH) were assessed in whole 96 hpf larval extracts. Activities of

COX, CS, and LDH were significantly decreased starting at an ATV concentration of 0.5 mg L^{-1} (Fig. 3.10). COX activities were fully recovered in the presence of CoQ10 and PTS; however only PTS recovery was significant (Fig. 3.10A). Similarly to COX, whole-body CS activity was fully recovered with CoQ10 and PTS treatments and in fact, activities in the presence of CoQ10 or PTS were significantly higher than in the ATV group (Fig. 3.10B). LDH activities were fully recovered with CoQ10 and PTS treatments, and at the highest ATV concentration (1 mg L^{-1}) in the presence of CoQ10 the activity was significantly increased compared with 1 mg L^{-1} ATV treatment alone (Fig. 3.10C).

3.1.5. Effects of ATV on molecular markers of muscle atrophy

Given that ATV-associated muscle damage was reported in previous studies (see Introduction for details), molecular markers of muscle atrophy (*atrogen-1*, *murf* and *pgc-1α*) were evaluated in 96 hpf zebrafish larvae following ATV exposure. The transcript abundance of *atrogen-1* was differentially affected by ATV exposure, such that it was significantly increased at ATV concentrations of 0.045 and 1 mg L^{-1}, but significantly decreased at 0.5 mg L^{-1} relative to the DMSO control group. This trend was also apparent in the presence of CoQ10, however at an ATV concentration of 1 mg L^{-1} there was a significantly increased abundance compared with the ATV treatment alone (Fig. 3.11A). Moreover, in the presence of ATV + PTS there was a significant increase in *atrogen-1* mRNA abundance at an ATV concentration of 1 mg L^{-1} and a significant decrease at ATV concentration of 0.045 mg L^{-1} compared to the ATV treatment group (Fig. 3.11A).

The transcript abundance of *murf* was also differentially affected. Although there were no significant differences within the ATV or CoQ10 treatment groups, there was an increase in presence of PTS. Moreover, there was a significant effect of treatment at 1 mg

L^{-1} ATV, such that *murf* mRNA abundance was significantly higher in CoQ10 and PTS treatments compared to the ATV group. Also, at 0.5 mg L^{-1} ATV, ATV + PTS significantly increased *murf* transcript abundance compared to their CoQ10- or ATV treated counterparts (Fig. 3.11B).

The transcript abundance of *pgc-1α* mRNA was significantly increased at ATV concentrations of 0.045 mg L^{-1} and decreased at ATV concentrations of 0.5 and 1 mg L^{-1}. Within the larvae that were treated with ATV and CoQ10, *pgc-1α* transcript abundance was significantly increased at an ATV concentration of 0.45 mg L^{-1} and significantly decreased at ATV concentration of 0.5 and 1 mg L^{-1}. However, the *pgc-1α* abundance at 0.045 mg L^{-1} ATV within the ATV + CoQ10 treatment group was significantly increased compared with the ATV and ATV +PTS groups. Moreover, within the larvae that were treated with ATV + PTS, *pgc-1α* abundance was significantly decreased at ATV concentrations of 0.45, 0.5 and 1 mg L^{-1}. The *pgc-1α* abundance at ATV concentration of 0.045 mg L^{-1} within ATV + PTS treatment was significantly decreased compared with the ATV group (Fig. 3.11C).

3.2. Effects of ATV on Zebrafish Adults

3.2.1. Effects of ATV on mortality

Treating adult zebrafish with an ATV concentration of 0.045 mg L^{-1} for 30 days resulted in no mortalities. Thus, this ATV concentration was not toxic to adult zebrafish.

3.2.2. Effects of ATV on adult behavior

Given that ATV exposure altered larval locomotor behaviors, a number of standard behavioral traits were also evaluated in adult zebrafish. There were no significant differences in the average speed, maximum speed, maximum swimming speed, and total displacement between control and ATV-treated zebrafish (Fig. 3.12).

3.2.3. Effects of ATV on muscle histology and apoptosis

The general structure and morphology of the skeletal muscle was assessed using hematoxylin and eosin staining. Preliminary results from one fish show no significant changes in cell size in red and white muscle from ATV-treated fish compared with the controls (Fig. 3.13C, D, F and G). However, treated zebrafish skeletal muscle cells appear to have gaps consistent with previous findings on rat skeletal muscle demonstrating gap formation as a result of ATV treatment (Elhaleem and Elsayed, 2011) (Fig. 3.13). Given the higher cell turnover in the cardiac muscle, it was used for the apoptosis assay. There were no significant changes in the number of apoptotic cells in the cardiac muscle (Fig. 3.14).

3.2.4. Effects of ATV on enzyme activities associated with oxidative capacity and mitochondrial function

Previously I demonstrated that ATV exposure reduced whole-body enzyme activities of COX, CS, and LDH in larval zebrafish. To establish whether ATV exposure would affect the activities of these enzymes in adults, these same enzymes were assayed in cardiac and skeletal muscles of adult zebrafish. ATV significantly increased COX activities in skeletal muscle but not cardiac muscle, whereas the activity of CS was significantly decreased in both cardiac and skeletal muscles (Fig. 3.15). The activity of LDH was not affected in either muscle type. The aerobic to anaerobic enzyme activity ratio was also evaluated in both muscles to assess whether ATV exposure results in a shift toward anaerobic metabolism as previously described in patients (Thompson *et al.*, 2003). There was a significant decrease in the CS:LDH ratio for cardiac and skeletal muscles compared

to control. However, the COX:LDH ratio significantly increased in skeletal muscle, but not in cardiac muscle (Fig. 3.16).

3.2.5. Effects of ATV on molecular markers of muscle atrophy

Similar to larval zebrafish, the markers of muscle atrophy were assessed in the adult zebrafish after a 30 d exposure to 0.045 mg L^{-1} ATV. There were no significant differences in mRNA transcript abundance of *atrogen-1*, *murf,* and *pgc-1α* in the skeletal muscle (Fig. 3.17A). However, there was a significant decrease in transcript abundance of *atrogen-1*, *murf,* and *pgc-1α* in the cardiac muscle (Fig. 3.17B).

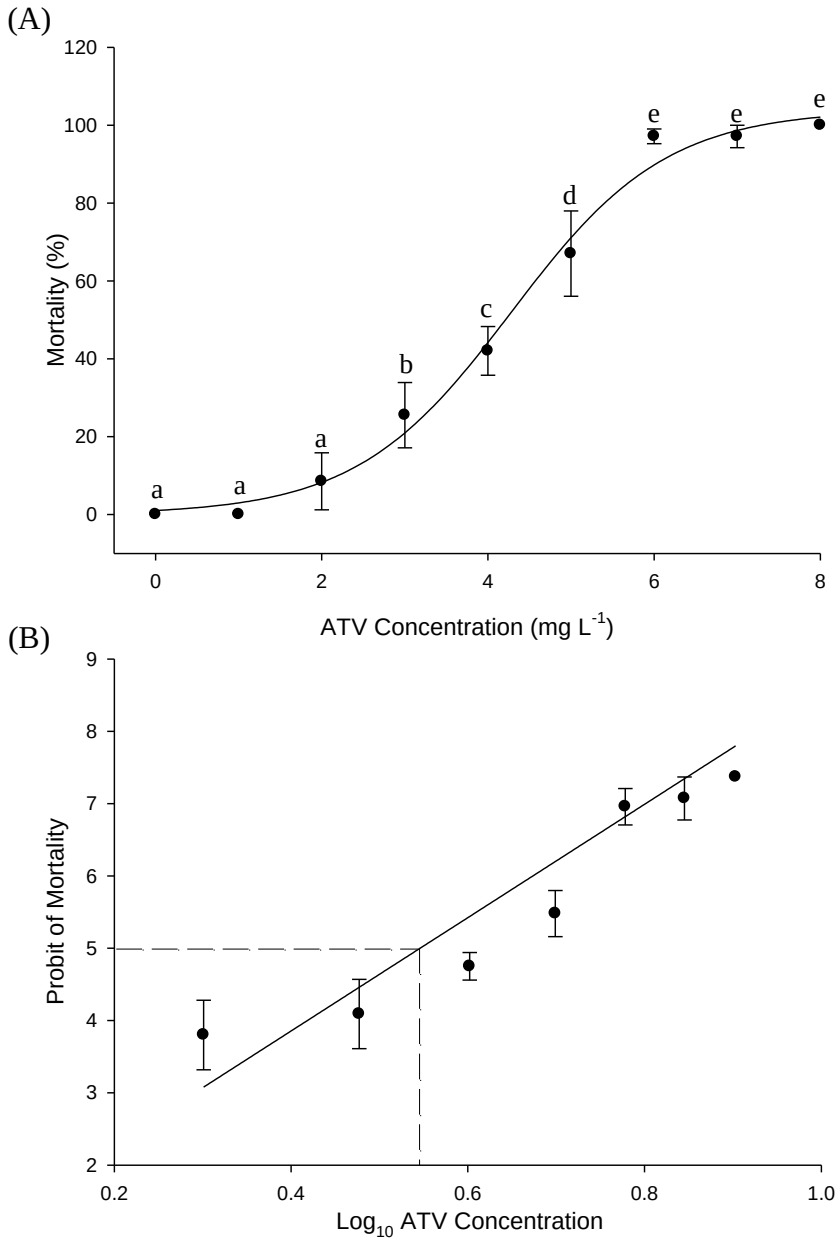

Figure 3.1: (A) Percent mortality of zebrafish larvae at 96 hpf after a continuous exposure (from 2 hpf) to a range of ATV concentrations. (B) Probit analysis of the mortality data (A). Different letters indicate significant differences assessed using one-way ANOVA followed by a Tukey's pair-wise multiple comparison test ($p < 0.05$ was considered significant). The extrapolated LC_{50} (Probit value of 5) is indicated by a dashed line corresponding to an ATV concentration of 3.3 mg L^{-1}. In both panels the data are presented as means ± SEM (n = 4 breedings for each ATV concentration).

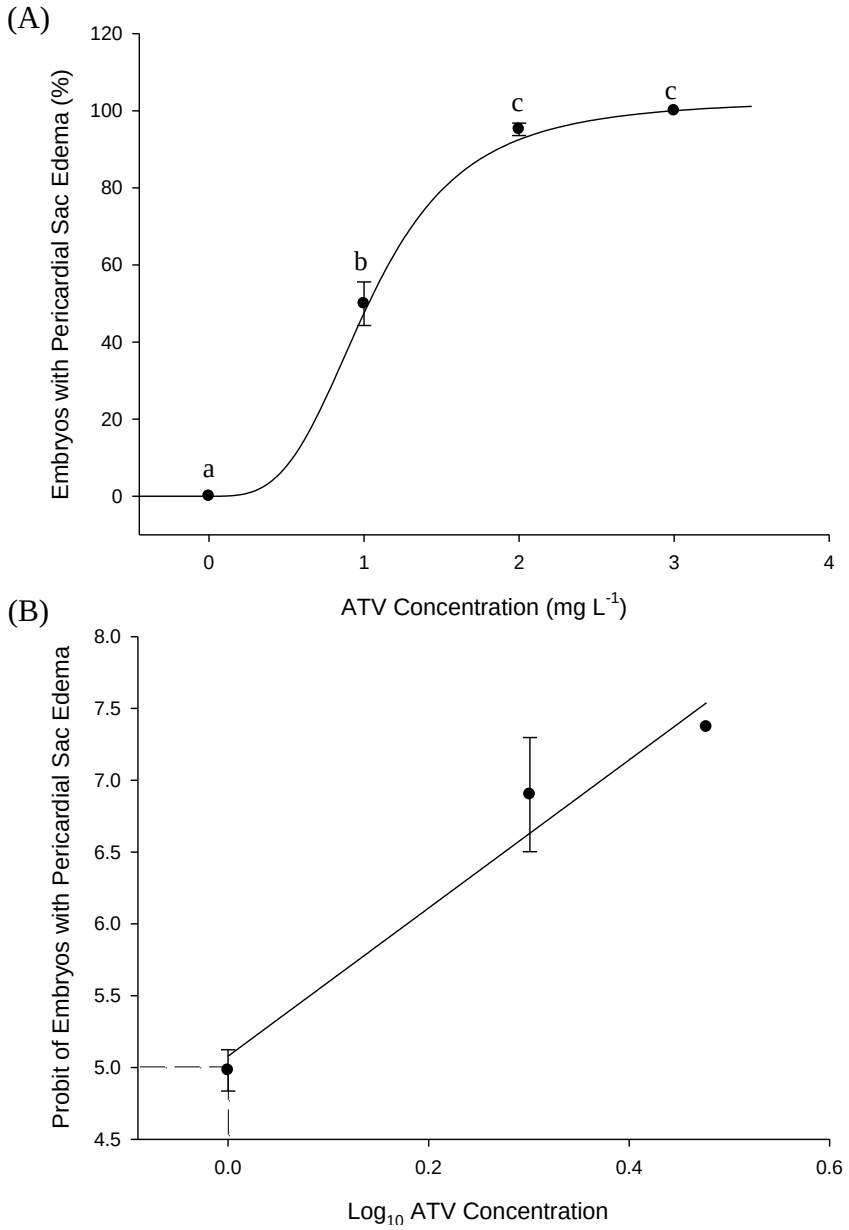

Figure 3.2: (A) Percent of pericardial sac edema in zebrafish larvae at 96 hpf after a continuous exposure (from 2 hpf) to a range of ATV concentrations. (B) Probit analysis of data in (A). Different letters indicate significant differences assessed using one-way ANOVA followed by a Tukey's pair-wise multiple comparison test ($p < 0.05$). The extrapolated LE_{50} (Probit value of 5) is indicated by a dashed line corresponding to an ATV concentration of 1 mg L^{-1}. In both cases the data are presented means ± SEM (n = 4 breedings for each ATV concentration).

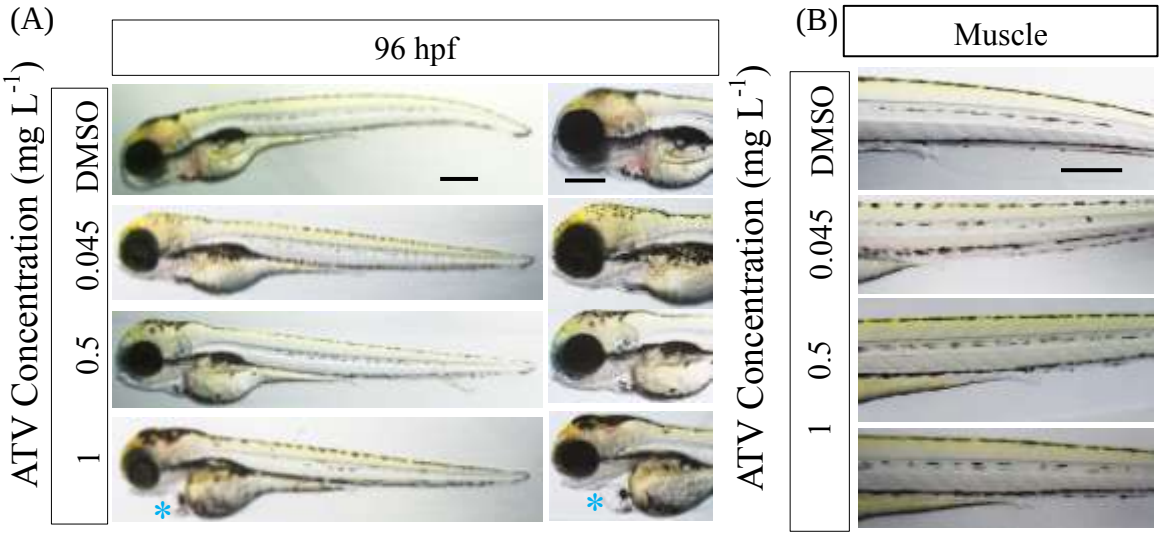

Figure 3.3: Representative photomicrographs of 96 hpf zebrafish larvae after a continuous exposure (from 2 hpf) to various ATV concentrations. (A) Overall larval morphology, and an enlarged image of the head region. The asterisk (*) denotes presence of pericardial sac edema. (B) Tail region of the corresponding larvae from panel A. Scale bar: 2 mm.

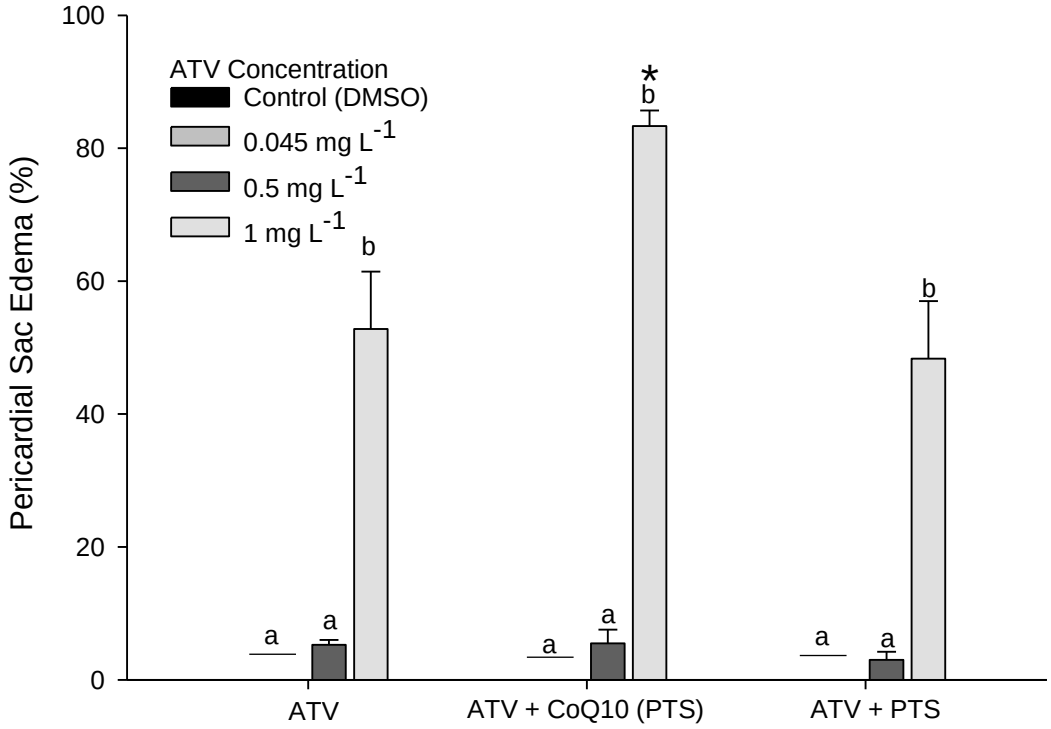

Figure 3.4: Percent pericardial sac edema observed in zebrafish larvae at 96 hpf after a continuous exposure (from 2 hpf) to three ATV concentrations with or without CoQ10 (4.5 mg L^{-1}) or vehicle (PTS; same amount as in CoQ10 treatment). Data are presented as means + SEM (n = 4 breeding for each ATV concentration). Different letters indicate statistical differences among various ATV concentrations within the same treatment group; the asterisk (*) denotes statistical differences within the same ATV concentration among treatment groups. A two-way ANOVA followed by a Holm-Sidak post-hoc test was used ($p < 0.05$ was considered significant).

Table 3.1: Heart rate of 96 hpf zebrafish larvae that were continuously exposed (from 2 hpf) to three ATV concentrations with or without CoQ10 (4.5 mg L^{-1}) or vehicle (PTS). Data are presented as means ± SEM in brackets (n=4 breeding for each ATV concentration). A two-way ANOVA indicated significant differences among treatment; however the Holm-Sidak post-hoc test could not find where the differences were ($p < 0.05$ was considered significant).

	Treatment (SEM)		
ATV Concentration	**ATV**	**ATV + CoQ10 (PTS)**	**ATV + PTS**
Control (DMSO)	152.5 (5.86)	143.5 (2.39)	158.2 (4.02)
0.045 mg L^{-1}	149 (4.88)	142 (3.62)	157 (4.14)
0.5 mg L^{-1}	140.2 (1.84)	142.75 (2.01)	155.7 (3.61)
1 mg L^{-1}	138 (2.46)	139 (3.85)	149 (3.87)

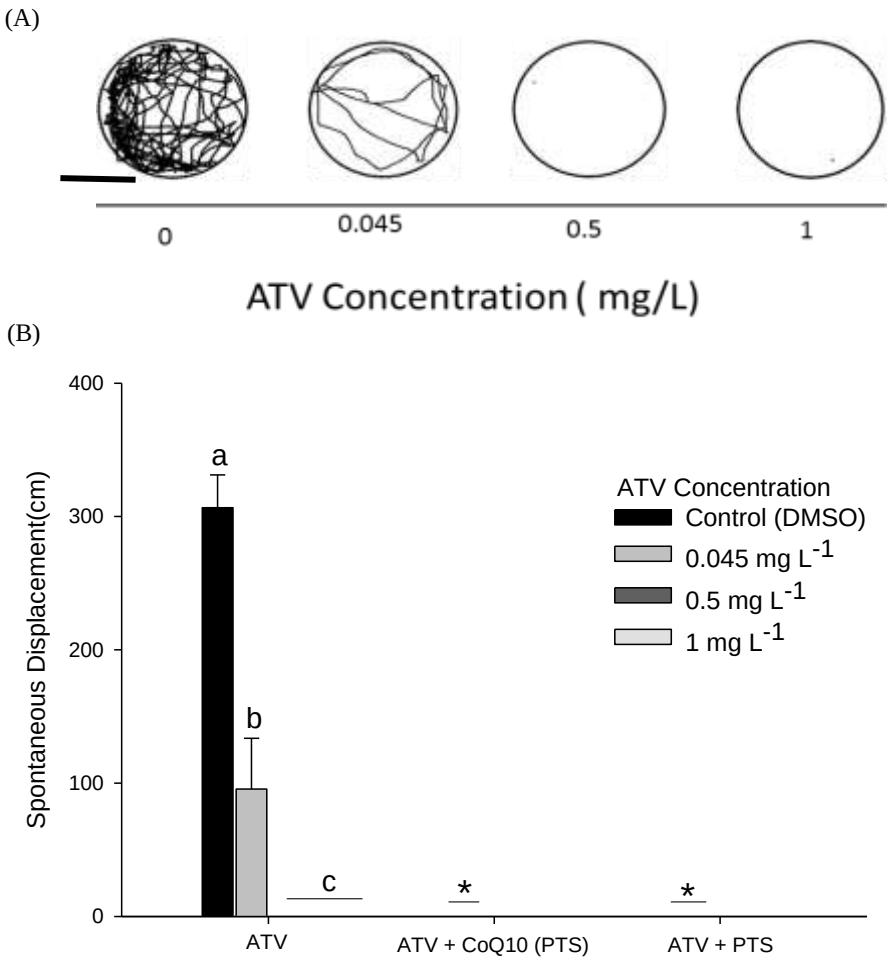

Figure 3.5: Spontaneous displacement of 96 hpf larvae that were continuously exposed (from 2 hpf) to three ATV concentrations with or without CoQ10 (4.5 mg mL^{-1}) or vehicle (PTS). Videos (see Materials and Methods) were taken for duration of 2 min. (A) Representative video trace of larva spontaneous displacement. Scale bar: 4.5 mm. (B) Average spontaneous displacement (cm) of zebrafish larvae over the 2 min video period. Data are presented as means + SEM (n = 4 larvae at each ATV concentration). Different letters denote significant differences between ATV concentrations within the same treatment, whereas an asterisk (*) denotes significant differences within the same ATV concentration among the different treatments. A two-way ANOVA analysis followed by a Holm-Sidak post-hoc test was conducted ($p < 0.05$ was considered significant).

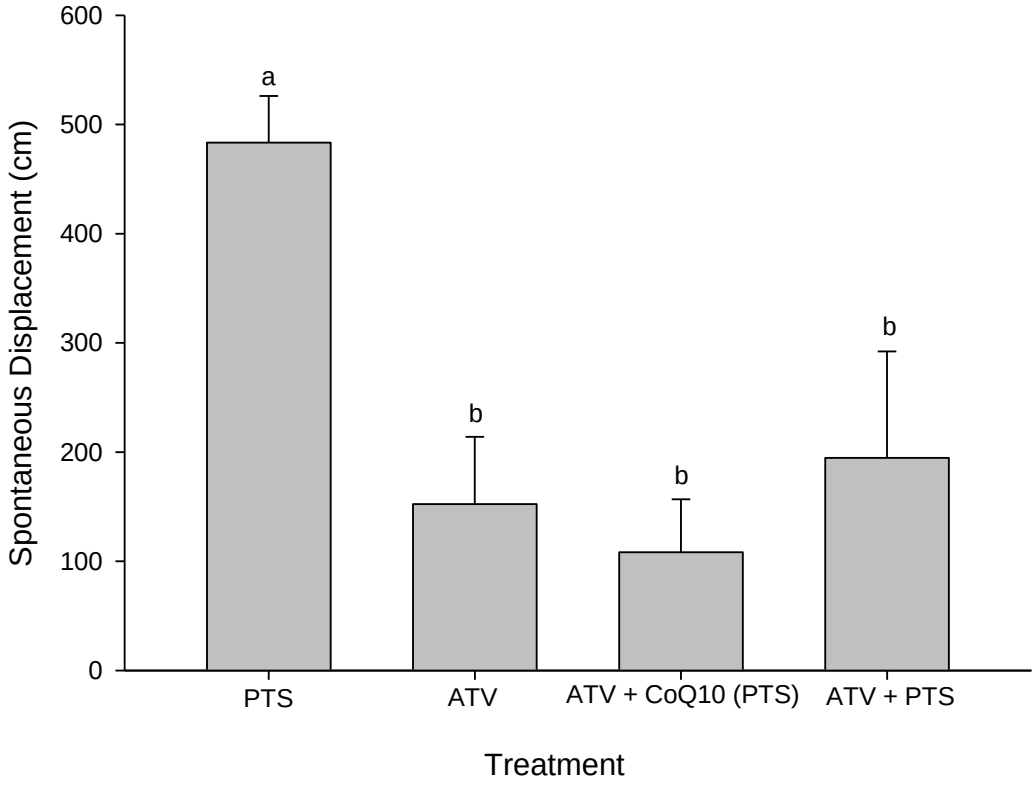

Figure 3.6: Spontaneous displacement of 120 hpf zebrafish larvae that were continuously exposed to 0.5 mg L^{-1} of ATV with or without CoQ10 (4.5 mg L^{-1}) or vehicle (PTS) starting at 2 hpf until 96 hpf, and then reared in EM in the absence of chemicals until 120 hpf. Videos were taken for a duration of 2 min. Data are presented as mean + SEM (n = 3 larvae for each treatment group). Different letters indicate significant differences among the treatment groups. One-way ANOVA followed by a Tukey's pair-wise multiple comparison test was conducted ($p < 0.05$ was considered significant).

Figure 3.7: Response to tactile stimulus of 96 hpf zebrafish larvae that were continuously exposed (from 2 hpf) to either (A) ATV alone, (B) ATV + CoQ10 (4.5 mg L^{-1}), or (C) ATV + vehicle (PTS). Data are presented as means + SEM (n = 30 larvae for each ATV concentration). Different letters denote significant differences among ATV concentrations within each response group; an asterisk (*) denotes significant differences within the same ATV dose across various treatment groups. A two-way ANOVA analysis followed by a Holm-Sidak post-hoc test was used to determine statistical differences ($p < 0.05$ was considered significant).

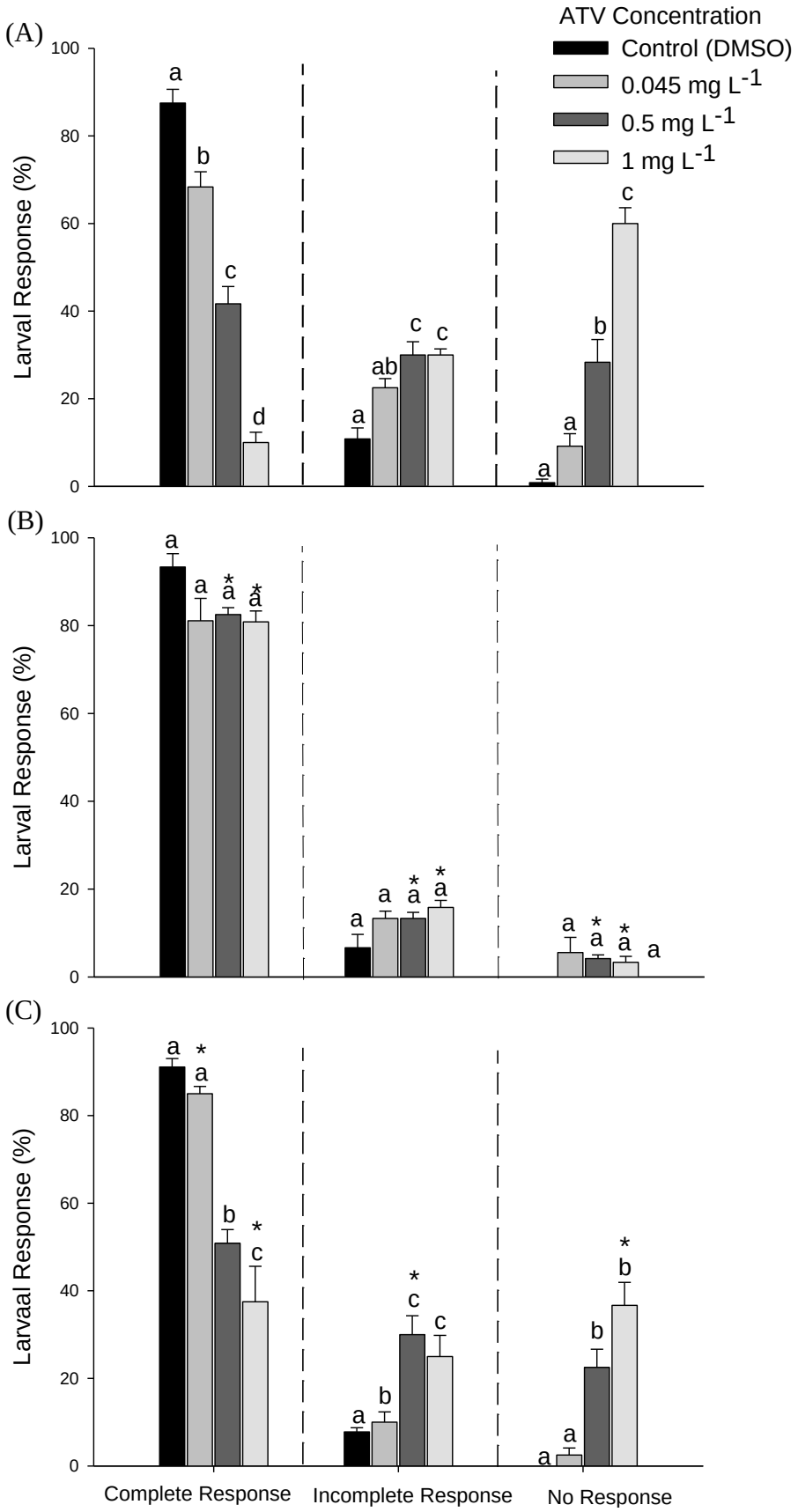
(A)
(B)
(C)
ATV Concentration
Control (DMSO)
0.045 mg L-1
0.5 mg L-1
1 mg L-1
Larval Response (%)
Larvaal Response (%)
Complete Response
Incomplete Response
No Response

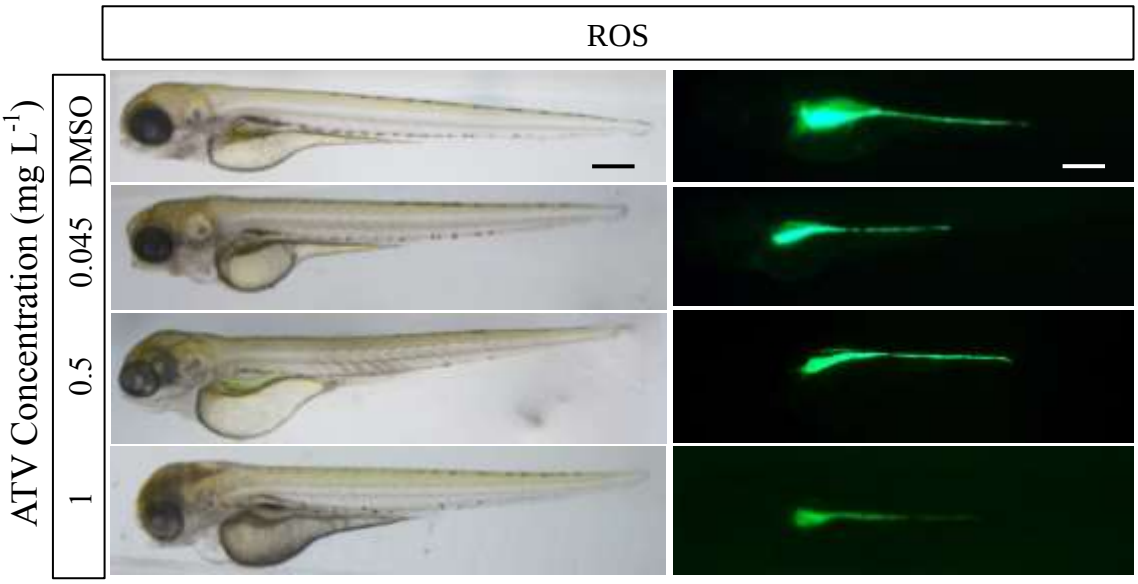

Figure 3.8: Reactive oxygen species (ROS) generation in 96 hpf zebrafish larvae that were continuously exposed (from 2 hpf) to various ATV concentrations. The left panel shows bright field images of larvae, whereas the right panel displays the same images using the GFP filter (wavelength of 469 nm). Scale bar: 2 mm.

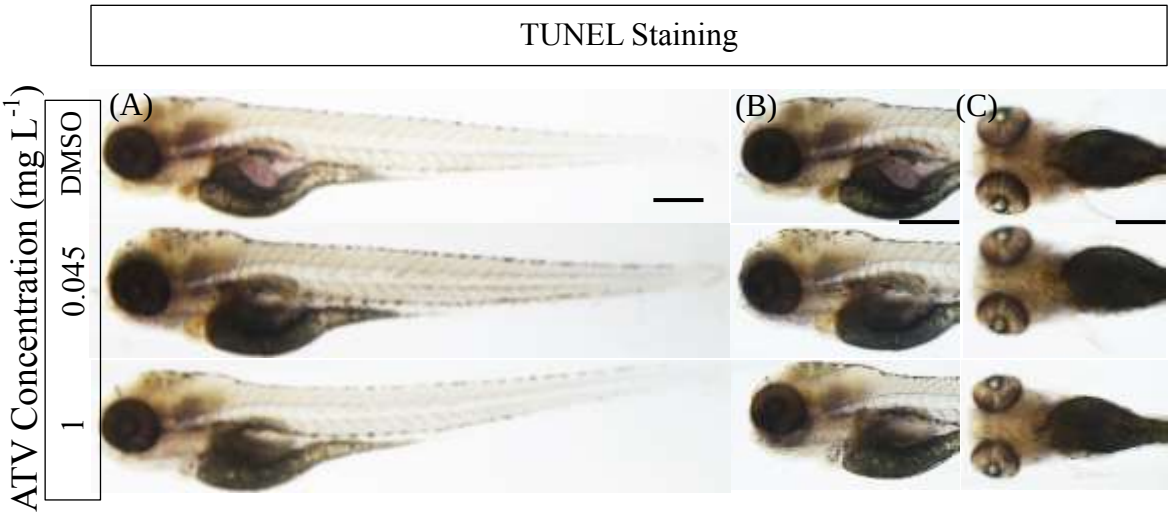

Figure 3.9: TUNEL staining in 96 hpf zebrafish larvae that were continuously exposed (from 2 hpf) to two ATV concentrations. (A) and (B) anterior facing left, and (C) ventral view. Scale bar: 2 mm.

Figure 3.10: Whole-body enzyme activities (assayed at 28 °C) of 96 hpf zebrafish larvae that were continuously exposed (from 2 hpf) to either ATV alone, ATV + CoQ10 (4.5 mg L^{-1}), or ATV + vehicle (PTS). Values are presented for (A) cytochrome oxidase (COX), (B) citrate synthase (CS), and (C) lactate dehydrogenase (LDH). Data are presented as means + SEM (n = 4 breedings for each ATV concentration). Different letters denote significant differences among ATV concentrations; an asterisk (*) denotes significant differences within a dose of ATV among treatment groups. A two-way ANOVA followed by a Holm-Sidak post-hoc test was conducted ($p < 0.05$ was considered significant).

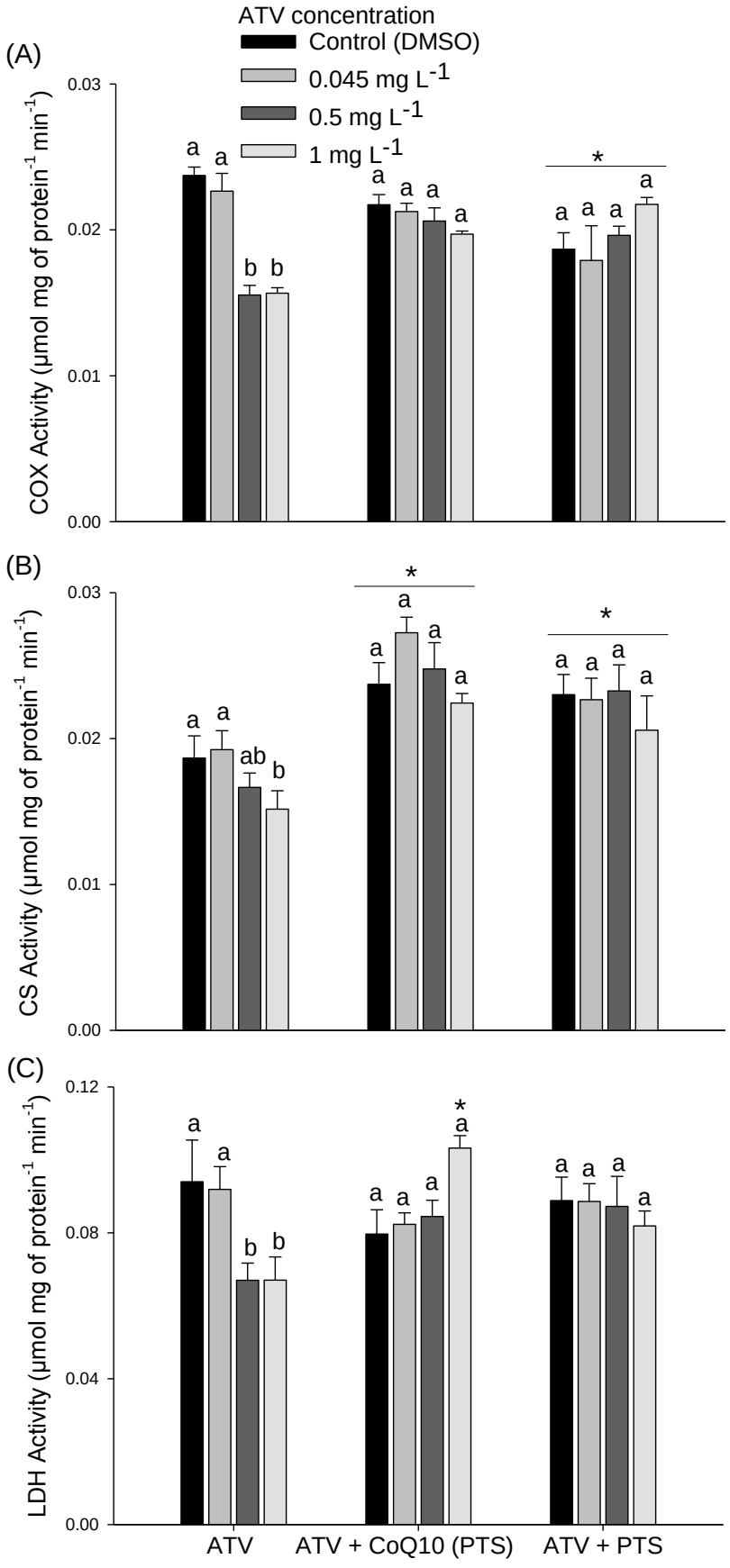
ATV concentration
Control (DMSO)
0.045 mg L-1
0.5 mg L-1
1 mg L-1
(A)
COX Activity (µmol mg of protein-1 min-1)
0.03
0.02
0.01
0.00
a a b b
a a a a
a a a a
*
(B)
CS Activity (µmol mg of protein-1 min-1)
0.03
0.02
0.01
0.00
a a ab b
a a a a
a a a a
*
*
(C)
LDH Activity (µmol mg of protein-1 min-1)
0.12
0.08
0.04
0.00
a a b b
a a a a
a a a a
*
ATV
ATV + CoQ10 (PTS)
ATV + PTS

Figure 3.11: Whole-body *atrogen-1* (A), *murf* (B), and *pgc-1α* (C) relative mRNA transcript abundance of 96 hpf zebrafish larvae that were continuously exposed to either ATV alone, ATV + CoQ10 (4.5 mg L^{-1}), or ATV + vehicle (PTS). Transcript abundance was normalized using NORMA-Gene. Data are presented as means + SEM (n=4 samples for each treatment with each sample being pooled from various petri dishes of a particular ATV treatment; see Materials and Methods). Different letters denote significant differences among ATV concentrations within treatments; an asterisk (*) denotes significant differences within the dose of ATV among treatment groups. A two-way repeated measures ANOVA followed by a Holm-Sidak test was conducted ($p < 0.05$ was considered significant).

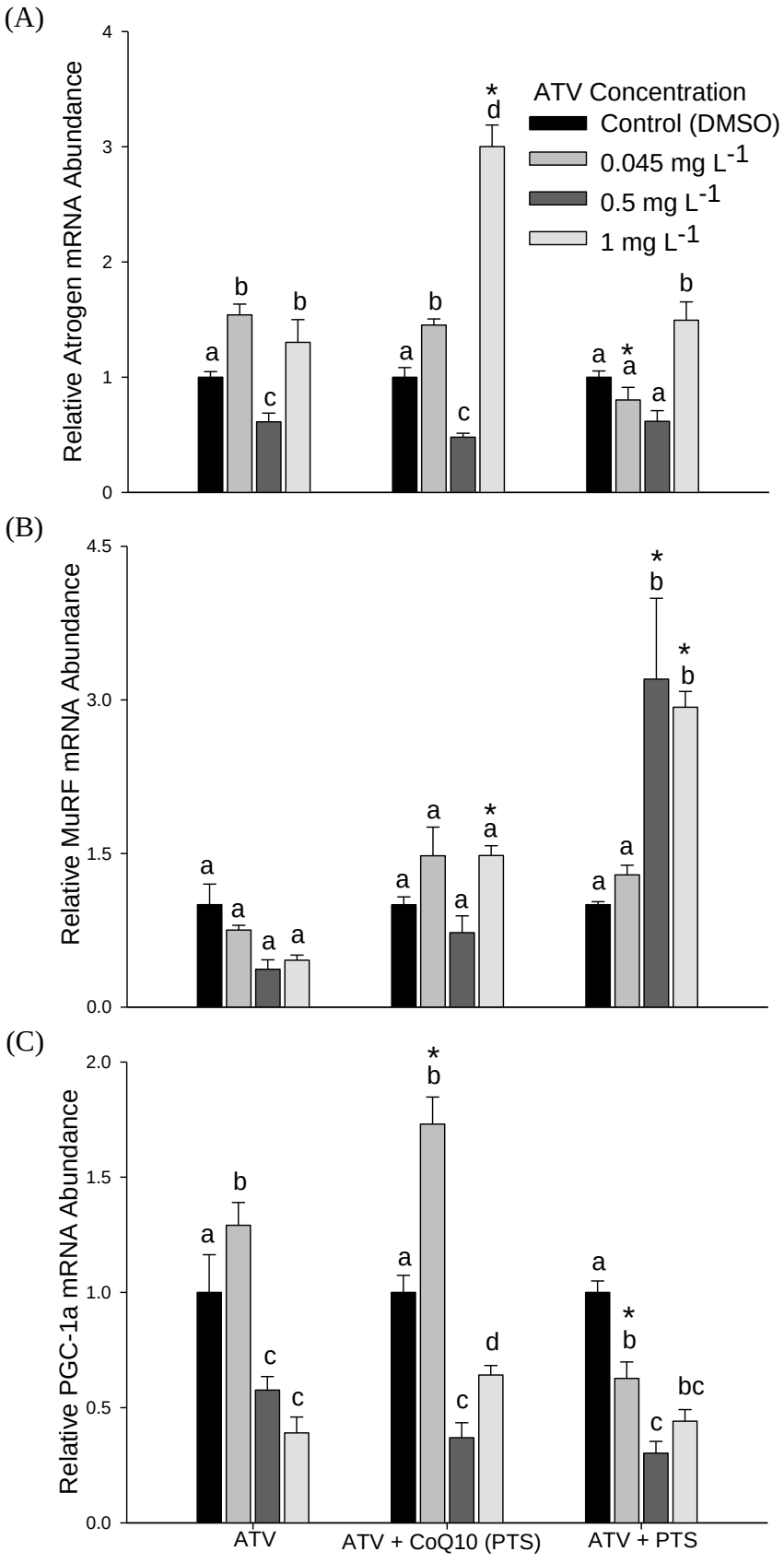
(A)
Relative Atrogen mRNA Abundance
ATV Concentration
Control (DMSO)
0.045 mg L-1
0.5 mg L-1
1 mg L-1
(B)
Relative MuRF mRNA Abundance
(C)
Relative PGC-1a mRNA Abundance
ATV
ATV + CoQ10 (PTS)
ATV + PTS

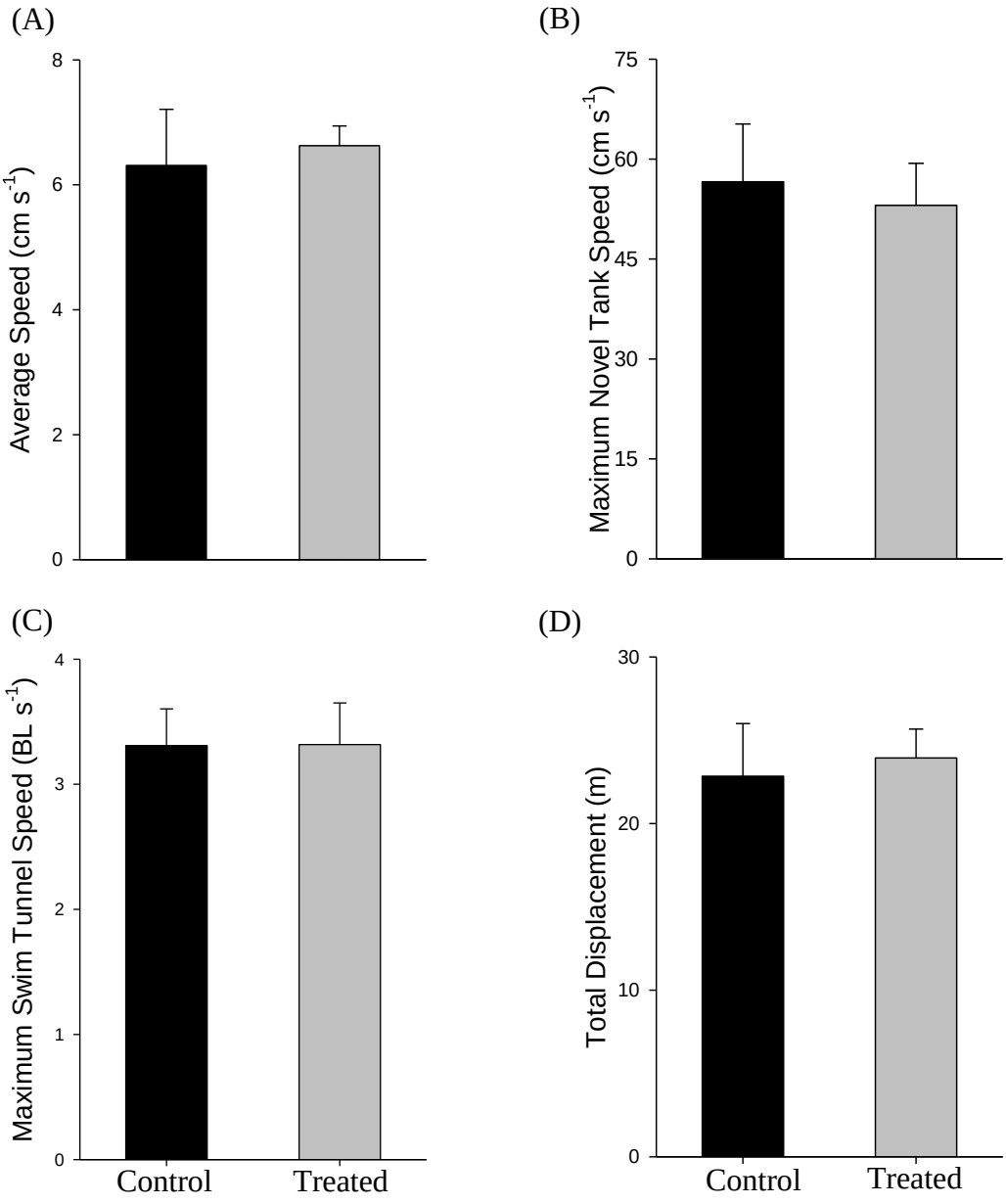

Figure 3.12: (A) Average speed (n=15 zebrafish), (B) maximum novel test speed (n=15 zebrafish), (C) maximum swimming tunnel speed (n=8 zebrafish), and (D) total displacement (n=15 zebrafish) within the first 5 min of adult zebrafish treated for 30 days with ATV (0.045 mg L^{-1}). Data are presented as means + SEM. There were no significant differences between groups.

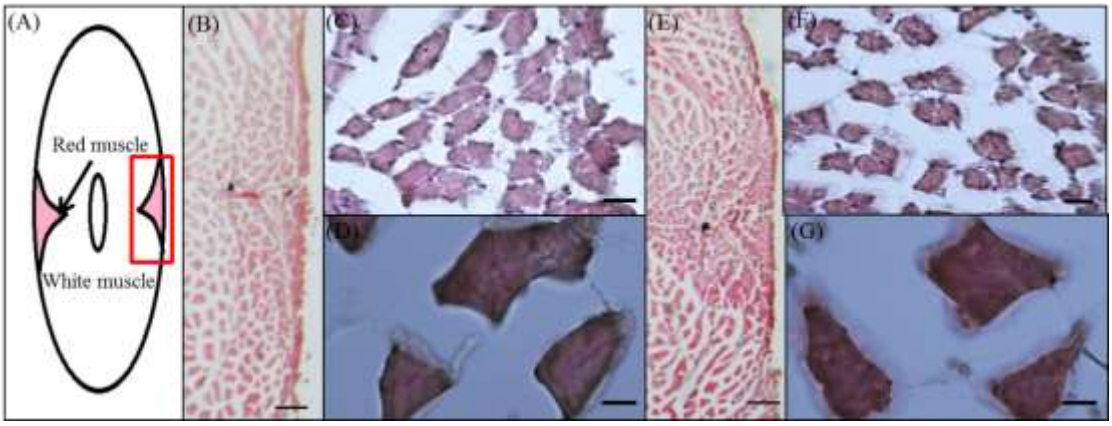

Figure 3.13: Hematoxylin and eosin staining of trunk skeletal muscle cross section from one adult zebrafish treated for 30 days with ATV (0.045 mg L^{-1}) compared with a control fish. (A) An illustration demonstrating the location of red and white muscle from which the sections were taken. Panels (B) and (E) demonstrate the section highlighted in the rectangle on panel (A). Scale bar 10 µm. Panels (C) and (F) are red muscle and panels (D) and (G) are white muscle. The panels B to D are from a control fish while E to G are from a ATV-treated fish. Scale bar: 32 nm.

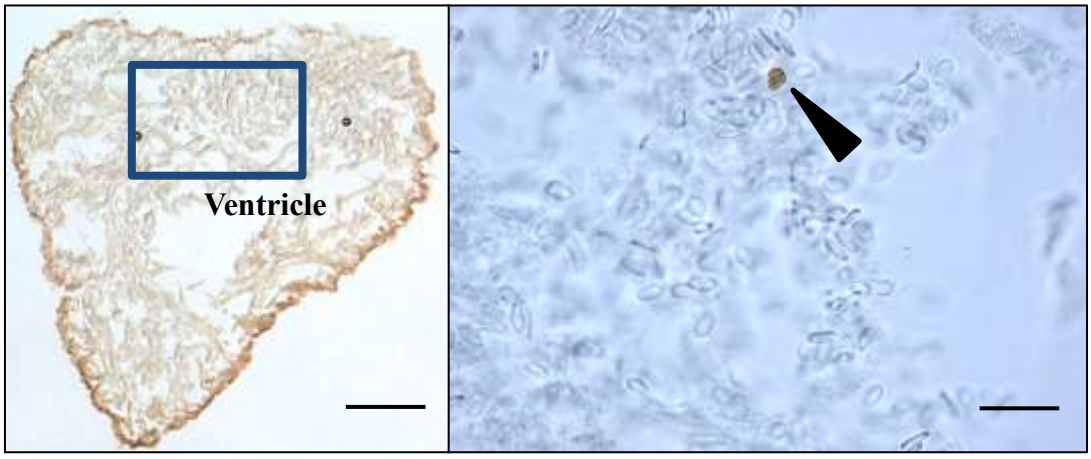

Figure 3.14: TUNEL staining of heart muscle from an adult zebrafish. (A) A representative micrograph of a whole-mount TUNEL stained heart taken from a control zebrafish (DMSO). Scale bar: 10 µm. (B) A higher magnification within an area similar to that shown in (A) of a TUNEL-positive cardiomyocyte (indicated by arrowhead). Scale bar: 21.5 nm. This experiment examined 4 adult zebrafish hearts taken from untreated controls (DMSO) or treated with 0.45 mg L^{-1} ATV for a period of 30 days.

Figure 3.15: Cardiac and skeletal muscle enzyme activities (assayed at 28°C) in adult zebrafish after exposure for 30 days to 0.45 mg mL^{-1} ATV compared with the controls. Values are presented for (A) cytochrome oxidase (COX), (B) citrate synthase (CS), and (C) lactate dehydrogenase (LDH). Data are presented as means + SEM (n=4 samples for each treatment group; see Materials and Methods). An asterisk (*) denotes significant differences compared to controls. A one-way ANOVA followed by a Tukey's pair-wise multiple comparison test was conducted ($p < 0.05$ was considered significant).

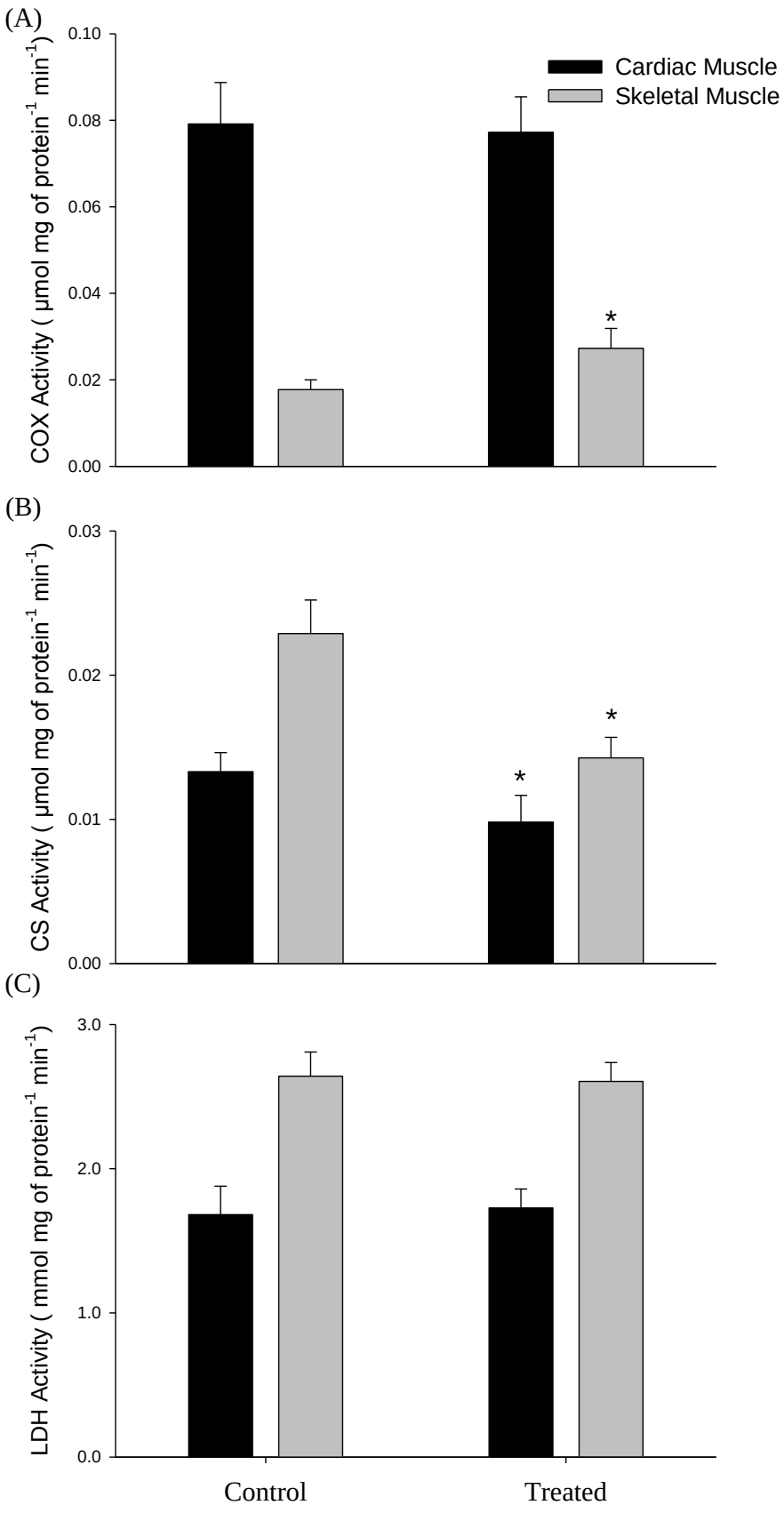
(A)
COX Activity (µmol mg of protein-1 min-1)
0.10
0.08
0.06
0.04
0.02
0.00
Cardiac Muscle
Skeletal Muscle
*
(B)
CS Activity (µmol mg of protein-1 min-1)
0.03
0.02
0.01
0.00
*
*
(C)
LDH Activity (mmol mg of protein-1 min-1)
3.0
2.0
1.0
0.0
Control
Treated

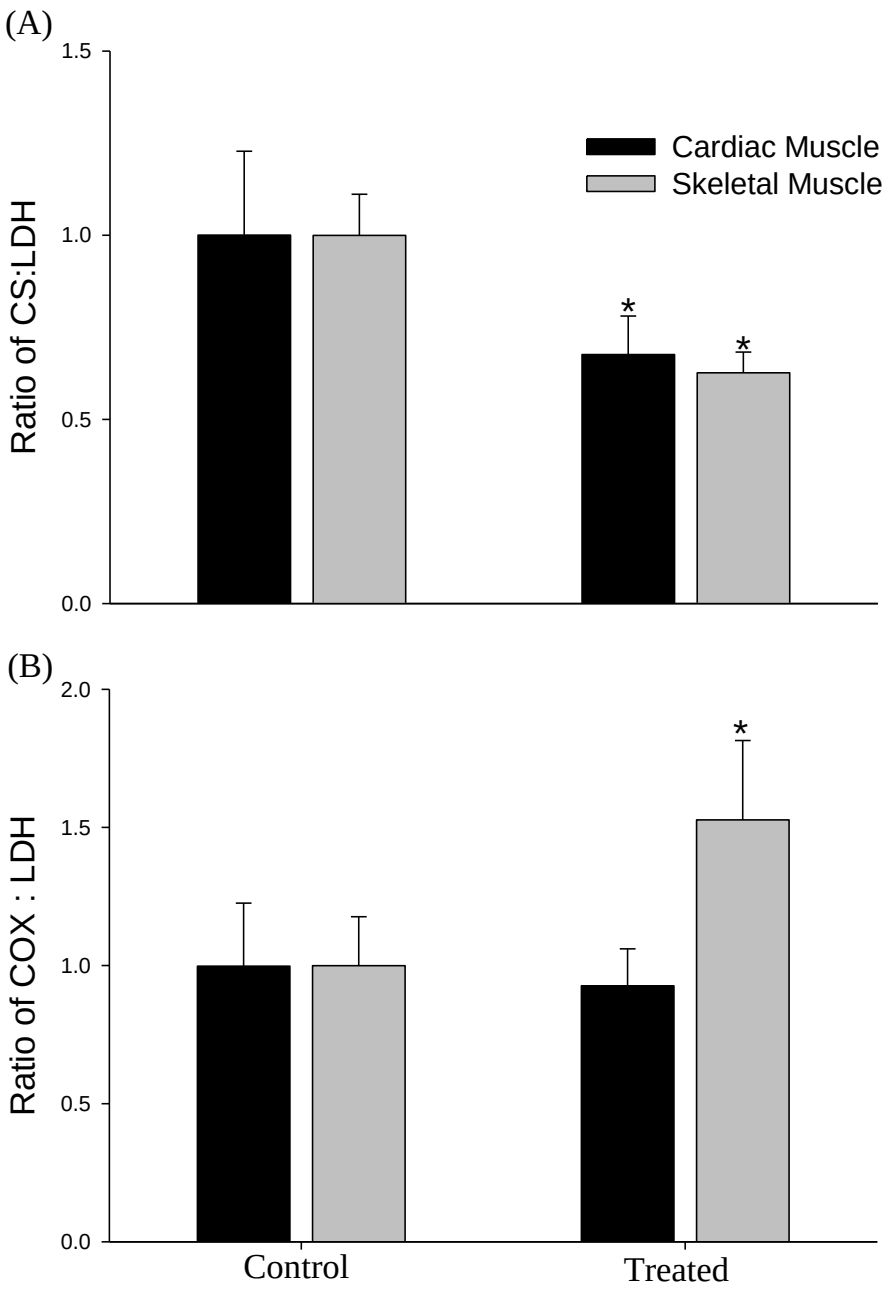

Figure 3.16: Ratios of (A) CS-to-LDH and (B) COX-to-LDH for adult zebrafish calculated from the data in Fig. 3.15. An asterisk (*) denotes significant differences compared to controls. A one-way ANOVA followed by a Tukey's pair-wise multiple comparison test was conducted ($p < 0.05$ was considered significant).

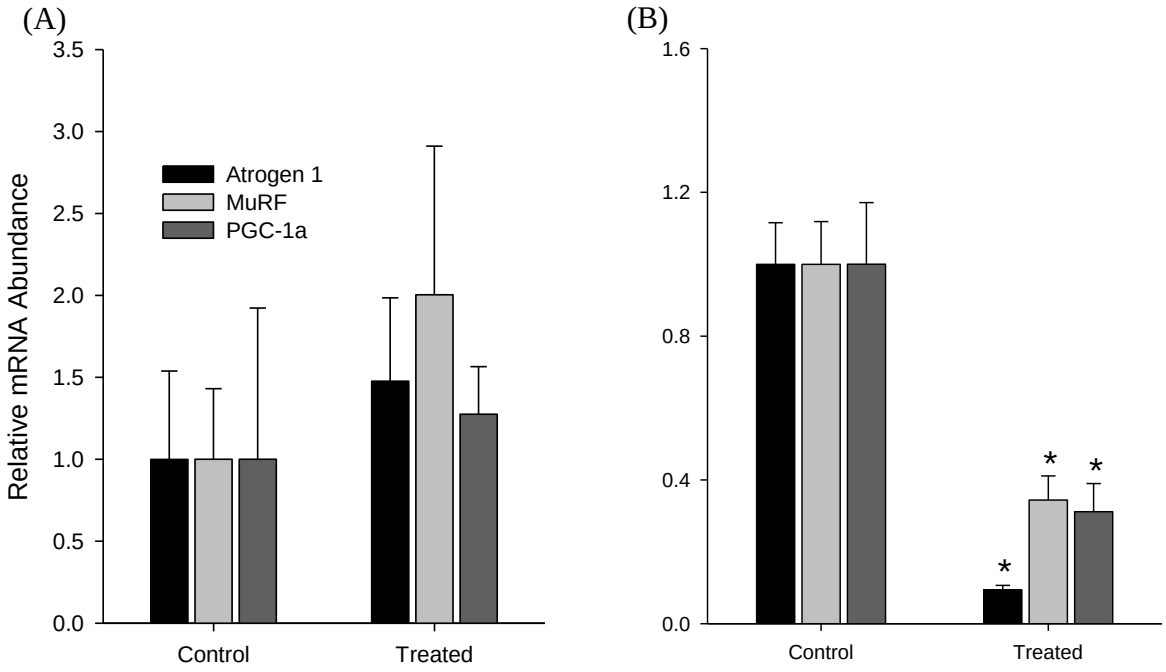

Figure 3.17: Relative mRNA transcript abundance (compared to control) in (A) skeletal muscle and (B) cardiac muscle of control and ATV-treated (0.045 mg L^{-1}) adult zebrafish. Transcript abundance was normalized using NORMA-Gene then relative abundance was calculated. Data represent means + SEM (n=4 samples for each treatment group). An asterisk (*) denotes significant differences compared to controls. A one-way ANOVA followed by a Tukey's pair-wise multiple comparison test was conducted ($p < 0.05$ was considered significant).

Chapter 4 – Discussion and Conclusion

Through a combination of assessments, I tested the hypothesis that ATV-exposed zebrafish (*Danio rerio)* embryos and adults would demonstrate cardiac and skeletal muscle damage and that this damage could be rescued by the exogenous treatment of CoQ10. Toxicological endpoints in larvae such as the LC_{50} and LE_{50}, as well as behavioral responses, tissue enzyme activities and transcript abundance of muscle atrophy were estimated in both larvae and adult zebrafish to address the hypothesis. Although the data did not fully support my hypothesis, this study demonstrated that ATV could pose a risk to zebrafish embryos/larvae and adults. ATV exposure in embryos/larvae did not only increase mortality and the incidence of pericardial edema, but also induced behavioral (locomotion), enzymatic (oxidative and glycolytic capacity), and transcriptional (muscle atrophy markers) changes. Some of these effects were also observed in ATV-exposed adult zebrafish. It is noteworthy that the ATV effects on response to tactile stimuli and enzyme activity were rescued by the addition of CoQ10.

4.1. Zebrafish embryos/larvae

4.1.1. Effects of ATV on mortality, pericardial sac edema, and heart rate

ATV treatment significantly increased zebrafish larvae mortality and the 96 h LC_{50} was reported at 3.3 mg L^{-1} (Fig. 3.1). This was in agreement with Key *et al.* (2009), who exposed mummichog *(Fundulus heteroclitus)* embryos for four days to simvastatin and reported a 96 h LC_{50} of 2.68 mg L^{-1}. Although the LC_{50} values are very similar, the minor variation might be a result of species differences. Nevertheless, these LC_{50} values are well above the highest reported environmental concentration of ATV (44 ng L^{-1}) (Metcalfe *et al*., 2003).

In addition, there was a higher incidence of pericardial sac edema in ATV-exposed larvae, such that the 96 h LE_{50} for the development of pericardial sac edema was 1 mg L^{-1} (Fig. 3.3 & 3.4). It has been reported previously that ATV exposure in zebrafish does not only induce pericardial sac edema, but also inhibits HMG-CoAR and hinders angiogenic processes in the trunk, including the anterior to posterior sprouting of intersegmental vessels of the dorsal aorta, thereby restricting circulation (Eisa-Baygi *et al.*, 2013). Consequently, it is possible that pericardial sac edema in combination with improper angiogenesis may have led to the increased mortality.

Despite the pericardial sac edema, ATV exposure did not alter the heart rate (Table 3.1). Heart rate in zebrafish embryos is commonly used as an indicator of health (Asharani *et al.*, 2008) and previous studies reported that exposing zebrafish to xenobiotic compounds including propranolol, fluoxetine, nicotine, and diphenhydramine (Schock *et al.*, 2012; Milan *et al.*, 2003; Nagel, 2002) during development reduced heart rate. However, the effects of statins on heart rate have not been reported to date and the absence of heart rate effects but higher mortality rates reported here suggest that heart rate may not the most appropriate health marker for ATV exposure.

4.1.2. Effect of ATV on larval behavior

In addition to the increased mortality and pericardial sac edema, ATV also decreased spontaneous larval displacement in a dose-dependent manner (Fig. 3.5). It should be noted that 96 hpf zebrafish larvae are capable of free swimming (Drapeau *et al.*, 2002) and several previous studies reported that spontaneous displacement in zebrafish larvae was reduced after exposures to various contaminants including propranolol, clozapine, fluoxetine, melatonin, diazepam, and pentobarbital (Barros *et al.*, 2008; Airhart and Lee,

2007; Boehmler *et al.*, 2007; Lockwood *et al.*, 2004; Zhdanova *et al.*, 2001), suggesting its applicability for testing drug effects on larval locomotor activity.

Interestingly, the rescue treatment with CoQ10 (prepared in PTS) did not restore the ATV-mediated reduction in spontaneous movement (Fig. 3.5). I hypothesized that this could be due to possible drug interactions of PTS, since the PTS-treated larvae displayed a similar pattern. Consequently, a follow up experiment was conducted to address the effects of CoQ10 and vehicle control (PTS) on larval spontaneous displacement. This experiment confirmed that ATV treatment significantly decreased spontaneous displacement behavior of larvae and that exposed larvae to PTS recovered its spontaneous displacement after the larvae were incubated for 24 h in treatment-free medium (Fig. 3.6). It should be noted that although PTS has been previously used in several cell culture models and in rats *in vivo* (Somayajulu *et al.*, 2009; Somayajulu *et al.*, 2005); PTS has not been tested in fish larvae. Therefore, future studies should examine the suitability of using PTS in the fish model as well as alternative means to solubilize CoQ10.

The effects of ATV on locomotor behavior were further investigated by assessing the larval response to tactile stimuli. Similarly to spontaneous displacement, ATV exposure led to a significant decline in the 'complete response' (response to both stimuli) and a significant increase in 'no response' (response to neither stimuli) to a tactile stimulus. Interestingly, in contrast to the spontaneous displacement, the treatment with CoQ10 or PTS fully recovered ATV-mediated effects on response to tactile stimuli. Although PTS effects were significant, the extent of recovery was less than with CoQ10 (Fig. 3.7). The difference between the 'tactile stimuli' and 'spontaneous displacement' experiments

suggests that PTS may not hinder the ability of the larvae to respond to stimuli, but rather affects their ability to swim.

It has been suggested previously that a decrease in tactile stimuli and swimming behavior could be the result of neurodegeneration, as was demonstrated in a *pink1* morphant zebrafish study (Xi *et al.*, 2011). It is thought that the Pink1 protein is involved in the zebrafish dopaminergic neuron development and function (Xi *et al.*, 2011), as well as mitochondrial function (Pilsl *et al.*, 2012). This leads me to speculate that the decrease in larval response to tactile stimuli and spontaneous displacement may be a result of neuronal degeneration due to depletion of proteins like Pink1 as a result of mitochondrial membrane destabilization.

Furthermore, previous studies using cell culture models and rats *in vivo* had demonstrated that CoQ10 effectively protected neurons from the toxic effects of paraquat, a herbicide that is linked to the development of Parkinson's disease (Somayajulu *et al.*, 2009; Somayajulu *et al.*, 2005). It was suggested that blockade of complex I of the oxidative phosphorylation pathway by paraquat and the inability of neurons to cope with free radicals are the triggers of neuronal death (Muthukumaran *et al.*, 2014). Therefore, the protective effects of CoQ10 and PTS may be due to their antioxidant properties. Oxidized CoQ10 is reduced to $CoQ10H_2$ in the mitochondria, and the reduced form is the only endogenously synthesized lipophilic antioxidant (Molyneux *et al.*, 2008). Moreover, PTS is an esterified form of vitamin E, analogous to α-tocopheryl acetate which a synthetic form of vitamin E (Borowy-Borowski *et al.*, 2004) and given that both CoQ10 and vitamin E are antioxidants, they are both capable of reducing the levels of free radicals. Hence it is possible that both CoQ10 and PTS can directly protect biological membranes against

potential ATV-mediated oxidation and thus protect against neuronal degeneration and cell death. Moreover, the protective effects of CoQ10 and PTS may be attributed to unknown interactions of PTS with ATV thus resulting in reduced toxicity of ATV.

4.1.3. Reactive oxygen species (ROS) generation and apoptosis

My results did not demonstrate ROS generation with ATV treatment (Fig. 3.8), at least under the given experimental conditions and using the methods described. If ATV results in a decrease in mitochondrial abundance due to membrane permeabilization as reported in Kaufmann *et al.* (2006), it is possible that fewer mitochondria are producing more ROS, which may result in similar ROS production compared with controls as shown in Fig. 3.8. Consequently, future studies should examine and quantify ROS production using different assays such as the fluorometric hydrogen peroxide in an attempt to assess changes among ATV treatments in larvae.

Additionally, no differences in apoptosis were found between ATV-treated and control larvae (Fig. 3.9) using the TUNEL assay. In contrast, Hanai *et al.* (2007) reported that simvastatin (0.01 mg L^{-1}) resulted in larval morphological muscle damage when stained with antibodies of the myosin heavy chain, suggesting induction of apoptosis. Therefore, it is likely that the TUNEL assay used here to detect apoptotic cells is not applicable for muscle damage detection as previously demonstrated by Hanai *et al.* (2007). Consequently, future studies should verify whether exposure to ATV concentrations results in larval muscle morphological damage by using a different method, such as the myosin heavy chain staining of 96 hpf larvae.

4.1.4. Effects of ATV on enzymes activity associated with oxidative capacity and mitochondrial function

In larvae, ATV exposure significantly decreased the whole-body enzyme activities of CS, and COX in a dose-dependent manner, suggesting ATV-mediated reduction in tissue aerobic and possibly anaerobic metabolic processes. Interestingly, the decline in all three enzyme activities in whole-body larvae was rescued by the addition of CoQ10 and PTS, although this effect was not statistically significant for LDH activity.

It should be noted that multiple mechanisms have been proposed to explain cell death resulting from mitochondrial dysfunction including the production of ROS, opening of the permeability transition pore, respiration, or ATP synthase changes (Chandra *et al.*, 2002; McClintock *et al.*, 2002). It is noteworthy that cell death due to mitochondrial dysfunction may be a result of one or several mechanisms occurring in parallel. Kaufmann *et al.* (2006) reported that ATV induces mitochondrial swelling in rat skeletal muscle cell lines (L6 cell lines) in a dose-dependent manner, resulting in openings of the mitochondrial permeability transition pore and the release of cytochrome c, ultimately resulting in cell death. Thus I speculate that the reduction in COX enzyme activity may be the result of permeabilization of the mitochondrial membrane due to opening of mitochondrial permeability transition pore and the release of cytochrome c. Moreover, the reduction in CS enzyme activity may also be accounted for in a similar manner. The reduction in LDH enzyme activity may be attributed to the reduction in protein content as shown in Fig. I (panel B). Furthermore, the recovery of aerobic enzyme activities upon CoQ10 and PTS treatment suggests that exogenous supply of CoQ10 and PTS are playing a role in reducing mitochondrial membrane permeability possibly by reducing oxidative stress.

4.1.5. Effects of ATV on molecular markers of muscle atrophy

It is important to note that the relative mRNA abundance of *atrogen-1*, *murf*, and *pgc-1α* were assessed in 25 whole-body zebrafish larvae. Consequently, this may potentially mask minor alteration in mRNA abundance within a tissue as a result of attenuation (i.e. larval skeletal muscle) and result in deceitful unchanged mRNA abundance as a result of variable alterations of mRNA abundance between tissues (i.e. an increase in cardiac muscle verses decrease in skeletal muscle). ATV exposure differentially affected the abundance of molecular markers of muscle atrophy. The abundance of *atrogen-1* mRNA was increased in larvae treated with 0.045 mg L^{-1}ATV and differentially altered in those treated with 0.5 and 1 mg L^{-1} ATV. Previously, Hanai *et al.* (2007) reported that treating 20 hpf zebrafish embryos with 0.5 μM (0.2 mg L^{-1}) ATV for 12 h increased *atrogen-1* mRNA and Atrogen-1 protein levels, similarly to what was observed at 0.045 mg L^{-1} ATV in this study. The results obtained with 0.5 and 1 mg L^{-1} ATV could be associated with the reduced larval tissue aerobic and anaerobic metabolism mentioned earlier, suggesting that at these higher ATV concentrations the abundance of *atrogen-1* reflects altered metabolism. Interestingly, differential patterns were also observed in CoQ10- and PTS-treated larvae, suggesting *atrogen-1* abundance is not CoQ10- and/or PTS-dependent. Moreover, the increase in *atrogen-1* abundance at 1 mg L^{-1} ATV in CoQ10-treated larvae, and the decrease in *atrogen-1* at 0.045 mg L^{-1} ATV in PTS-treated larvae, suggest that PTS and CoQ10 may have an independent effect on *atrogen-1* abundance during development through unknown mechanisms. Given my results demonstrate differential alterations in *atrogen-1*transcipt abundance, future studies are needed to assess Atrogen-1 protein levels in order to address associations of ATV-mediated

atrogen-1 abundance to Atrogen-1 protein concentration. Alternatively, the differential effects on *atrogen-1* mRNA levels could be due to the dynamic gene expression during larval development. For example, in the developing embryo/larvae, different genes are regulated at different developmental period and the interactions between genes are what drive cell growth and differentiation (Ton *et al.*, 2002). Moreover, given that adaptation is driven by the dynamic interactions of genes with physiological or pathological stimuli (Ton *et al.*, 2002), it is therefore possible that the larvae development was affected (e.g. delayed) by ATV exposure, which would then translate into differences in gene expression profiles in 96 hpf larvae.

No differences in *murf* abundance were found between the different concentrations of ATV in 96 hpf larvae. This may suggest that *murf* may not be an appropriate marker for ATV-mediated muscle atrophy in the developing zebrafish. However, since it was demonstrated previously that *murf* abundance in adult zebrafish increases in response to after a 7 day food deprivation (Amaral and Johnston, 2011); it is possible that *murf* is a marker specifically for adult zebrafish muscle atrophy. Differential patterns were observed in CoQ10- and PTS-treated larvae suggesting that *murf* abundance is not CoQ10- and/or PTS-dependent. Moreover, the increase in *murf* abundance at 1 mg L^{-1} ATV in CoQ10-treated larvae, and the decrease in *murf* at 0.5 and 1 mg L^{-1} ATV in PTS-treated larvae suggest that PTS and CoQ10 may have an independent effect on *murf* abundance during development through unknown mechanisms.

The abundance of *pgc-1α* increased in ATV-treated larvae at a concentration of 0.045 mg L^{-1} and decreased at concentrations of 0.5 and 1 mg L^{-1}. A central function of *pgc-1α* is linked to mitochondrial biogenesis and the detoxification of ROS (St-Pierre *et al.*,

2006; Valle *et al.*, 2005; St-Pierre *et al.*, 2003). *Pgc-1α* controls ROS removal by regulating the expression of superoxide dismutase 2 (SOD2), which removes superoxide radicals, and glutathione peroxidase 1 (GPX1), which detoxifies hydrogen peroxide (St-Pierre *et al.*, 2003), as well as various mitochondrial, cytoplasmic, and peroxisomal ROS-detoxifying enzymes (St-Pierre *et al.*, 2006; Valle *et al.*, 2005). Thus, the increase in *pgc-1α* abundance may have been a response to the increase in ROS in an attempt to protect tissues from ATV-mediated oxidative stress. This is consistent with the enzyme activities results, which did not change. However, at the higher ATV concentrations *pgc-1α* abundance was reduced, suggesting that ATV-mediated damage passed a threshold at which *pgc-1α* could no longer protect tissue from ATV-mediated effects. This was also consistent with ATV-mediated effects on tissue enzyme activity at concentrations of 0.5 and 1 mg L^{-1}. Similarly to *atrogen-1* and *murf*, differential patterns were observed in CoQ10- and PTS-treated larvae suggesting that *pgc-1α* abundance is not CoQ10- and/or PTS-dependent. Moreover, the increase in *pgc-1α* abundance at 0.045 mg L^{-1} ATV in CoQ10-treated larvae, and the decrease in *pgc-1α* at 0.045 mg L^{-1} ATV in PTS-treated larvae suggest that PTS and CoQ10 may have an independent effect on *pgc-1α* abundance during development through unknown mechanisms. Therefore, future studies are needed to assess Pgc-1α protein levels in ATV-treated larvae to assess the protective role of CoQ10 and PTS and whether they have an effect on Pgc-1α protein levels.

4.2. Effects of ATV on Zebrafish Adults

4.2.1. Effects of ATV on adult behaviors

Similarly to larval zebrafish, the effect of ATV on adult zebrafish locomotor behavior was also assessed. My results, however indicated that a 30 d ATV exposure at

0.045 mg L^{-1} did not affect the average speed, maximum novel test speed, maximum swimming tunnel speed or total displacement (Fig. 3.12). These results suggested that ATV does not disrupt the motor or neurological ability of adult zebrafish, at least under the experimental conditions used here.

As discussed in Chapter 1 (see section *1.3.2*). ATV can result in inhibition of endogenous production of CoQ10, an important cofactor for the production of ATP in the cell mitochondria. Given that CoQ10 serves an important function in every cell of the body, impairing its synthesis could be detrimental to all tissues, but in particular those tissues with high energy requirements (Abou-Sleiman *et al.*, 2006; Molyneux *et al.*, 2009). This suggests that perhaps higher concentrations of ATV are necessary to observe effects on swimming performance associated with a potential decrease in CoQ10 levels; this should be tested in future experiments.

4.2.2. Muscle staining

Concomitant with the lack of effects on swimming performance, ATV exposure did not lead to apoptosis in zebrafish cardiac muscle (Fig. 3.13), at least under the given experimental conditions. This contrasts with the report of Dubey and Hesong (2006), who demonstrated that treating Wistar rats with ATV (10 mg Kg^{-1}) for 3 days resulted in apoptosis (assessed using TUNEL assay) in cardiomyocytes. This inconsistency could be due to 1) ATV concentration was not adequate to result in cardiomyocyte apoptosis in zebrafish, 2) the difference in the route of drug administration, or 3) species-specific differences. Therefore, the effect of ATV on zebrafish cardiac muscle should be examined further. Also, as this was my first use of tissue sectioning, further efforts in acquiring better sections might assist in this regard.

Zebrafish skeletal muscle morphology showed that ATV exposure did not result in significant changes in cell size (Appendix C, Fig. IV); however, there may be effects on cell shape (Fig. 3.14). Elhaleem and Elsayed (2011) reported that ATV-treated adult male Sprague Dawley rats (oral administration of 1.44 mg day^{-1} for 3 months) showed histological changes in skeletal muscle (using hematoxylin and eosin staining), suggesting ATV-induced degeneration of skeletal muscle and the formation of small cavities in sarcoplasm and mitochondria. Given that my observations are preliminary, future studies are needed to confirm the findings in multiple fish in order to produce cohesive morphological observations between treatments.

4.2.3. Effect of ATV on enzymes activity associated with oxidative capacity and mitochondrial function

Zebrafish adult exposed to ATV at 0.045 mg L^{-1} for 30 d resulted in differential effects on muscle COX, CS, and LDH activities compared with what I found for zebrafish larvae. ATV significantly increased COX activity in skeletal muscle, but not cardiac muscle, suggesting a tissue-specific ATV effect. The increase in COX activity observed in this study may suggest compensatory responses of skeletal muscle possibly to address ATV-mediated effects on tissue metabolism. These results contradict Bouitbir *et al.* (2011) who reported that treatment of adult male Wistar rats with ATV (10 mg kg^{-1} per day) for two weeks increased COX activity in cardiac muscle and decreased skeletal muscle COX activity. It is possible that the ATV-mediated effects on tissue aerobic and anaerobic metabolism are concentration-dependent, thus my results may suggest that at low concentrations ATV improves tissue aerobic metabolism. Unfortunately, similar studies involving ATV effects on fish COX enzyme activity could not be found, therefore this

should be tested in future experiments to confirm whether increasing ATV concentrations results in different effects on COX enzyme activities in skeletal and cardiac muscle in fish.

Moreover, ATV significantly decreased CS activity in both cardiac and skeletal muscles (Fig. 3.14), suggesting a lower mitochondrial abundance (Rooyackers *et al.*, 1996). Cell death due to mitochondrial dysfunction may occur as a result of one or several mechanisms occurring in parallel including the production of ROS, opening of the permeability transition pore, decrease in respiration or ATP synthase (Chandra *et al.*, 2002; McClintock *et al.*, 2002). Thus, decreases in mitochondria may result from cardiac and skeletal muscle damage, sequentially affecting cardiac and skeletal muscle function. Cardiac and skeletal muscle damage in fish can have a significant impact on fish development, fecundity, and survivability, including their capability to evade predation. Thus, future studies are needed to address these physiological effects of ATV on the overall fitness of fish.

The activity of LDH was not affected in either the cardiac or skeletal muscles (Fig.3.15), suggesting that at ATV concentration of 0.045 mg L^{-1} it did not affect the anaerobic capacity in either tissue. The absence of an effect on LDH activity is consistent with my larval exposure studies (0.045 mg L^{-1}), as well as a previous study that indicated unchanged tissue LDH in rats treated with a low dose of ATV or simvastatin (Elhaleem and Elsayed, 2011).

Furthermore, De Pinieux *et al.* (1996) reported that analogs of statins (lovastatin, simvastatin, pravastatin, or fluvastatin) increased the blood serum ratios of lactate to pyruvate in treated patients. The authors suggested statin use resulted in a shift towards anaerobic metabolism (De Pinieux et al., 1996). Consequently the aerobic to anaerobic

ratios were also calculated to verify whether ATV exposure in adult zebrafish led to a similar metabolic shift. There was a significant decrease in CS:LDH ratio in cardiac and skeletal muscles, suggesting a shift towards anaerobic metabolism consistent with De Pinieux *et al.* (1996). However, the COX:LDH ratio significantly increased in skeletal, but not cardiac, muscle (Fig. 3.16). Given that LDH activity did not change, the increase in COX:LDH ratio was a result in the increased COX activity.

4.2.4. Effects of ATV on molecular markers of muscle atrophy

The transcriptional abundance of *atrogen-1* and *murf* has been previously reported to increase during muscle atrophy in fish and mammals and consequently are considered to be early markers of muscle degradation (see section 1.4). However, my results demonstrated that there were no differences in the skeletal muscle abundance of *atrogen-1*, *murf*, and *pgc-1α* between 0.045 mg L^{-1} ATV-treated and control adult zebrafish. These results suggested that ATV does not result in muscle atrophy, at least under my experimental conditions. It should be noted that not all individuals are equally susceptible to xenobiotic exposure (Depledge, 1996), and this may explain the large variations between fish (represented by error bars). Therefore, to address this variation, future research should repeat the assessment of *atrogen-1*, *murf*, and *pgc-1α* abundance in a larger sample size.

Although treatment of adult zebrafish with an ATV concentration of 0.045 mg L^{-1} for 30 d did not alter skeletal muscle abundance of *atrogen-1*, *murf*, and *pgc-1α*, all three markers were reduced in cardiac muscle. Zyzynska-Granica and Koziak (2012) demonstrated that for each particular tissue or cell type and specific experimental designs, there is a difference in gene expression. Muscle growth and muscle atrophy vary among tissues due to differences in fiber types, contractile activities, abundance of *pgc-1α*,

differences in protein turnover, and cell/nuclear turnover (Schiaffino *et al.*, 2013). For example, *atrogen-1* promotes degradation of MyoD, an important activator of protein synthesis (Csibi *et al.*, 2010). While, in the heart, *atrogen-1* reduces the levels of calcineurin A, an important factor triggering cardiac hypertrophy (Li *et al.*, 2004). Bouitbir et al. (2010) suggested that statins protected cardiac muscle by stimulating mitochondrial biogenesis and antioxidant defence through ROS-induced *pgc-1α* expression. The authors also reported that statins are toxic for mitochondria in skeletal muscle of rat and in deltoid muscle of some patients due to the low abundance of *pgc-1α*, and that an adequate antioxidant therapy should prevent muscle damage. This suggests that the ATV-mediated decrease in the abundance of all three markers may be tissue-specific, but whether ATV protects against cardiac muscle atrophy is yet to be demonstrated in zebrafish.

4.3. General Conclusions

Contributing to the increase in statin use, the appearance of these drugs in aquatic environments raises environmental concerns. Since the effects of statins in aquatic species are yet to be fully understood, my thesis aimed to examine the physiological and behavioral alterations occurring as a result of ATV exposure in zebrafish and if there was a role of CoQ10 in mitigating these changes. I hypothesized that ATV exposure in zebrafish embryos/larvae and adults would lead to cardiac and skeletal muscle damage and that this damage could be rescued by the addition of CoQ10. Toxicological endpoints such as the LC_{50} and LE_{50}, behavioral responses, enzyme activities, as well as transcript abundance in larval and adult zebrafish were estimated to address the hypothesis.

My results demonstrated that ATV exposure in zebrafish alters both physiological and behavioral responses in larvae and specific physiological, but not behavioral, responses

in adults. ATV exposure increased mortality and pericardial sac edema, but did not affect larval heart rate. Moreover, the larval spontaneous displacement and response to stimuli were affected by ATV, and some of these changes were rescued by CoQ10 treatment. The whole-body activities of COX, CS, and LDH were also affected and showed a decrease in response to ATV treatment. There were also alterations in transcript levels of muscle atrophy markers; however, no clear trends were observed. Furthermore, the results from adult zebrafish experiments indicated that ATV did not affect swimming behavior or tissue histology, but did differentially affect enzyme activities. The activity of COX was increased in skeletal muscle, whereas that of CS decreased in both cardiac and skeletal muscle, and that of LDH was not affected. Also, the transcript abundance of all three biomarkers was significantly reduced only in cardiac tissue.

The major conclusions that I can draw from these assessments are: 1) ATV exposure reduced the response to tactile stimuli that can be rescued by the addition of antioxidants, CoQ10 and PTS; 2) behavioral analyses were sensitive to ATV exposure only in larval stages but whether these changes have longer consequences in unknown; 3) decreases in enzyme activities supports that ATV mediates effects on tissue metabolism in larvae and thus may effect fish development and fecundity; and, 4) tissue enzyme activities and transcriptional abundance for muscle atrophy should be investigated further in ATV-exposed adult zebrafish.

4.4. Prospective Future Research

Although larval results from this study demonstrate that CoQ10 may have a protective role in ATV-mediated effects, it is still unclear whether ATV-mediated effects in fish are a result of reduced CoQ10 levels in tissue mitochondria. Therefore, further

research should include the repetition of the larval and adult exposure studies in order to quantify the CoQ10 levels. Given that fish have a lower capacity to metabolize xenobiotic compounds compared to mammals (Wolf and Wolfe, 2005), especially during early life stages (Andersson and Forlin, 1992; Walker and Peterson, 1991), more tests should be done to examine the effects of low chronic exposure of ATV on fecundity and whether the effects could be transgenerational.

An alternative option is to repeat ATV exposures in a larger fish species such as the rainbow trout. This would allow the assessment of plasma CoQ10 and ATV levels as well as other parameters including myoglobin, potassium, creatine phosphokinase, which may increase the range of feasible experimental methods. Intraperitoneal injections of ATV or CoQ10 are possible in larger fish, thus such studies could provide a better understanding of the role of CoQ10 in ATV-mediated effects.

Another area that has received little attention is the impact of ATV on swimming and mating in fish, whether chronic exposure could lead to reductions in growth, swimming and fecundity. The effects on growth could be examined in ATV-exposed zebrafish larvae that are raised to adulthood. Once these fish are a few months of age several experiments could be conducted including swimming behavior, counting viable embryos, as well as measuring estrogen and testosterone levels.

Much remains to be discovered about the factors that determine ATV bioavailability in fish, the influence of environmental parameters such as pH on the bioavailability and toxicity need to be investigated further. This is important for acidic pharmaceuticals, such as ATV where the metabolites and speciation can influence toxicity. Therefore, experiments on the effects of environmental parameters as well as different

ATV metabolites on fish will enhance our understanding of ATV bioavailability and the potential toxicity to aquatic organisms. These experiments would be more environmentally relevant.

4.5. Significance

There is concern that aquatic species such as fish will be affected by statins since they share similar physiological processes with humans. For example, zebrafish possess orthologs to 86% of tested human gene drug targets (Gunnarssan *et al.*, 2009). Previous studies have examined the effects of ATV on zebrafish embryo development and muscle damage; however, these studies do not report the potential physiological changes that may threaten fish development and ultimately performance. Therefore, this thesis examined the physiological as well as behavioral effects of ATV on zebrafish larvae as well as adults, and the role of CoQ10 in ATV-mediated effects in zebrafish larvae. So far, most of the attention has been channeled towards the traditional toxicological assessment in fish exposed to ATV, while little has been done on the behavioral effects. No studies have examined the effects of ATV on the transcript levels of *pgc-1α* and *murf*, and there has been little work on the cardiac and skeletal muscle enzymatic activities in response to ATV. Furthermore, this is the first study to examine the behavioral alterations in fish larvae and adults while being exposed to ATV and the role of CoQ10 in ATV-mediated changes in larvae.

From an environmental perspective, as the concentrations of ATV rise, there is increased concern that aquatic wildlife may be negatively affected by ATV exposure. This study provides evidence that the increase in environmental concentrations of ATV can affect tissue metabolism and thus may have an effect on fish development and

survivability. Decreases in tactile stimulus and spontaneous movement in larvae may be the most significant finding in this study in that it could lead to a diminished capability of fish to respond to situations in their environment like predation. It is also interesting to note that both CoQ10 and PTS significantly recovered ATV mediated reduction in larval whole-body enzymatic activities as well as response to tactile stimuli. Therefore, it may be relevant to pursue more studies regarding the role of antioxidants including CoQ10 and vitamin E in ATV-mediated changes.

References

Abou-Sleiman P, Muqit M, Wood N (2006) Expanding insights of mitochondrial dysfunction in Parkinson's disease. Nat Rev Neurosci 7:207-219.

Adams V, Linke A, Wisloff U, Doering C, Erbs S, Kraenkel N, Witt CC, Labeit S, Mueller-Werdan U, Schuler G, Hambrecht R (2007) Myocardial expression of *murf-1* and *mafbx* after induction of chronic heart failure: Effect on myocardial contractility. Cardiovasc Res 73:120-129.

Airhart MJ, Lee DH, Wilson TD, Miller BE, Miller MN, Skalko RG (2007) Movement disorders and neurochemical changes in zebrafish larvae after bath exposure to fluoxetine (PROZAC). Neurotoxicol Teratol 29:652-664.

Albano C, Muralikrishnan D, Ebadi M (2002) Distribution of coenzyme Q homologues in brain. Neurochem Res 27:359-368.

Al-habsi A (2012). Personal communication.

Amaral IPG, Johnston IA (2011) Insulin-like growth factor (IGF) signalling and genome-wide transcriptional regulation in fast muscle of zebrafish following a single-satiating meal. J Exp Biol 214:2125-2139.

Amsterdam A, Hopkins N (2006) Mutagenesis strategies in zebrafish for identifying genes involved in development and disease. Trends Genet 22:473-478.

Anand V, Cehnniappan, Kalavathy, Uma, Saravanan, Kumar S (2008) Redeeming measure of atorvastatin in the risk factors of cardiovascular disease. Int J Pharmacol 4:305-309.

Andersson T, Forlin L (1992) Regulation of the Cytochrome-P450 Enzyme-System in Fish. Aquat Toxicol 24:1-19.

Asharani PV, Wu YL, Gong Z, Valiyaveettil S (2008) Toxicity of silver nanoparticles in zebrafish models. Nanotechnology 19:255102.

Barros TP, Alderton WK, Reynolds HM, Roach AG, Berghmans S (2008) Zebrafish: an emerging technology for *in vivo* pharmacological assessment to identify potential safety liabilities in early drug discovery. Brit J Pharmacol 154:1400-1413.

Battino M, Ferri E, Gorini A, Villa R, Huertas J, Fiorellap P, Genova M, Lenaz G, MarchettiI M (1990) Natural distribution and occurrence of coenzyme-Q homologs. Membr Biochem 9:179-190.

Bdolah Y, Segal A, Tanksale P, Karumanchi SA, Lecker SH (2007) Atrophy-related ubiquitin ligases *atrogin-1* and *murf-1* are associated with uterine smooth muscle involution in the postpartum period. Am J Physiol Reg Integr Comp Physiol 292:R971-R976.

Benotti MJ, Trenholm RA, Vanderford BJ, Holady JC, Stanford BD, Snyder SA (2009) Pharmaceuticals and endocrine disrupting compounds in US drinking water. Environ Sci Technol 43:597-603.

Bhagavan H, Chopra R (2006) Coenzyme Q10: Absorption, tissue uptake, metabolism and pharmacokinetics. Free Radical Res 40:445-453.

Boehmler W, Carr T, Thisse C, Thisse B, Canfield VA, Levenson R (2007) D4 Dopamine receptor genes of zebrafish and effects of the antipsychotic clozapine on larval swimming behaviour. Genes Brain Behav 6:155-166.

Borowy-Borowski H, Sodja C, Docherty J, Walker P, Sikorska M (2004) Unique technology for solubilization and delivery of highly lipophilic bioactive molecules. J Drug Target 12:415-424.

Bouitbir J, Charles A, Echaniz-Laguna A, Kindo M, Daussin F, Auwerx J, Piquard F, Geny B, Zoll J (2012) Opposite effects of statins on mitochondria of cardiac and skeletal muscles: a omitohormesis' mechanism involving reactive oxygen species and *pgc-1*. Eur Heart J 33:1397-1407.

Cachat J, Stewart A, Grossman L, Gaikwad S, Kadri F, Chung KM, Wu N, Wong K, Roy S, Suciu C, Goodspeed J, Elegante M, Bartels B, Elkhayat S, Tien D, Tan J, Denmark A, Gilder T, Kyzar E, Dileo J, Frank K, Chang K, Utterback E, Hart P, Kalueff AV (2010) Measuring behavioral and endocrine responses to novelty stress in adult zebrafish. Nat Protoc 5:1786-1799.

Caminada D, Zaja R, Smital T, Fent K (2008) Human pharmaceuticals modulate *p-gp1* (ABCB1) transport activity in the fish cell line PLHC-1. Aquat Toxicol 90:214-222.

Campuzano V, Montermini L, Molto M, Pianese L, Cossee M, Cavalcanti F, Monros E, Rodius F, Duclos F, Monticelli A, Zara F, Canizares J, Koutnikova H, Bidichandani S, Gellera C, Brice A, Trouillas P, DeMichele G, Filla A, DeFrutos R, Palau F, Patel P, DiDonato S, Mandel J, Cocozza S, Koenig M, Pandolfo M (1996) Friedreich's ataxia: Autosomal recessive disease caused by an intronic GAA triplet repeat expansion. Science 271:1423-1427.

Cao P, Hanai J, Tanksale P, Imamura S, Sukhatme VP, Lecker SH (2009) Statin-induced muscle damage and atrogin-1 induction is the result of a geranylgeranylation defect. FASEB J 23:2844-2854.

Carballa M, Omil F, Lema J, Llompart M, Garcia-Jares C, Rodriguez I, Gomez M, Ternes T (2004) Behavior of pharmaceuticals, cosmetics and hormones in a sewage treatment plant. Water Res 38:2918-2926.

Chandra D, Liu J, Tang D (2002) Early mitochondrial activation and cytochrome c up-regulation during apoptosis. J Biol Chem 277:50842-50854.

Charlton-Menys V, Durrington PN (2008) Human cholesterol metabolism and therapeutic molecules. Exp Physiol 93:27-42.

Christensen AM, Markussen B, Baun A, Halling-Sørensen B (2009) Probabilistic environmental risk characterization of pharmaceuticals in sewage treatment plant discharges. Chemosphere 77:351-358.

Cilla Jr. DD, Gibson DM, Whitfield LR, Sedman AJ (1996) Pharmacodynamic effects and pharmacokinetics of atorvastatin after administration to normocholesterolemic subjects in the morning and evening. J Clin Pharmacol 36:604-609.

Cleveland BM, Evenhuis JP (2010) Molecular characterization of Atrogin-1/F-box protein-32 (FBXO32) and F-box protein-25 (FBXO25) in rainbow trout (*Oncorhynchus mykiss*): Expression across tissues in response to feed deprivation. Comp Biochem Physiol 157B:248-257.

Corcoran J, Winter MJ, Tyler CR (2010) Pharmaceuticals in the aquatic environment: A critical review of the evidence for health effects in fish. Crit Rev Toxicol 40:287-304.

Corsini A, Bellosta S, Baetta R, Fumagalli R, Paoletti R, Bernini F (1999) New insights into the pharmacodynamic and pharmacokinetic properties of statins. Pharmacol Therapeut 84:413-428.

Crane F, Hatefi Y, Lester R, Widmer C (1957) Isolation of a quinone from beef heart mitochondria. Biochim Biophys Acta 25:220-221.

Csibi A, Cornille K, Leibovitch M, Poupon A, Tintignac LA, Sanchez AMJ, Leibovitch SA (2010) The translation regulatory subunit *eif3f* controls the kinase-dependent mTOR signaling required for muscle differentiation and hypertrophy in mouse. PLoS Biol 5:e8994.

Daughton C, Ternes T (1999) Pharmaceuticals and personal care products in the environment: Agents of subtle change? Environ Health Persp 107:907-938.

DePinieux G, Chariot P, AmmiSaid M, Louarn F, Lejonc J, Astier A, Jacotot B, Gherardi R (1996) Lipid-lowering drugs and mitochondrial function: Effects of HMG-CoA reductase inhibitors on serum ubiquinone and blood lactate/pyruvate ratio. Brit J Clin Pharmaco 42:333-337.

Depledge M (1996) Genetic ecotoxicology: An overview. J Exp Mar Biol Ecol 200:57-66.

Di Bernardo S, Fato R, Casadio R, Fariselli P, Lenaz G (1998) A high diffusion coefficient for coenzyme Q10 might be related to a folded structure. FEBS Lett 426:77-80.

Drapeau P, Saint-Amant L, Buss R, Chong M, McDearmid J, Brustein E (2002) Development of the locomotor network in zebrafish. Prog Neurobiol 68:85-111.

Dubey L, Hesong Z (2006) Atorvastatin inhibits Fas expression in ischemia-reperfusion induced myocardial cell injury. J Res Med Sci 11:137-145.

Eisa-Beygi S, Hatch G, Noble S, Ekker M, Moon TW (2013) The 3-hydroxy-3-methylglutaryl-CoA reductase (HMGCR) pathway regulates developmental cerebral-vascular stability via prenylation-dependent signalling pathway. Dev Biol 373:258-266.

Elhaleem Z, Elsayed A (2011) Coenzyme Q10 Ameliorates statin-related myotoxicity: A biochemical and histological study. J Pharmacol Toxicol 6:258-271.

Ellesat KS, Holth TF, Wojewodzic MW, Hylland K (2012) Atorvastatin up-regulate toxicologically relevant genes in rainbow trout gills. Ecotoxicology 21:1841-1856.

Elmberger PG, Kalen A, Brunk UT, Dallner G (1989) Discharge of newly-synthesized dolichol and ubiquinone with lipoproteins to rat-liver perfusate and to the bile. Lipids 24:919-930.

Endo A (2010) A historical perspective on the discovery of statins. Proc Jpn Acad B-Phys Biol Sci 86:484-493.

Ernster L, Dallner G (1995) Biochemical, physiological and medical aspects of ubiquinone function. Biochim Biophys Acta - Mol Basis Dis 1271:195-204.

Estey C, Chen X, Moon TW (2008) 3-Hydroxy-3-methylglutaryl coenzyme A reductase in rainbow trout: Effects of fasting and statin drugs on activities and mRNA transcripts. Comp Biochem Physiol 147C:386-398.

Fato R, Battino M, Esposti MD, Castelli GP, Lenaz G (1986) Determination of partition and lateral diffusion coefficients of ubiquinones by fluorescence quenching of n-(9-anthroyloxy)stearic acids in phospholipid vesicles and mitochondrial membranes. Biochemistry-US 25:3378-3390.

Fent K, Weston A, Caminada D (2006) Ecotoxicology of human pharmaceuticals. Aquat Toxicol 76:122-159.

Forkers K, Wolaniuk J, Simonsen R, Morishita M, Vadhanavikit S (1985) Biochemical rationale and the cardiac response of patients with muscle disease to therapy with coenzyme-Q10. Proc Nat Acad Sci USA 82:4513-4516.

Fraysse B, Mons R, Garric J (2006) Development of a zebrafish 4-day toxicity of embryo-larval bioassay to assess chemicals. Ecotox Environ Safe 63:253-267.

Fujita T, Tanayama S, Shirakaw Y, Suzuoki Z (1971) Metabolic fate of ubiquinone-7 .1. absorption, excretion and tissue distribution in rats. J Biochem 69:53-61.

Gagné F, Blaise C, André C (2006) Occurrence of pharmaceutical products in a municipal effluent and toxicity to rainbow trout (*Oncorhynchus mykiss*) hepatocytes. Ecotox Environ Safe 64:329-336.

Galasso G, De Rosa R, Piscione F, Iaccarino G, Vosa C, Sorriento D, Piccolo R, Rapacciuolo A, Walsh K, Chiariello M (2010) Myocardial expression of FOXO3a-Atrogin-1 pathway in human heart failure. Eur J Heart Fail 12:1290-1296.

Gazzerro P, Proto MC, Gangemi G, Malfitano AM, Ciaglia E, Pisanti S, Santoro A, Laezza C, Bifulco M (2012) Pharmacological actions of statins: A critical appraisal in the management of cancer. Pharmacol Rev 64:102-146.

Geromel V, Darin N, Chrétien D, Bénit P, DeLonlay P, Rötig A, Munnich A, Rustin P (2002) Coenzyme Q10 and idebenone in the therapy of respiratory chain diseases: Rationale and comparative benefits. Mol Genet Metab 77:21-30.

Gibson DM, Stern RH, Abel RB, (1997) Absolute bioavailability or atorvastatin in man. Pharm Res 14:S253.

Gin P, Hsu A, Rothman S, Jonassen T, Lee P, Tzagoloff A, Clarke C (2003) The Saccharomyces cerevisiae COQ6 gene encodes a mitochondrial flavin-dependent monooxygenase required for coenzyme Q biosynthesis. J Biol Chem 278:25308-25316.

Gold D, Cohen B (2001) Treatment of mitochondrial cytopathies. Semin Neurol 21:309-325.

Gomes M, Lecker S, Jagoe R, Navon A, Goldberg A (2001) Atrogin-1, a muscle-specific F-box protein highly expressed during muscle atrophy. Proc Nat Acad Sci USA 98:14440-14445.

Gotto Jr. AM (2002) Statins: Powerful drugs for lowering cholesterol: Advice for patients. Circulation 105:1514-1516.

Granato M, vanEeden F, Schach U, Trowe T, Brand M, FurutaniSeiki M, Haffter P, Hammerschmidt M, Heisenberg C, Jiang Y, Kane D, Kelsh R, Mullins M, Odenthal J, NussleinVolhard C (1996) Genes controlling and mediating locomotion behavior of the zebrafish embryo and larva. Development 123:399-413.

Greenberg S, Frishman WH (1990) Co-enzyme Q10: a new drug for cardiovascular disease. J Clin Pharmacol 30:596-608.

Gunnarsson L, Jauhiainen A, Kristiansson E, Nerman O, Larsson DGJ (2008) Evolutionary conservation of human drug targets in organisms used for environmental risk assessments. Environ Sci Technol 42:5807-5813.

Hajipour B, Somi MH, Dibazar F, Asl NA, Vatankhah AM (2010) Anti-oxidative effect of simvastatin in liver and lung tissue after hepatic ischemia/reperfusion in rat. J Med Sci 10:66-70.

Halling-Sorensen B, Nielsen S, Lanzky P, Ingerslev F, Lutzhoft H, Jorgensen S (1998) Occurrence, fate and effects of pharmaceutical substances in the environment - A review. Chemosphere 36:357-394.

Han PK, Gong WC, Gill MA (2012) In: http://secure.pharmacytimes.com/lessons/html/dislipidemia.htm#BEHAVIORAL%20OBJECTIVES. Accessed 06/15 2012.

Hanai J, Cao P, Tanksale P, Imamura S, Koshimizu E, Zhao J, Kishi S, Yamashita M, Phillips PS, Sukhatme VP, Lecker SH (2007) The muscle-specific ubiquitin ligase *atrogin-1*/MAFbx mediates statin-induced muscle toxicity. J Clin Invest 117:3940-3951.

Heart and Stroke Foundation (2012) In: http://www.heartandstroke.com/site/c.ikIQLcMWJtE/b.3483991/k.34A8/Statistics.htm#cost. Accessed 05/03 2012.

Helenius IT, Yeh JJ (2012) Small zebrafish in a big chemical pond. J Cell Biochem 113:2208-2216.

Hernando MD, Aguera A, Fernandez-Alba AR (2007) LC-MS analysis and environmental risk of lipid regulators. Anal Bioanal Chem 387:1269-1285.

Ho RH, Kim RB (2005) Transporters and drug therapy: Implications for drug disposition and disease. Clin Pharmacol Ther 78:260-277.

Hsiang B, Zhu Y, Wang Z, Wu Y, Sasseville V, Yang W, Kirchgessner T (1999) A novel human hepatic organic anion transporting polypeptide (OATP2) - Identification of a liver-specific human organic anion transporting polypeptide and identification of rat and human hydroxymethylglutaryl-CoA reductase inhibitor transporters. J Biol Chem 274:37161-37168.

Huckins J, Tubergen M, Manuweera G (1990) Semipermeable-membrane devices containing model lipid - a new approach to monitoring the bioavailability of lipophilic contaminants and estimating their bioconcentration potential. Chemosphere 20:533-552.

IMS, Top Line Market Data (2011) In: http://www.imshealth.com/deployedfiles/ims/Global/Content/Corporate/Press%20Room/TopLine%20Market%20Data%20&%20Trends/Top_20_Global_Products.pdf. Accessed 08/07 2012.

Itagaki M, Takaguri A, Kano S, Kaneta S, Ichihara K, Satoh K (2009) Possible mechanisms underlying statin-induced skeletal muscle toxicity in L6 fibroblasts and in rats. J Pharmacol Sci 109:94-101.

Jackevicius CA, Chou MM, Ross JS, Shah ND, Krumholz HM (2012) Generic atorvastatin and health care costs. New Engl J Med 366:201-204.

Jelic A, Gros M, Ginebreda A, Cespedes-Sanchez R, Ventura F, Petrovic M, Barcelo D (2011) Occurrence, partition and removal of pharmaceuticals in sewage water and sludge during wastewater treatment. Water Res 45:1165-1176.

Jemiota-Rzeminska M, Latowski D, Strzalka K (2001) Incorporation of plastoquinone and ubiquinone into liposome membranes studied by HPLC analysis. The effect of side chain length and redox state of quinone. Chem Phys Lipids 110:85-94.

Jonassen T, Clarke CF (2001) Genetic analysis of coenzyme Q biosynthesis. CRC press, Boca Raton.

Kalen A, Norling B, Appelkvist E, Dallner G (1987) Ubiquinone biosynthesis by the microsomal fraction from rat-liver. Biochim Biophys Acta 926:70-78.

Key PB, Hoguet J, Chung KW, Venturella JJ, Pennington PL, Fulton MH (2009) Lethal and sublethal effects of simvastatin, irgarol, and PBDE-47 on the estuarine fish, *Fundulus heteroclitus*. J Environ Sci Health B 44:379-382.

Kiernan JA (1999). In: Histological and Histochemical Methods: Theory and Practice, 3rd edition, Oxford.

Kishi T, Yamada A, Okamatsu S, Sunagawa K (2009) Atorvastatin might improve ventricular electrostability and decelerate the deterioration of renal function in patients with heart failure and diabetes mellitus. J Cardiol 53:341-348.

Kolpin D, Furlong E, Meyer M, Thurman E, Zaugg S, Barber L, Buxton H (2002) Pharmaceuticals, hormones, and other organic wastewater contaminants in US streams, 1999-2000: A national reconnaissance. Environ Sci Technol 36:1202-1211.

Kommuru T, Ashraf M, Khan M, Reddy I (1999) Stability and bioequivalence studies of two marketed formulations of coenzyme Q(10) in beagle dogs. Chem Pharm Bull 47:1024-1028.

Konig J, Cui Y, Nies A, Keppler D (2000) A novel human organic anion transporting polypeptide localized to the basolateral hepatocyte membrane. Am J Physiol Gastrointest Liver Physiol 278:G156-G164.

Kurokawa H, Aoki Y, Nakamura S, Ebe Y, Kobayashi D, Tanaka M (2006) Time-lapse analysis reveals different modes of primordial germ cell migration in the medaka *Oryzias latipes*. Dev Growth Diff 48:209-221.

Kyoto Encyclopedia of Genes and Genomes (2012) In: http://www.genome.jp/kegg-bin/show_pathway?dre00130+M00128. Accessed 08/14 2012.

Lahti M, Brozinski J, Jylha A, Kronberg L, Oikari A (2011) Uptake from water, biotransformation, and biliary excretion of pharmaceuticals by rainbow trout. Environ Toxicol Chem 30:1403-1411.

Lee H, Peart TE, Lewina Svoboda M, Backus S (2009) Occurrence and fate of rosuvastatin, rosuvastatin lactone, and atorvastatin in Canadian sewage and surface water samples. Chemosphere 77:1285-1291.

Lee J, Na D, Ju B (2007) Zebrarish chorion as an extracellular matrix for cell culture. IFMBE Proc 2006, Vol 14, Pts 1-6 14:3379-3381.

Lemasters J, Qian T, Bradham C, Brenner D, Cascio W, Trost L, Nishimura Y, Nieminen A, Herman B (1999) Mitochondrial dysfunction in the pathogenesis of necrotic and apoptotic cell death. J Bioenerg Biomembr 31:305-319.

LeMoine CMR, Walsh PJ (2013) Ontogeny of ornithine-urea cycle gene expression in zebrafish (*Danio rerio*). Am J Physiol Regul Integr Comp Physiol 304:R991-R1000.

Lenaz G, Fato R, Castelluccio C, Genova ML, Bovina C, Estornell E, Valls V, Pallotti F, Parenti Castelli G (1993) The function of coenzyme Q in mitochondria. Clin Investigator, Supplement 71:S 66-S 70.

Lennernäs H (2003) Clinical pharmacokinetics of atorvastatin. Clin Pharmacokinet 42:1141-1160.

Lessman CA (2011) The developing zebrafish (*Danio rerio*): A vertebrate model for high-throughput screening of chemical libraries. Birth Defects Res C - Embryo Today: Reviews 93:268-280.

Li H, Kedar V, Zhang C, McDonough H, Arya R, Wang D, Patterson C (2004) *Atrogin-1*/muscle atrophy F-box inhibits calcineurin-dependent cardiac hypertrophy by participating in an SCF ubiquitin ligase complex. J Clin Invest 114:1058-1071.

Lockwood B, Bjerke S, Kobayashi K, Guo S (2004) Acute effects of alcohol on larval zebrafish: a genetic system for large-scale screening. Pharmacol Biochem Behav 77:647-654.

Lyons KS, McVeigh GE, Harbinson MT (2011) Statins in heart failure-where do we stand? Cardiovasc Drugs Ther 25:99-104.

Maggini M, Raschetti R, Traversa G, Bianchi C, Caffari B, Da Cas R, Panei P (2004) The cerivastatin withdrawal crisis: a "post-mortem" analysis. Health Policy 69:151-157.

Mancini A, Festa R, Raimondo S, Pontecorvi A, Paolo G (2011) Hormonal influence on coenzyme Q_{10} levels in blood plasma. Int J Mol Sci 12:9216-9225.

Marcoff L, Thompson PD (2007) The role of coenzyme Q10 in statin-associated myopathy - A systematic review. J Am Coll Cardiol 49:2231-2237.

Massarsky A, Dupuis L, Tylor J, Eisa-Beygi S, Strek L, Vance L, Moon T (2013) Assessment of nanosilver toxicity during zebrafish (Danio rerio) development. Chemosphere 92(1): 59-66.

McClelland G, Dalziel A, Fragoso N, Moyes C (2005) Muscle remodeling in relation to blood supply: implications for seasonal changes in mitochondrial enzymes. J Exp Biol 208:515-522.

McClintock D, Santore M, Lee V, Brunelle J, Budinger G, Zong W, Thompson C, Hay N, Chandel N (2002) *Bcl-2* family members and functional electron transport chain regulate oxygen deprivation-induced cell death. Mol Cell Biol 22:94-104.

McGrath P, Li C (2008) Zebrafish: a predictive model for assessing drug-induced toxicity. Drug Discov Today 13:394-401.

McKenney JM (2003) Pharmacologic characteristics of statins. Clin Cardiol 26:III32-III38.

Metcalfe CD, Miao X-, Koenig BG, Struger J (2003) Distribution of acidic and neutral drugs in surface waters near sewage treatment plants in the lower Great Lakes, Canada. Environ Toxicol Chem 22:2881-2889.

Miao X, Metcalfe CD (2003) Determination of cholesterol-lowering statin drugs in aqueous samples using liquid chromatography-electrospray ionization tandem mass spectrometry. J Chromatogr A 998:133-141.

Milan D, Peterson T, Ruskin J, Peterson R, MacRae C (2003) Drugs that induce repolarization abnormalities cause bradycardia in zebrafish. Circulation 107:1355-1358.

Molyneux SL, Florkowski CM, Richards AM, Lever M, Young JM, George PM (2009) Coenzyme Q10; an adjunctive therapy for congestive heart failure. N Z Med J 122:74-79.

Musumeci O, Naini A, Slonim A, Skavin N, Hadjigeorgiou G, Krawiecki N, Weissman B, Tsao C, Mendell J, Shanske S, De Vivo D, Hirano M, DiMauro S (2001) Familial cerebellar ataxia with muscle coenzyme Q10 deficiency. Neurology 56:849-855.

Muthukumaran K, Leahy S, Harrison K, Sikorska M, Sandhu JK, Cohen J, Keshan C, Lopatin D, Miller H, Borowy-Borowski H, Lanthier P, Weinstock S, Pandey S (2014) Orally delivered water soluble Coenzyme Q10 (Ubisol-Q10) blocks on-going neurodegeneration in rats exposed to paraquat: Potential for therapeutic application in Parkinson's disease. BMC Neurosci 15.

Nagel R (2002) DarT: The embryo test with the zebrafish *Danio rerio* - a general model in ecotoxicology and toxicology. Altex Altern Tierexp 19:38-48.

Ottmar KJ, Colosi LM, Smith JA (2010) Sorption of statin pharmaceuticals to wastewater-treatment biosolids, terrestrial soils, and freshwater sediment. J Environ Eng-Asce 136:256-264

Palinski W (2001) New evidence for beneficial effects of statins unrelated to lipid lowering. Arterioscl Throm Vas 21:3-5.

Pan H, Triscari J, Devault A, Smith S, Wangiverson D, Swanson B, Willard D (1991) Pharmacokinetic interaction between propranolol and the HMG-CoA Reductase inhibitors pravastatin and lovastatin. Brit J Clin Pharmacol 31:665-670.

Pérez F, Granger BE (2007) IPython: A system for interactive scientific computing. Comput Sci Eng 9:21-29.

Pilsl A, Winklhofer KF (2012) Parkin, pink1 and mitochondrial integrity: Emerging concepts of mitochondrial dysfunction in Parkinson's disease. Acta Neuropathol 123:173-188.

Pojana G, Fantinati A, Marcomini A (2011) Occurrence of environmentally relevant pharmaceuticals in Italian drinking water treatment plants. Int J Environ An Ch 91:537-552.

Prueksaritanont T, Subramanian R, Fang X, Ma B, Qiu Y, Lin J, Pearson P, Baillie T (2002) Glucuronidation of statins in animals and humans: A novel mechanism of statin lactonization. Drug Metab Dispos 30:505-512.

Prueksaritanont T, Tang C, Qiu Y, Mu L, Subramanian R, Lin J (2002) Effects of fibrates on metabolism of statins in human hepatocytes. Drug Metab Dispos 30:1280-1287.

Prueksaritanont T, Zhao J, Ma B, Roadcap B, Tang C, Qiu Y, Liu L, Lin J, Pearson P, Baillie T (2002) Mechanistic studies on metabolic interactions between gemfibrozil and statins. J Pharmacol Exp Ther 301:1042-1051.

Puigserver P, Spiegelman B (2003) Peroxisome proliferator-activated receptor-gamma coactivator 1 alpha (*pgs-1* alpha): Transcriptional coactivator and metabolic regulator. Endocr Rev 24:78-90.

Quinn PJ, Esfahani MA (1980) Ubiquinones have surface-active properties suited to transport electrons and protons across membranes. Biochem J 185:715-722.

Randall D, Connell D, Yang R, Wu S (1998) Concentrations of persistent lipophilic compounds in fish are determined by exchange across the gills, not through the food chain. Chemosphere 37:1263-1270.

Rawson D, Zhang T, Kalicharan D, Jongebloed W (2000) Field emission scanning electron microscopy and transmission electron microscopy studies of the chorion, plasma membrane and syncytial layers of the gastrula-stage embryo of the zebrafish *Brachydanio rerio*: A consideration of the structural and functional relationships with respect to cryoprotectant penetration. Aquat Res 31:325-336.

Rea PA (2008) Statins: From fungus to pharma - The curiosity of biochemists, mixed with some obvious economic incentives, created a family of powerful cardiovascular drugs. Am Sci 96:408-415.

Rooyackers O, Adey D, Ades P, Nair K (1996) Effect of age on in vivo rates of mitochondrial protein synthesis in human skeletal muscle. Proc Nat Acad Sci USA 93:15364-15369.

Rotig A, Appelkvist E, Geromel V, Chretien D, Kadhom N, Edery P, Lebideau M, Dallner G, Munnich A, Ernster L, Rustin P (2000) Quinone-responsive multiple respiratory-chain dysfunction due to widespread coenzyme Q(10) deficiency. Lancet 356:391-395.

Sacheck JM, Ohtsuka A, McLary SC, Goldberg AL (2004) IGF-I stimulates muscle growth by suppressing protein breakdown and expression of atrophy-related ubiquitin ligases, *atrogin-1* and *murf1*. Am J Physiol Endocrinol Metab 287:E591-E601.

Sacheck J, Ohtsuka A, McLary S, Goldberg A (2004) IGF-I stimulates muscle growth by suppressing protein breakdown and expression of atrophy-related ubiquitin ligases, *atrogin-1* and *murf1*. Am J Physiol Endocrinol Metab 287:E591-E601.

Salem M, Kenney PB, Rexroad EIII, Yao J (2006) Microarray gene expression analysis in atrophying rainbow trout muscle: a unique nonmammalian muscle degradation model. Physiol Genomics 28:33-45.

Sathyapalan T, Atkin SL (2010) Evidence for statin therapy in polycystic ovary syndrome. Ther Adv Endocrinol Metabolis 1:15-22.

Schachter M (2005) Chemical, pharmacokinetic and pharmacodynamic properties of statins: an update. Fund Clin Pharmacol 19:117-125.

Schiaffino S, Dyar KA, Ciciliot S, Blaauw B, Sandri M (2013) Mechanisms regulating skeletal muscle growth and atrophy. FEBS J 280:4294-4314.

Schindler S, Lichtenthaler H, Dizengremel P, Rustin P, Lance C (1984) Distribution and significance of different ubiquinone homologues in purified mitochondria and intact plant tissue. Dev Plant Biol 9: 267-272.

Schock EN, Ford WC, Midgley KJ, Fader JG, Giavasis MN, McWhorter ML (2012) The effects of carbaryl on the development of zebrafish (*Danio rerio*) embryos. Zebrafish 9:169-178.

Seiliez I, Panserat S, Skiba-Cassy S, Fricot A, Vachot C, Kaushik S, Tesseraud S (2008) Feeding status regulates the polyubiquitination step of the ubiquitin-proteasome-dependent proteolysis in rainbow trout (*Oncorhynchus mykiss*) muscle. J Nutr 138:487-491.

Shapiro S, Saliou C (2001) Role of vitamins in skin care. Nutrition 17:839-844.

Somayajulu M, McCarthy S, Hung M, Sikorska M, Borowy-Borowski H, Pandey S (2005) Role of mitochondria in neuronal cell death induced by oxidative stress; neuroprotection by Coenzyme Q(10). Neurobiol Dis 18:618-627.

Somayajulu-Nitu M, Sandhu JK, Cohen J, Sikorska M, Sridhar TS, Matei A, Borowy-Borowski H, Pandey S (2009) Paraquat induces oxidative stress, neuronal loss in substantia nigra region and Parkinsonism in adult rats: Neuroprotection and amelioration of symptoms by water-soluble formulation of Coenzyme Q(10). BMC Neurosci 10:88.

Spinazzi M, Casarin A, Pertegato V, Salviati L, Angelini C (2012) Assessment of mitochondrial respiratory chain enzymatic activities on tissues and cultured cells. Nat Protoc 7:1235-1246.

Spisni A, Masotti L, Lenaz G, Bertoli E, Pedulli GF, Zannoni C (1978) Interactions between ubiquinones and phospholipid bilayers. A spin-label study. Arch Biochem Biophys 190:454-458.

Spitsbergen JM, Kent ML (2003) The state of the art of the zebrafish model for toxicology and toxicologic pathology research - advantages and current limitations. Toxicol Pathol 31:62-87.

Stancu C, Sima A (2001) Statins: mechanism of action and effects. J Cell Mol Med 5:378-387.

Stern R, Gibson D, Whitfield L (1998) Cimetidine does not alter atorvastatin pharmacokinetics or LDL-cholesterol reduction. Eur J Clin Pharmacol 53:475-478.

St-Pierre J, Lin J, Krauss S, Tarr P, Yang R, Newgard C, Spiegelman B (2003) Bioenergetic analysis of peroxisome proliferator-activated receptor gamma coactivators 1 alpha and 1 beta (PGC-1 alpha and PGC-1 beta) in muscle cells. J Biol Chem 278:26597-26603.

St-Pierre J, Drori S, Uldry M, Silvaggi JM, Rhee J, Jager S, Handschin C, Zheng K, Lin J, Yang W, Simon DK, Bachoo R, Spiegelman BM (2006) Suppression of reactive oxygen species and neurodegeneration by the *pgc-1* transcriptional coactivators. Cell 127:397-408.

Stumpf M, Ternes T, Wilken R, Rodrigues S, Baumann W (1999) Polar drug residues in sewage and natural waters in the state of Rio de Janeiro, Brazil. Sci Total Environ 225:135-141.

Ternes T (1998) Occurrence of drugs in German sewage treatment plants and rivers. Water Res 32:3245-3260.

Thompson P, Clarkson P, Karas R (2003) Statin-associated myopathy. JAMA-J Am Med Assoc 289:1681-1690.

Thorpe J, Doitsidou M, Ho S, Raz E, Farber S (2004) Germ cell migration in zebrafish is dependent on HMGCoA reductase activity and prenylation. Dev Cell 6:295-302.

Ton C, Stamatiou D, Dzau V, Liew C (2002) Construction of a zebrafish cDNA microarray: gene expression profiling of the zebrafish during development. Biochem Biophys Res Commun 296:1134-1142.

Traber M, Lane J, Lagmay N, Kayden H (1992) Studies on the transfer of tocopherol between lipoproteins. Lipids 27:657-663.

Tran UC, Clarke CF (2007) Endogenous synthesis of coenzyme Q in eukaryotes. Mitochondrion 7:S62-S71.

Ulrich EL, Girvin ME, Cramer WA, Markley JL (1985) Location and mobility of ubiquinones of different chain lengths in artificial membrane vesicles. Biochemistry (NY) 24:2501-2508.

Vagelos P (1991) Are prescription drug prices high. Science 252:1080-1084.

Valle I, Alvarez-Barrientos A, Arza E, Lamas S, Monsalve M (2005) *pgc-1* alpha regulates the mitochondrial antioxidant defense system in vascular endothelial cells. Cardiovasc Res 66:562-573.

Vasyuk YA, Perlamutrov YN, Shkolnik MN, Shkolnik EL (2010) Possibilities of atorvastatin in complex management of extensive psoriasis in patients with arterial hypertension. Kardiologiya 50:37-46.

Walker M, Peterson R (1991) Potencies of polychlorinated dibenzo-para-dioxin, dibenzofuran, and biphenyl congeners, relative to 2,3,7,8-tetrachlorodibenzo-para-dioxin, for producing early life stage mortality in rainbow-trout (*Oncorhynchus mykiss*). Aquat Toxicol 21:219-238.

Wang J, Salem M, Qi N, Kenney PB, Rexroad EIII, Yao J (2011) Molecular characterization of the *murf* genes in rainbow trout: Potential role in muscle degradation. Comp Biochem Physiol 158B:208-215.

Wolf J, Wolfe M (2005) A brief overview of nonneoplastic hepatic toxicity in fish. Toxicol Pathol 33:75-85.

Wu X, Whitfield L, Stewart B (2000) Atorvastatin transport in the Caco-2 cell model: Contributions of P-glycoprotein and the proton-monocarboxylic acid co-transporter. Pharmacol Res 17:209-215.

Wu Y, Lin CY, Tsai M, Chen Y, Lu Y, Huang C, Cheng C, Hwang SL (2011) beta-Lapachone induces heart morphogenetic and functional defects by promoting the death of erythrocytes and the endocardium in zebrafish embryos. J Biomed Sci 18:70.

Xi Y, Ryan J, Noble S, Yu M, Yilbas AE, Ekker M (2010) Impaired dopaminergic neuron development and locomotor function in zebrafish with loss of *pink1* function. Eur J Neurosci 31:623-633.

Zhang X, Oakes KD, Cui S, Bragg L, Servos MR, Pawliszyn J (2010) Tissue-specific *in vivo* bioconcentration of pharmaceuticals in rainbow trout (*Oncorhynchus mykiss*) using space-resolved solid-phase microextraction. Environ Sci Technol 44:3417-3422.

Zhdanova I, Wang S, Leclair O, Danilova N (2001) Melatonin promotes sleep-like state in zebrafish. Brain Res 903:263-268.

Zyzynska-Granica B, Koziak K (2012) Identification of suitable reference genes for real-time PCR analysis of statin-treated human umbilical vein endothelial cells. PLoS One 7:e51547.

Appendix A – Matlab Commends

```
clear  displacement  histarray ytophalf latencytotop yhist
% import file into workspace as MATRIX
% input data file name here:
filename='Control1';
eval(['file=',filename,';']);
%file=data;  %imported VP (x,y) data in 'm'
tcol=1; % time
xcol=2; % x in 'cm'
ycol=3; % y in 'cm'
samples=size(file,1);  % 1500 for 5min, 3000 for 10min
timedelta=file(2,tcol)-file(1,tcol);  % assume consistent sample frequency e.g. 5 frames/sec
tmax=max(file(:,tcol));
time=timedelta*(1:samples-1);

%tank dimensions in cm
xmin=-15;  xmax=15;
ymin=-10;  ymax=10; ywater=11;
%starting point
xp=file(1,xcol); yp=file(1,ycol);

%% %calculate first latency to reach top half of tank (i.e. y>0)
ytophalf=find(file(:,ycol)>0);
latencytotop=timedelta*min(ytophalf);

%% %2D histogram %%%

binx=(xmin:xmax)';   % ie 1cm bin size
biny=(ymin:ymax)';
binnumx=length(binx); binnumy=length(biny);

histarray=zeros(binnumx,binnumy);

for a=1:samples;
   for b=1:binnumx-1;
   if file(a,xcol)>binx(b) & file(a,xcol)<binx(b+1)
      c=1;
```

```
      for c=1:binnumy-1;
         if file(a,ycol)>biny(c) & file(a,ycol)<biny(c+1)
            histarray(b,c)=histarray(b,c)+1;
         end
      end
   end
   end
end

notvisited=size(find(histarray==0),1);
fractionvisited=((binnumx*binnumy)-notvisited)/(binnumx*binnumy);
%% displacement, speed
displacement=sqrt((diff(file(:,xcol))).^2+(diff(file(:,ycol))).^2);  % get point-point dist
totaldisplacement=sum(displacement);
speed=displacement/timedelta; % speed in cm/sec
avgspeed=mean(speed);

sbins=(0:50);  %i.e. centers of bins, 1cm/sec resolution
[speedhist,speedbins]=hist(speed,sbins);

%% y histograms
bins=(ymin:ymax);  %i.e. centers of bins, 1cm resolution
[yhist,distbins]=hist(file(:,ycol),bins);
maxyfish=max(file(:,ycol));
minyfish=min(file(:,ycol));
yhistmode=distbins(find(yhist==max(yhist)));
yfishmean=mean(file(:,ycol));
yfishstd=std(file(:,ycol));
yhigh=timedelta*size(find(file(:,ycol)>0),1); % time above y=0

%% y above 0 over time

yfish=file(:,ycol);
ii=1;
for tbins=60:60:round(tmax) % one minute intervals
   time_index=find((tbins-60)<time & time<tbins);
   yhigh_index=find(yfish(time_index)>0);
   yhightime(ii)=timedelta*size(yhigh_index,1); % time above y=0
   ii=ii+1;
end;
```

```
%% mean speed over time
ii=1;
for tbins=60:60:round(tmax) % one minute intervals
   time_index=find((tbins-60)<time & time<tbins);
   speed_mean_time(ii)=mean(speed(time_index));
   speed_sd_time(ii)=std(speed(time_index));
   ii=ii+1;
end;


%% output
FIGURE4_speed_distn=zeros(length(speedbins),2);
FIGURE4_speed_distn(:,1)=speedbins;
FIGURE4_speed_distn(:,2)=timedelta*speedhist;
FIGURE6_speed_time=zeros(length(speed_mean_time),3);
FIGURE6_speed_time(:,1)=(1:length(speed_mean_time))';
FIGURE6_speed_time(:,2)=speed_mean_time;
FIGURE6_speed_time(:,3)=speed_sd_time;

%% %%%%%%%  PLOTTING %%%%%%%%%%%%%%%%%%%
figure(1);
plot(file(:,xcol),file(:,ycol)); % data in cm [0 0 0] for black,[0 0 1] for blue
hold on;
%axis([xmin xmax ymin ymax]);
axis([xmin xmax ymin ymax]);
set(gca,'DataAspectRatio',[1 1 1]);  % set uniform aspect ratio
xlabel('X (cm)'); ylabel('Y (cm)');
text(-10,-8,['latency to top half = ',num2str(latencytotop),'sec']);
title(['total displacement: ', num2str(round(10*totaldisplacement)/10),' cm']);
hold off;

figure(2);
surface(binx,biny,histarray','EdgeAlpha',0); view(2); %no grid lines, default 2D view
axis([xmin xmax ymin ymax]);
set(gca,'DataAspectRatio',[1 1 1]);  % set uniform aspect ratio
xlabel('X (cm)'); ylabel('Y (cm)');
title('2D HISTOGRAM');
hold off;
```

```
figure(3);   % distribution of y-values
bar(distbins,yhist/samples); hold on;  % scale with time bin to assess dwell-times
title('distribution over tank depth (y)');
text(5,0.2,['y mean = ',num2str(yfishmean)]);
text(5,0.18,['y std = ',num2str(yfishstd)]);
text(5,0.16,['t (y>0) = ',num2str(yhigh),'sec']);
xlabel('y (cm)'); ylabel('relative freq');
hold off;

figure(4);   % velocity trace in time
bar(speedbins,timedelta*speedhist); hold on;
%plot(speedbins,cumsum(timedelta*speedhist),'r');
xlabel('speed (cm/s)'); ylabel('time');
title('distribution of speeds');
hold off;

% figure(4);   % velocity trace in time
% plot(file(2:samples,tcol),speed); hold on;
% xlabel('time (sec)'); ylabel('speed (cm/s)');
% title(['average speed: ',num2str(avgspeed),'cm/s']);
% %title('instantaneous speed ');
% hold off;

figure(5);   % y high time
bar(yhightime); hold on;  % scale with time bin to assess dwell-times
title('y>0 over time');
xlabel('time (sec)'); ylabel('trial time (sec)');
hold off;

figure(6);   % y high time
subplot(2,1,1)
bar(speed_mean_time); hold on;  % scale with time bin to assess dwell-times
title('mean speed over time');
xlabel('time (sec)'); ylabel('speed (cm/sec)');
hold off;
subplot(2,1,2)
bar(speed_sd_time); hold on;  % scale with time bin to assess dwell-times
title('SD speed over time');
xlabel('time (sec)');
hold off
```

Appendix B – Python Commends

```
import import numpy as np
import matplotlib.pyplot as plt
from glob import glob
import os

def distance(point_1, point_2):
    """Returns euclidean distance between two points."""
    dist = point_1-point_2
    return sqrt(np.dot(dist,dist))

def percent_done(i, length, percent_increments=5):
    """Tells when a multiple of percent_increments done, about.
    An example would be every 5%.
    Useful for long loops that take  their sweet time.
    """
    incr = int(length*percent_increments/100.)
    if (i+1)%incr == 0:
            print '%s of %s done. %s percent done.' % \
                (i+1, length, int(round((i+1.)/length*100)))
    elif i == length-1:
        print '100% done'

def run_all(out_dir):
    files = glob(out_dir+'/*txt')
    fout = open(out_dir+'Marilyn_data.csv', 'w')
    fout.write('Fish,latency,number of transitions,time above,mean entry duration,top to
bottom ratio, total distance, top to bottom distance ratio, max speed, mean speed, num
times frozen,duration frozen,frozen times\n')
```

```
    for i, filename in enumerate(files):
        base = os.path.basename(filename)[:-4]
        print 'Fish %s' % base
        datum = examine_file(filename)
        fout.write(base+',')
        for j in range(len(datum)-1):
            fout.write(str(datum[j]))
            fout.write(',')
        fout.write('\n')
        try:
            percent_done(i, len(files))
        except:
            pass
    fout.close()

def examine_file(filename):
    """This can be used to give all examinations needed."""
    data = init_txt_file(filename)
    base = os.path.basename(filename)[:-4]
    lat = latency(data)
    transitions = transitions_to_top(data)
    above_time = time_above(data)
    mean_entry_duration = average_entry_duration(above_time,
                                        transitions)
    top2bottom = top_to_bottom_ratio(above_time, data)
    tot_distance = total_distance(data)
    top2bott_dist_ratio = top_to_bott_dist_ratio(distance_on_top(data),
                                        tot_distance)
    max_speed = np.amax(velocity_list(data))
    mean_speed = np.mean(velocity_list(data))
    frozen_times = find_frozen(data, limit=0.0)
```

```
    frozen_x_times = times_frozen(frozen_times)
    frozen_this_long = length_time_frozen(frozen_times)
    coord = coordinates(data)
    plot_trace_plot(coord, os.path.dirname(filename)+'/Fig1_'+base)
    make_heatmap(coord, os.path.dirname(filename)+'/Fig2_'+base)
    return lat, transitions, above_time, mean_entry_duration, \
          top2bottom, tot_distance, top2bott_dist_ratio, max_speed, \
          mean_speed, frozen_x_times, frozen_this_long, frozen_times, \
          coord

def init_txt_file(filename):
    """Initiates the file"""
    f = open(filename, 'r')
    lines = f.readlines()
    data = []
    for i in range(len(lines)):
        data.append(lines[i].split())
        if lines[i][:3] == '360':
            print lines[i]
            return data[7:]

def latency(data):
    """Latency to reach the upper portion of the tank"""
    for i in range(len(data)):
        if float(data[i][2]) > 0.0:
            return data[i][0]

def transitions_to_top(data):
    """Number of times the fish goes above y = 0"""
    count = 0
    for i in range(len(data)):
```

```
        if float(data[i][2]) > 0.0 and float(data[i-1][2]) <= 0.0:
            count += 1
    return count


def time_above(data):
    """Total time spent in the upper portion of the tank. Upon a transition,
    time starts at half the amount of time between t1 and t2.
    """
    times = []
    for i in range(1, len(data)):
        t1, t2 = float(data[i-1][2]), float(data[i][2])
        if t2 > 0.0 and t1 <= 0.0:
            times.append([str((float(data[i][0])+float(data[i-1][0]))/2)])
        elif t1 > 0.0 and t2 <= 0.0:
            times[-1].append(str((float(data[i][0])+float(data[i-1][0]))/2))
    if len(times) > 0 and len(times[-1]) == 1:
        times[-1].append(data[-1][0])
    time = 0
    for i in range(len(times)):
        time += float(times[i][1]) - float(times[i][0])
    return time


def average_entry_duration(time_above, transitions_to_top):
    """Time spent in the top divided by the number of entries to the top."""
    if transitions_to_top != 0:
        return time_above/transitions_to_top
    else:
        return 0.


def top_to_bottom_ratio(time_above, data):
    """The ratio of top to bottom: amount of time on the top divided by the
```

```
    amount of time on the bottom.
    """
    return time_above/(float(data[-1][0]) - time_above)

def distance_on_top(data):
    """Total time spent in the upper portion of the tank. Upon a transition,
    time starts at half the amount of time between t1 and t2.
    """
    distances = 0
    for i in range(1, len(data)):
        t1, t2 = float(data[i-1][2]), float(data[i][2])
        if (t2 > 0.0 and t1 <= 0.0) or (t1 > 0.0 and t2 <= 0.0):
            dist = distance(np.array([float(data[i-1][1]), float(data[i-1][2])]),
                            np.array([float(data[i][1]), float(data[i][2])]))
            distances += dist/2
        elif t1 > 0.0 and t2 > 0.0:
            dist = distance(np.array([float(data[i-1][1]), float(data[i-1][2])]),
                            np.array([float(data[i][1]), float(data[i][2])]))
            distances += dist
    return distances

def total_distance(data):
    """Give total distance the fish traveled"""
    dist = 0
    for i in range(1, len(data)):
        dist += distance(np.array([float(data[i-1][1]), float(data[i-1][2])]),
                         np.array([float(data[i][1]), float(data[i][2])]))
    return dist

def top_to_bott_dist_ratio(distance_on_top, total_distance):
    return distance_on_top/(total_distance - distance_on_top)
```

```
def velocity_list(data):
    """Returns a list of velocities, so that the mean and max velocities
    can be measured, maybe even freeze points...
    """
    velocities = []
    for i in range(1, len(data)):
        dist = distance(np.array([float(data[i-1][1]), float(data[i-1][2])]),
                        np.array([float(data[i][1]), float(data[i][2])]))
        time = float(data[i][0]) - float(data[i-1][0])
        velocities.append(dist/time)
    return np.array(velocities)


def find_frozen(data, limit=0.0):
    """Counts as frozen when fish didn't move for at least two seconds.
    Not moving is defined as ..."""
    velocities = []
    for i in range(1, len(data)):
        dist = distance(np.array([float(data[i-1][1]), float(data[i-1][2])]),
                        np.array([float(data[i][1]), float(data[i][2])]))
        time = float(data[i][0]) - float(data[i-1][0])
        velocities.append([float(data[i][0]), dist/time])
    freezes = []
    times = []
    for i in range(len(velocities)):
        if (velocities[i][1] <= limit and velocities[i-1][1] > limit) or \
           (velocities[i][1] <= limit and i==0):
            freezes.append([velocities[i][0] - velocities[i-1][0]])
            times.append([velocities[i][0]])
        elif velocities[i][1] <= limit and velocities[i-1][1] <= limit:
            freezes[-1].append(velocities[i][0] - velocities[i-1][0])
```

```
            times[-1].append(velocities[i][0])
    list_times = []
    for i in range(1, len(freezes)):
        if sum(freezes[i]) >= 2.0:  # 2 seconds is considered frozen.
            list_times.append([times[i][0], times[i][-1]])
 #   print len(list_times), list_times
    list_in_min = []
    for i in range(len(list_times)):
        list_in_min.append([sec2min(list_times[i][0]), sec2min(list_times[i][1])])
  #  print len(list_times), list_in_min
    return list_times

def times_frozen(frozen_times):
    """This assumes find_frozen worked, although unlikely.
    Needs to be double checked.
    Returns amount of times the fish freezes for at least 2 seconds.
    """
    return len(frozen_times)

def length_time_frozen(frozen_times):
    """This assumes find_frozen worked, although unlikely.
    Needs to be double checked.
    Returns total amount of time the fish was frozen.
    """
    time_sum = 0
    for i in range(len(frozen_times)):
        time_sum += frozen_times[i][1] - frozen_times[i][0]
    return time_sum

def sec2min(time):
    l = time/60.
```

```
    return '%s min %s s' % (int(l), ((l-int(l))*60))

def plot_trace_plot((x,y), name2save):
    plt.plot(x,y)
    plt.xlabel('X (cm)')
    plt.ylabel('Y (cm)')
    plt.xlim(xmax=15)
    plt.xlim(xmin=-15)
    plt.ylim(ymax=10)
    plt.ylim(ymin=-10)
##    plt.plot([x1,x2,x3,x4,x1],[y1,y2,y3,y4,y1])
    plt.savefig(name2save+'.png', dpi=None,
                facecolor='w', edgecolor='w', orientation='portrait',
                papertype=None, format=None, transparent=True,
                bbox_inches=None, pad_inches=0.1)
##    plt.show()
    plt.clf()
    return

def make_heatmap((x,y), name2save):
    """Plots heatmap for a x and y coordinates."""
    x,y = np.array(x), np.array(y)
    plt.hist2d(x,y,bins=(30,20), range=([[-15,15],[-10,10]]))
    plt.xlabel('X (cm)')
    plt.ylabel('Y (cm)')
    plt.colorbar()
    plt.savefig(name2save+'.png', dpi=None,
                facecolor='w', edgecolor='w', orientation='portrait',
                papertype=None, format=None, transparent=True,
                bbox_inches=None, pad_inches=0.1)
##    plt.show()
```

```
    plt.clf()
    return

def coordinates(data):
    """Returns all x,y coordinates, independent of time."""
    x, y = [], []
    for i in range(len(data)):
        x.append(float(data[i][1]))
        y.append(float(data[i][2]))
    return np.array(x), np.array(y)

run_all(os.getcwd())
```

Appendix C – Protein Content and Cell size

Figure I: Protein content in homogenate that contained 25 of 96 hpf larvae that were continuously exposed (from 2 hpf) to three ATV concentrations with or without CoQ10 (4.5 mg mL^{-1}) or vehicle (PTS). Protein content was used to calculate (A) COX enzyme activity (B) LDH enzyme activity (C) CS enzyme activities. Data are presented as means + SEM (n=4 samples for each treatment with each sample being pooled from various petri dishes of a particular ATV treatment; see Materials and Methods). The letters denote significant differences among ATV concentrations within treatments, whereas an asterisk (*) denotes significant differences within the dose of ATV among treatment groups. A two-way ANOVA analysis followed by a Holm-Sidak post-hoc test was conducted ($p < 0.05$ was considered significant).

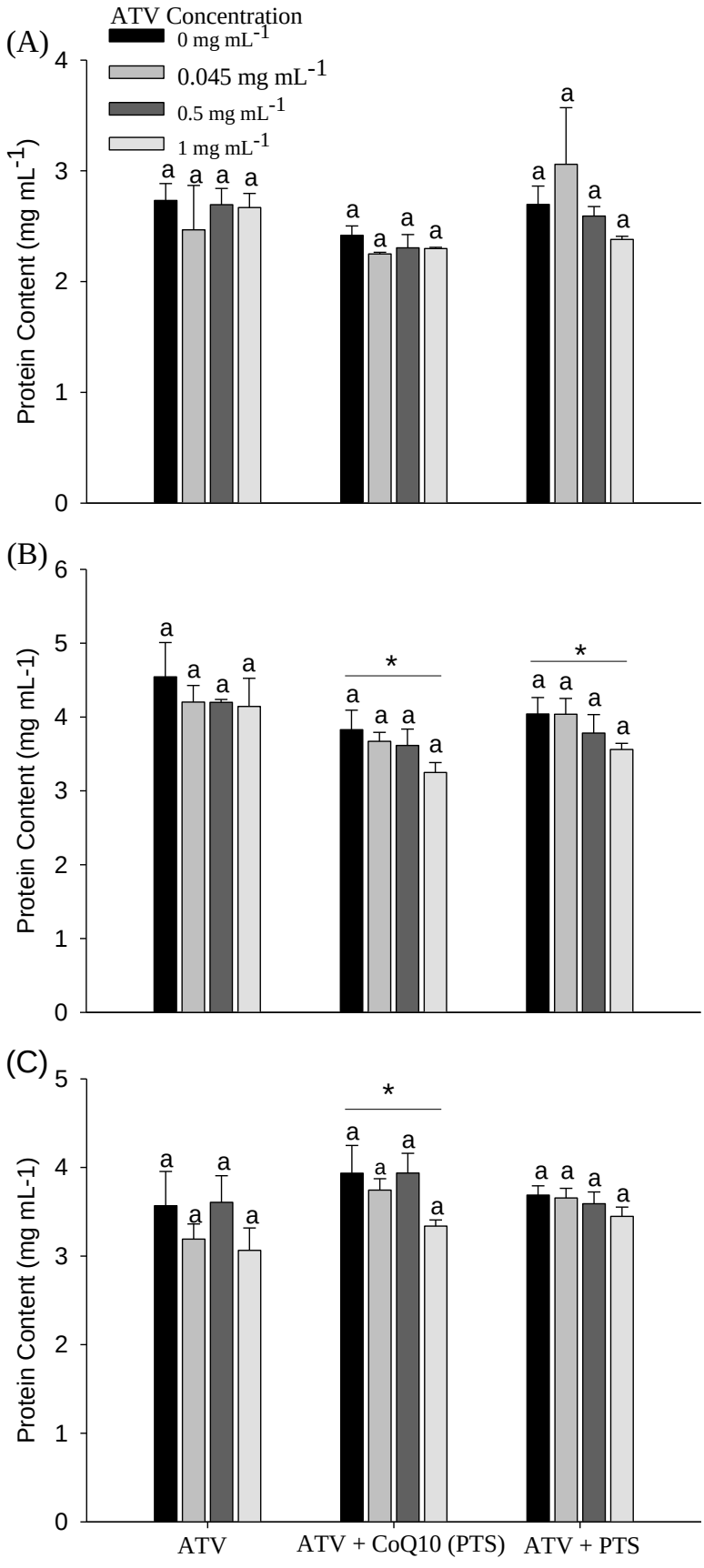
ATV Concentration
0 mg mL-1
0.045 mg mL-1
0.5 mg mL-1
1 mg mL-1
(A)
(B)
(C)
Protein Content (mg mL-1)
Protein Content (mg mL-1)
Protein Content (mg mL-1)
ATV
ATV + CoQ10 (PTS)
ATV + PTS

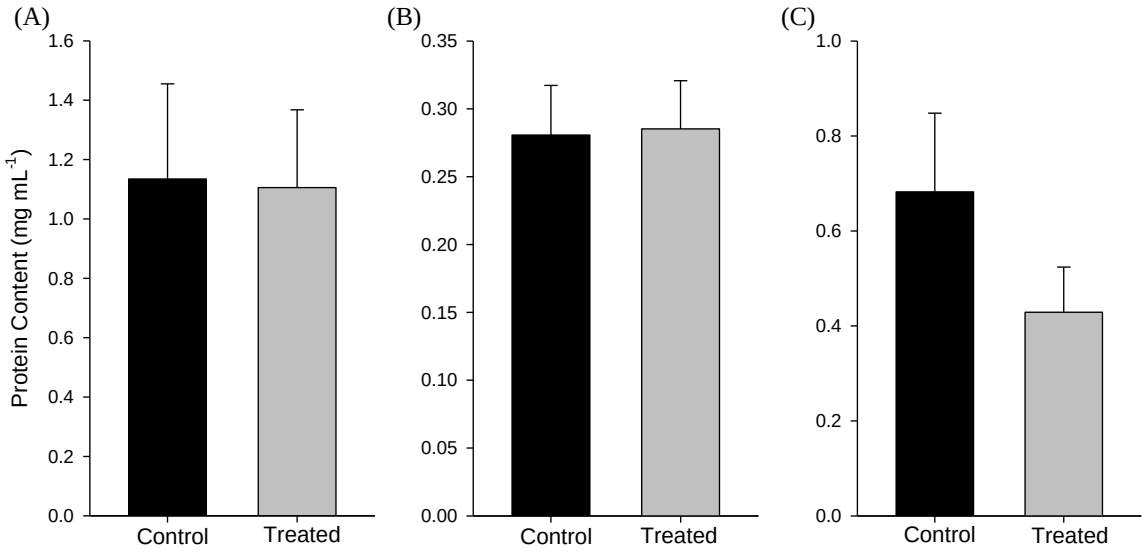

Figure II: Protein content in homogenate that contained 4 hearts from adult zebrafish treated for 30 days with ATV (0.045 mg L^{-1}). Protein content was used to calculate (A) COX enzyme activity, (B) CS enzyme activity, and (C) LDH enzyme activity. Data are presented as means + SEM (n = 4 samples at each treatment). A one-way ANOVA analysis found no differences between treatments.

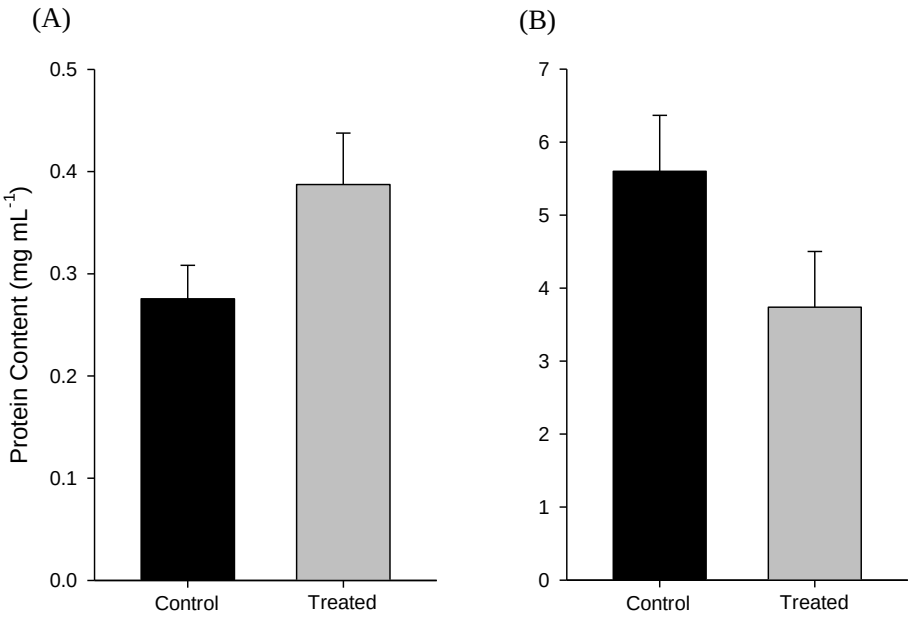

Figure III: Protein content in homogenate that contained one skeletal muscle from adult zebrafish treated for 30 days with ATV (0.045 mg L^{-1}). Protein content was used to calculate (A) COX enzyme activity, (B) CS and LDH enzyme activity. Data are presented as means + SEM (n = 4 samples at each treatment). A one-way ANOVA analysis found no differences between treatments.

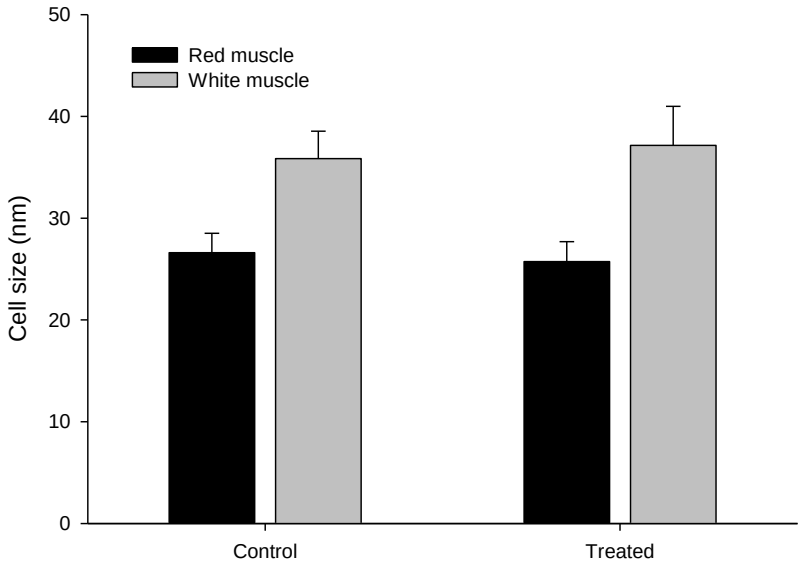

Figure IV: Cell size from red and white muscle in hematoxylin and eosin staining from adult zebrafish treated for 30 days with ATV (0.045 mg L^{-1}). Data are presented as means + SEM (n = 20 cells). A one-way ANOVA analysis found no differences between treatments.